

Synthesis and Applications of Functional Pyridines for Metamaterials and Fluorophores

Zur Erlangung des akademischen Grades eines

DOKTORS DER NATURWISSENSCHAFTEN

(Dr. rer. nat.)

von der KIT-Fakultät für Chemie und Biowissenschaften

des Karlsruher Instituts für Technologie (KIT)

genehmigte

DISSERTATION

von

M.Sc. Hannes Fabian Kühner

aus Bad Friedrichshall

1. Referent: Prof. Dr. Stefan Bräse

2. Referent: Prof. Dr. Christof Wöll

Tag der mündlichen Prüfung: 09.02.2023

“And the only way to do great work is to love what you do. If you haven't found it yet, keep looking. Don't settle. As with all matters of the heart, you'll know when you find it. ” – ***Steve Jobs, 2005***

Honesty Declaration

This work was carried out from September 01st 2019, through January 9th 2023, at the Institute of Organic Chemistry, Faculty of Chemistry and Biosciences at the Karlsruhe Institute of Technology (KIT) under the supervision of Prof. Dr. STEFAN BRÄSE.

Die vorliegende Arbeit wurde im Zeitraum vom 01. September 2019 bis 31. Dezember 2022 am Institut für Organische Chemie (IOC) an der Fakultät für Chemie und Biowissenschaften am Karlsruher Institut für Technologie (KIT) unter der Leitung von Prof. Dr. STEFAN BRÄSE angefertigt.

Hiermit versichere ich, HANNES FABIAN KÜHNER, die vorliegende Arbeit selbstständig verfasst und keine anderen als die angegebenen Hilfsmittel verwendet, sowie Zitate kenntlich gemacht zu haben. Die Dissertation wurde bisher an keiner anderen Hochschule oder Universität eingereicht.

Hereby I, HANNES FABIAN KÜHNER, declare that I completed the work independently, without any improper help and that all material published by others is cited properly. This thesis has not been submitted to any other university before.

German Title of this Thesis

**Synthese und Anwendungen von
Funktionellen Pyridinen für
Metamaterialien und Fluorophore**

Preface

Some of the presented results were published or submitted during the preparation of this thesis. The relevant content is reprinted with the permission of WILEY-VCH publishing. If some of the presented results have already been partly discussed elsewhere, it is stated at the beginning of the respective chapters.

Table of Contents

HONESTY DECLARATION.....	I
GERMAN TITLE OF THIS THESIS.....	III
PREFACE.....	V
KURZZUSAMMENFASSUNG	1
ABSTRACT	3
1 INTRODUCTION.....	5
1.1 PYRIDINE	5
1.2 4,4'-BIPYRIDINE.....	7
1.3 SUPRAMOLECULAR ARCHITECTURES.....	8
1.3.1 MOFs.....	10
1.3.2 SURMOFs	13
1.3.3 METAMATERIALS.....	14
1.3.4 NONLINEAR OPTICAL MATERIALS.....	15
1.4 FLUOROPHORES	18
1.4.1 INTRODUCTION TO FLUORESCENCE	18
1.4.2 HINA AS SMALL FLUOROPHORE.....	21
2 OBJECTIVE.....	23
3 MAIN SECTION	25
3.1 NON-CENTROSYMMETRIC 4,4'-BIPYRIDINES FOR MATERIALS SCIENCE.....	25
3.1.1 SYNTHESIS OF NON-CENTROSYMMETRIC 4,4'-BIPYRIDINES.....	25
3.1.1.1 General Synthesis Strategy - Cross-coupling of 4,4'-Bipyridines.....	25
3.1.1.2 Preliminary Work on the Synthesis of Non-centrosymmetric 4,4'-Bipyridines.....	26
3.1.1.3 Scope of Non-centrosymmetric 4,4'-Bipyridines.....	28
3.1.1.4 Photoswitchable Azo-benzene Containing Non-centrosymmetric Linkers.....	32
3.1.1.5 Protection Strategy and Synthesis of SURMOF Linkers.....	41
3.1.1.6 Photocleavage of PPG-bipyridine Conjugates.....	45
3.1.2 SURMOF PREPARATION AND CHARACTERIZATION	48
3.1.2.1 SURMOF Preparation with PPG-linker Conjugate.....	48
3.1.2.2 SURMOF Preparation with Unprotected Non-centrosymmetric 4,4'-Bipyridines	50
3.2 SYNTHESIS AND CHARACTERIZATION OF FLUORINATED HINA DERIVATIVES.....	53

3.2.1	SYNTHESIS OF FLUORINATED HINA DERIVATIVES.....	53
3.2.2	UV/VIS- AND FLUORESCENCE SPECTROSCOPY OF NICOTINALDEHYDES	62
4	SUMMARY AND OUTLOOK.....	65
4.1	SYNTHESIS OF NON-CENTROSYMMETRIC 4,4'-BIPYRIDINES FOR SURMOF PREPARATION	65
4.2	SYNTHESIS AND CHARACTERIZATION OF FLUORINATED HINA DERIVATIVES	68
5	EXPERIMENTAL SECTION	70
5.1	GENERAL REMARKS	70
5.2	CHARACTERIZATION OF COMPOUNDS.....	74
5.2.1	BIPYRIDINES	74
5.2.2	HINA DERIVATIVES	102
6	LIST OF ABBREVIATIONS.....	115
7	BIBLIOGRAPHY	117
8	APPENDIX.....	127
8.1	CURRICULUM VITAE.....	127
8.2	LIST OF PUBLICATIONS	128
8.3	ACKNOWLEDGEMENTS	129

Kurzzusammenfassung

Nichtlineare optische Materialien, die für eine Reihe wichtiger Anwendungen wie Frequenz- oder Wellenlängenumwandlung eingesetzt werden, erfordern einen nicht-zentrosymmetrischen Aufbau (fehlende Inversionssymmetrie). Oberflächenverankerte metallorganische Gerüstverbindungen (SURMOFs) sind kristalline Dünnschichtstrukturen. Um SURMOFs zu entwickeln, die sich nichtlinear verhalten, sollten die organischen Linker so gestaltet sein, dass sie nicht-zentrosymmetrisch sind und sich in einer Vorzugsrichtung im SURMOF orientieren. Dies würde die Möglichkeit eröffnen, solche orientierten SURMOFs als neue nichtlineare optische Materialien zu verwenden.

In dieser Arbeit lag der Schwerpunkt auf der Synthese von nicht-zentrosymmetrischen 4,4'-Bipyridinen. Verschiedene Strategien zur Ausrichtung der nicht-zentrosymmetrischen Moleküle im SURMOF wurden in Betracht gezogen und auf synthetischer Basis erforscht. Es wurde eine breite Palette von funktionalisierten Bipyridinen mit elektronenschiebenden oder -ziehenden Gruppen hergestellt. Darüber hinaus wurden zusätzliche Funktionalitäten in die Strukturen implementiert, wie z. B. eine photoschaltbare Azobenzolgruppe. Außerdem wurden Schutzkonzepte erforscht, um eine gerichtete Selbstorganisation der SURMOFs zu gewährleisten, einschließlich eines Schützungs-/Entschützungsansatzes unter Verwendung photospaltbarer Schutzgruppen (PPGs).

Durch sorgfältiges Design der Bipyridine war es möglich, die *Center-Symmetry Trap* bei der SURMOF-Synthese zu vermeiden. Die Anlagerung von elektronenziehenden oder -schiebenden Gruppen an nicht-zentrosymmetrische 4,4'-Bipyridine führt zu einer ungleichen Verteilung der Elektronen an den beiden koordinierenden Stickstoffatomen. Auf diese Weise wurden SURMOFs mit nichtlinearer optischer Aktivität und einem starken Frequenzverdopplungssignal (SHG) hergestellt.

In einem weiteren Projekt wurden fluorierte Isonicotinsäuren (HINAs) synthetisiert. Nicht-fluoriertes HINA ist ein vielversprechender kleiner grün-emittierender Fluorophor, der vor Kurzem von KANG *et al.* entdeckt wurde.¹ Durch die Synthese fluoriertem Derivate wurde erwartet, dass eine Rotverschiebung der Emission beobachtet werden würde. Es stellte sich heraus, dass die elektronenarmen HINAs recht instabil waren, so dass nur eines der beiden erfolgreich synthetisierten fluorierten HINA-Derivate getestet werden konnte. Die angestrebte Rotverschiebung von 16 nm wurde schlussendlich erreicht.

Abstract

Nonlinear optical materials, which have a variety of important applications such as frequency or wavelength conversion, require a non-centrosymmetric constitution (lack of inversion symmetry). Surface-mounted metal-organic frameworks (SURMOFs) are crystalline thin film structures. To develop SURMOFs that behave nonlinearly, the organic linkers should be designed to be non-centrosymmetric and oriented in a preferred direction in the SURMOF. This would allow using such oriented SURMOFs as new nonlinear optical materials.

In this work, the focus was on the synthesis of non-centrosymmetric 4,4'-bipyridines. Different strategies to direct the orientation of the non-centrosymmetric molecules in the SURMOF were explored on a synthetic base. A broad set of functionalized bipyridines having electron donating or withdrawing groups, such as halides or alkyl chains in different positions on one pyridine, was prepared. Furthermore, added functionality was implemented in the structures, such as a photoswitchable azobenzene group. In addition, protection strategies were explored to ensure directed self-assembly of the SURMOFs, including a protection/deprotection approach using photocleavable protecting groups (PPGs).

Through careful design of the bipyridines, it was possible to avoid the center-symmetry trap during SURMOF synthesis. The addition of electron withdrawing or donating groups to non-centrosymmetric 4,4'-bipyridines leads to an unequal distribution of electrons on the two coordinating nitrogen atoms. SURMOFs with nonlinear optical activity and strong second-harmonic generation (SHG) signal were fabricated.

In another project, fluorinated isonicotinic acids (HINAs) were synthesized. Nonfluorinated HINA is a promising small green-emissive fluorophore that was recently discovered by KANG *et al.*¹ By synthesizing fluorinated derivatives, it was expected that a red-shift in the emission would be observed. This work fabricated three new nicotinic acid derivatives *via* a newly developed synthesis strategy. It turned out that the electron-deficient HINAs were quite unstable, so only one of the two successfully synthesized fluorinated HINA derivatives could be tested. The targeted red-shift of 16 nm was ultimately achieved.

1 Introduction

For millennia, materials have shaped the development of civilizations through structures and devices. Using better tools and weapons made disruptive advances possible, as illustrated by the designation of historical eras by their predominant material, such as the Stone Age, Bronze Age, or Iron Age. The current age is called the Silicon or Polymer Age because semiconductors containing silicon are used in modern devices, and polymers are used in many products of our lives. Polymer production exceeded that of steel as early as 1980.^{2,3} In the last 50 years, materials science has shifted towards an interdisciplinary field across science and engineering, bringing researchers together to combine biological materials, organics, ceramics, and metals at near molecular precision in porous structures.

In this work, tailor-made structures are used to design and fine-tune the properties of these materials rationally. Therefore, this work includes a brief introduction to the basic properties of the chemicals used, as well as classifications and properties of the materials.

1.1 Pyridine

Heterocyclic derivatives are ubiquitous in many agrochemicals, pharmaceuticals, natural products, and optoelectronic materials. Among the wide variety of heterocycles, pyridines are by far the most predominant structure.⁴ It belongs to the pyridine alkaloids group, including the plant alkaloids nicotine and anabasine, both of which are found in the common tobacco plant *Nicotiana tabacum*.⁵ In addition, pyridine alkaloids can be found within the animal kingdom, such as epibatidine, which was found in the skin of Ecuadorian frogs (Figure 1).⁶

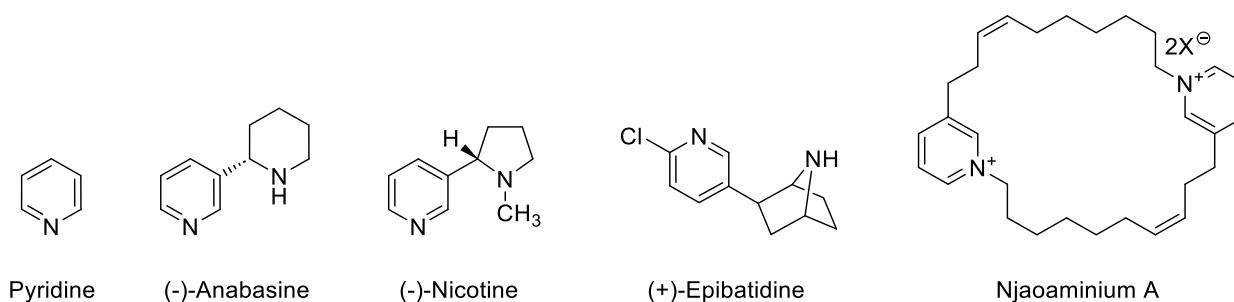
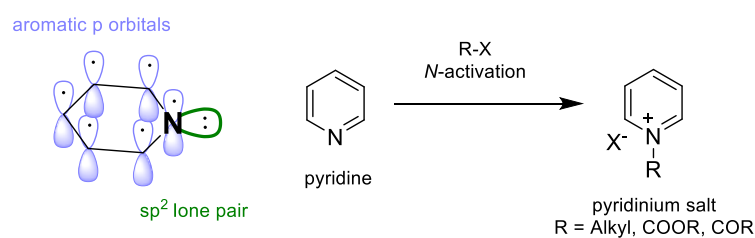


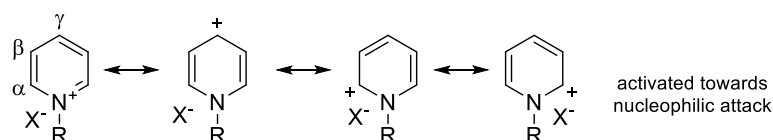
Figure 1. Natural products that contain pyridine components and pyridine.

Pyridine itself was first isolated in pure form by the Scottish chemist THOMAS ANDERSON, who extracted it from animal bone pyrolysate in 1851.⁷ Its final structure was proposed by DEWAR AND KÖRNER just five years after KEKULÉ had suggested the conjugated structure of benzene. Pyridine is a colorless, unreactive liquid with varying bond lengths compared to benzene. This is due to the electronegative nitrogen atom, which distorts the electronic distribution, which results in differing bond lengths in the ring.⁸ Furthermore, the nitrogen induces a dipole moment of 2.22 D, making it a π -deficient heterocycle.⁹ Compared to piperidines, pyridines are weak bases; they react with BRØNSTED acids like HCl to generate pyridinium ions and LEWIS acids like aluminum chloride to form stable pyridinium complexes.⁸ Electrophilic aromatic substitution on the ring-C-atoms only proceeds under harsh conditions. Nucleophilic aromatic substitutions proceed much more easily, owing to the electron-deficient nature of the pyridine heterocycle.¹⁰ When subject to hydration with hydrogen and a suitable catalyst, pyridine reacts to piperidine.¹¹⁻¹³

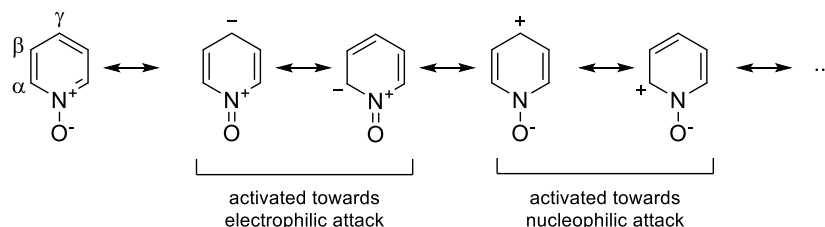
Pyridine reactivity:



Pyridinium salts:



Pyridine-N-oxide:



Scheme 1. Orbitals of pyridine (top left) and synthesis of *N*-activated pyridinium salts (top right). Mesomeric structures of pyridinium salts (middle) and pyridine *N*-oxide (bottom). Modified after 14, 15

Reactions with organic halides yield pyridinium salts, which have a positive charge in the pyridine ring and change the reactivity significantly. In comparison to pyridine heterocycles, pyridinium salts are much more polarized. Pyridinium salts are present in natural products, such as Njaoaminium A, found in marine sponges (Figure 1).¹⁶ 1-Alkylpyridinium salts are an important intermediate in several natural product syntheses and can be used as ionic liquids in synthesis and catalysis.^{14, 17} Moreover, it is important to notice that pyridinium salts retain the aromatic sextet. The lone pair electrons from the nitrogen lie in a plane with the ring in an sp^2 -orbital that does not overlap the p-orbitals. At the 2/6- and 4-positions of the ring, the pyridinium salt features reactive sites toward nucleophilic attacks, favored by the positive charge (Scheme 1).⁹ Thus, when a nucleophile attacks, combinations of 1,2- and 1,4-substituted dihydropyridines are obtained.¹⁸

In some cases, adducts can be isolated. However, they are unstable and undergo further reactions, such as disproportioning, ring opening, or substitution reactions. Electrophilic substitutions are rare due to the positive charge and are only possible if strongly activating substituents and strong electrophiles are used.¹⁹ Pyridine *N*-oxides are, in contrast to pyridinium salts, not only activated towards additions but also undergo nucleophilic substitutions. This can be explained by the mesomeric structures of pyridine *N*-oxide shown in Scheme 1. Both additions occur likewise at the ring's 2/6- and 4-positions.²⁰

1.2 4,4'-Bipyridine

According to IUPAC, compounds consisting of two pyridines linked together *via* a C-C bond are bipyridines.²¹ 2,2'-Bipyridine is the most widely used bipyridine, as it is an excellent chelating ligand. This work, however, solely concentrates on 4,4'-bipyridines, as they can be used as versatile linear ditopic linkers which find applications in pillared layered MOFs and other supramolecular architectures.²²⁻²⁷

The first documented synthesis of 4,4'-bipyridine was reported by THOMAS ANDERSON in 1870 by heating pyridine with sodium metal.²⁸ However, ANDERSON stated that the empirical formula of 4,4'-bipyridine was $C_{10}H_{10}N_2$ which was corrected to $C_{10}H_8N_2$ by WEIDEL and RUSSO in 1882.²⁹ Pyridine undergoes radical homocouplings, which resulted in the selective formation of either 2,2'-bipyridine when Raney Nickel is present or 4,4' bipyridine when elemental sodium is used.³⁰

Today, 4,4'-bipyridine is mainly produced as an intermediate in the production of paraquat, a broadly used herbicide. Due to its toxicity to humans, it was banned from the European Union in 2007; however, in the United States, it is used today, and the estimated consumption represented by the US Geological Survey exceeded 6800 tons of paraquat in 2018.³¹

In research, because of its coordinating abilities, 4,4'-bipyridine is an ambiguous building block used in materials chemistry. In 1982, the X-ray single crystal structure of the first 4,4'-bipyridine coordination polymer was reported (Figure 2).³²

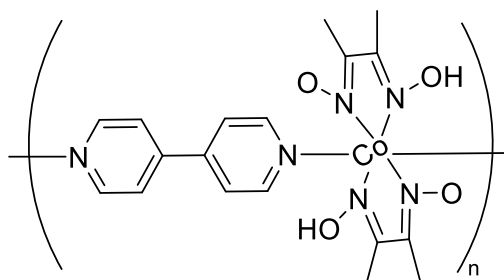


Figure 2. First coordination polymer with 4,4'-bipyridine was published by KUBEL and STRÄHLE in 1982.³²

Due to the following characteristics, the 4,4'-bipyridine ligand is a suitable connector between transition metal atoms for the propagation of coordination networks: It features two possible binding sites that are positioned on opposite sides; it has a solid structure that will facilitate the prediction of network geometries; the length of the ligand is suitable to construct molecular-sized spaces in the coordination networks with metal atoms. The pyridyl groups of 4,4'-bipyridine can theoretically twist around the connecting C-C link. Nonetheless, the rotation does not affect the orientation of the two lone pairs. Consequently, 4,4'-bipyridine can be considered a stiff bridging linker. The basic nitrogen of the bipyridines can coordinate most transition metals due to its σ -donating and π -accepting molecular orbitals.^{33,34}

1.3 Supramolecular Architectures

The Nobel Prize laureate in chemistry in 1987, Jean-Marie Lehn, defined supramolecular chemistry as “the chemistry of the intermolecular bond, covering the structures and functions of the entities formed by association of two or more chemical species.”³⁵ And in

contrast to this definition, he defined molecular chemistry as “the chemistry of the covalent bond, [that] is concerned with uncovering and mastering the rules that govern the structures, properties, and transformations of molecular species.”³⁵ This definition of supramolecular chemistry means that the field looks at all interactions between atoms or molecules other than covalent bonds. Historically, the term arose from host-guest interactions of, *e.g.*, crown ethers or spherands with metal cations.^{36, 37} Supramolecular chemistry has evolved to include any structure in which intermolecular interactions link together two or more chemical entities. All self-assembling systems, including films, gels, liquid crystals, nanostructures, and polymers, are assigned to supramolecular chemistry.³⁸

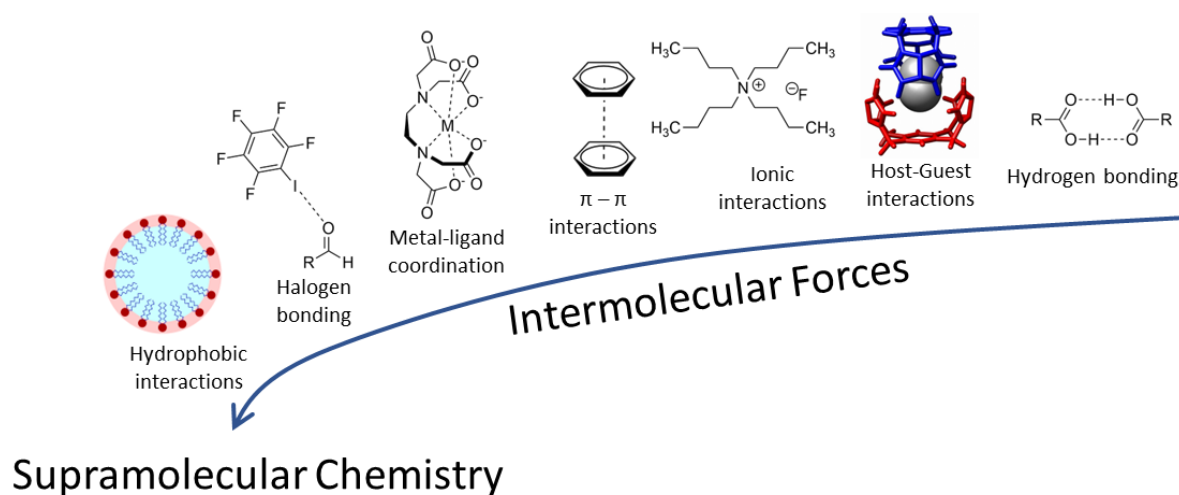


Figure 3. Depiction of intermolecular forces that can contribute to forming supramolecular assemblies, modified after ref. [39].

Supramolecular chemistry can be subdivided into coordination polymers that include metals and networks based on other non-covalent interactions between the components. These interactions can be based on hydrogen bonding, halogen bonding, ion-ion, ion-dipole, π - π -stacking, and Van-der-Waals forces, but also on hydrophobic and solvation effects –to name a few (Figure 3).³⁷ Metal-organic frameworks belong to the coordination polymers and are porous supramolecules consisting of organic ligands and metal components, which was defined by the IUPAC task group Coordination Polymers and Metal Organic Frameworks in 2013.⁴⁰

1.3.1 MOFs

Metal-organic frameworks (MOFs), also known as porous coordination polymers (PCPs), are well-known composite materials made up of multitopic organic linker molecules that form a crystalline, highly porous network together with inorganic metal nodes.⁴¹ They are crystalline three-dimensional networks with high pore volumes and high surface areas of up to 10000 m²g⁻¹.⁴² The metal nodes are also referred to as secondary building units (SBUs). They are metal-carboxylate clusters with various connectivities and diverse geometries, a prerequisite for constructing different MOF structures.⁴³ Even though the first coordination materials date back as far as 1959, MOFs are a relatively new class of materials whose importance in science is growing, especially since the beginning of the 21st century. This is evident when looking at the publications published recently in this field (Figure 4).⁴⁴

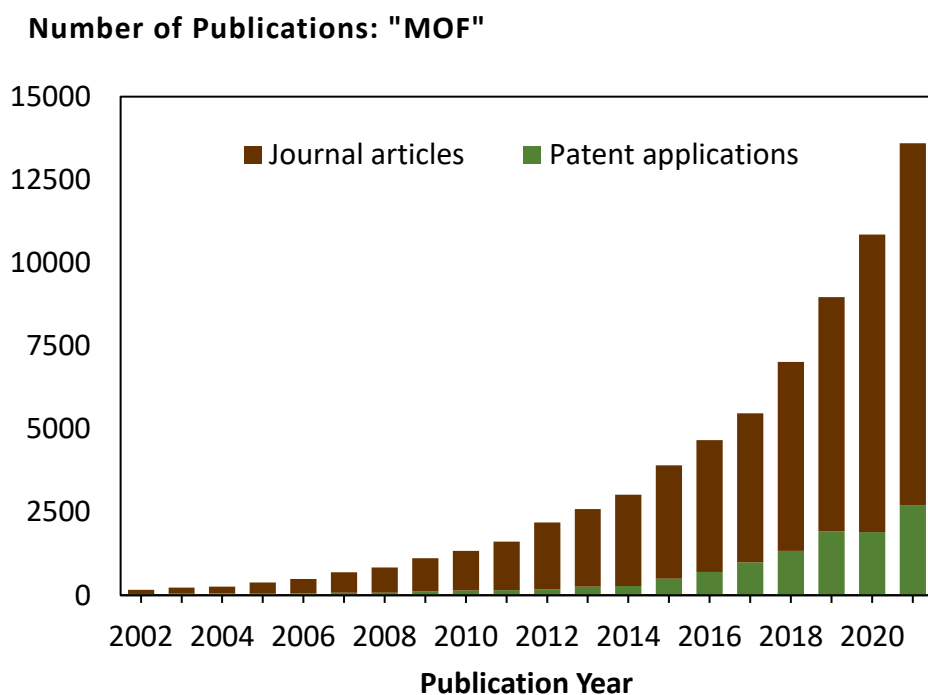


Figure 4. The growing field of MOF research is visualized by showing the yearly publications containing the topic "MOF" (Source: SciFinder[®]).

OMAR YAGHI pioneered MOF research in the 90s and coined the term "metal-organic frameworks".⁴⁵⁻⁴⁷ In his first examples, he used 4,4'-bipyridine as ditopic linkers to create a 2D square grid coordination network based on a Cd²⁺ SBU (Figure 5, left).⁴⁸ Later, using charged carboxylic acid-functionalized linkers became popular, as the increased bond

strength resulted in higher thermal stability. The MOF-5 structure was published in 1999 and was named after the well-known zeolite ZMS-5. It demonstrated the potential of MOFs, as it came with a large pore and a Brunauer-Emmett-Teller (BET) surface area of $2320 \text{ m}^2\text{g}^{-1}$, which exceeded that of common porous inorganic materials at that time.^{49, 50} YAGHI also visualized the large pore of MOF-5 by drawing a yellow-colored ball into the pore (Figure 5, right).

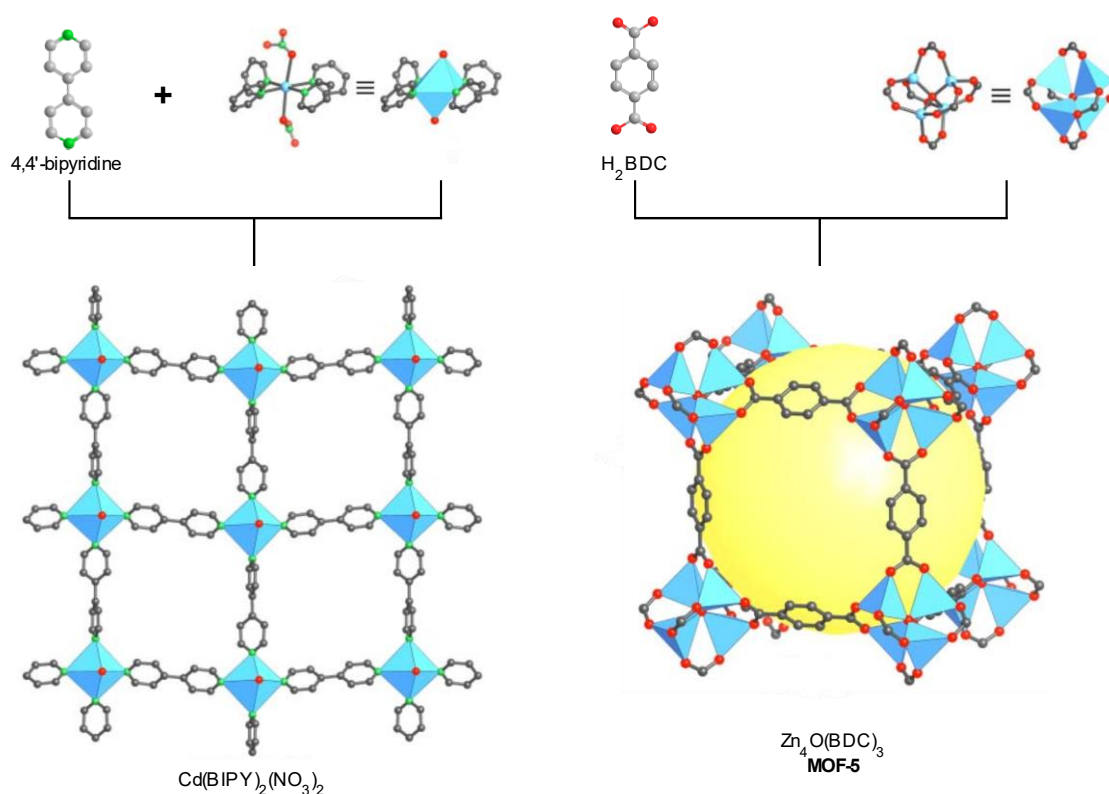


Figure 5. Early MOF structure containing 4,4'-bipyridine (BIPY) with a Cd^{2+} SBU (left), iconic depiction of the large pore of **MOF-5** (yellow, right). Hydrogens and guest atoms are omitted for clarity. Color Code: Cd or Zn, blue; C, gray; N, green; O, red; modified after ref. [48].

Most MOFs are based on linkers with similar functional groups, namely carboxylic acids and *N*-heterocyclic compounds such as bipyridines.⁵¹ They can be subcategorized regarding their topicity (Figure 6). The simplest and most often used linkers are ditopic carboxylic acids linkers of the H₂-BDC- and H₂-BPDC-type. They can be modified with functional groups such as amines (H₂-BDC-NH₂), ethers (H₂DE-BDC), and many more. By varying the linker length, the pore size of the resulting networks can be set. Tritopic linkers (H₃-BTC), tetratopic (H₄-atc), and other multitopic linkers can change the network structure with appropriate SBUs. Furthermore, chirality can be added to the framework using chiral linkers such as the (*R*)-BINOL-based linker. *N*-heterocyclic linkers can also vary in size. They are

often based on pyridyl- or azole-functional groups. Due to the weak donor-strength of the linear ditopic pyridine-based linkers, they are generally more challenging to grow than carboxylic acid linkers.⁵¹ However, their linear ditopic architecture makes rectangular architectures possible. Imidazolate linkers result in a special type of MOF, namely zeolitic imidazolate frameworks (ZIFs), which coordinate more strongly but are not of a linear type.⁴⁹

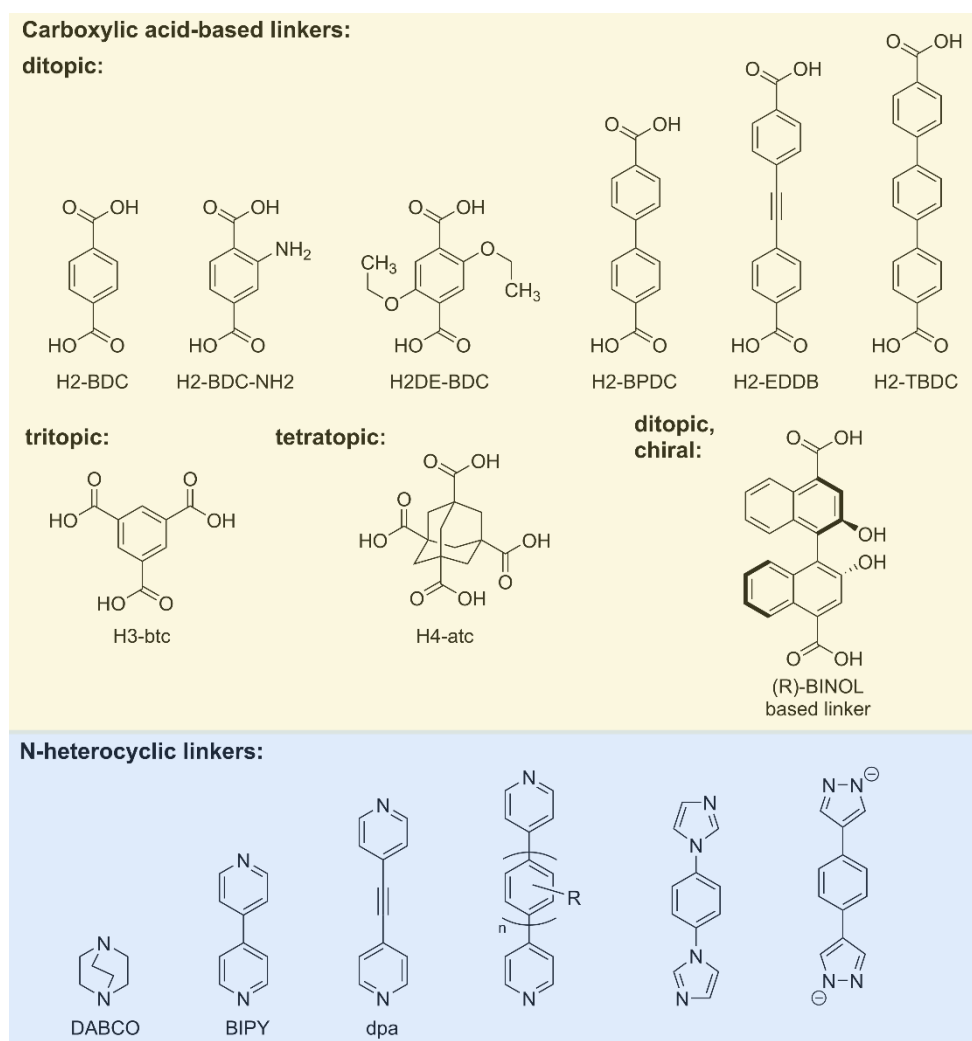


Figure 6. Common organic linkers for preparation of MOFs. Carboxylic acid-based linkers are shown on top (yellow background), and *N*-heterocyclic linkers are shown on the bottom (blue background).

1.3.2 SURMOFs

One of the most promising routes towards precisely constructing functional nanomaterials is molecular self-assembly, a so-called "bottom-up" approach in nanotechnology.⁵²⁻⁵⁶ Strongly linked to this approach is the controlled growth of MOF thin films, which several different techniques can achieve. Spin coating, dip coating, and hydro- or solvothermal growth from MOF suspensions, respectively, from reactant solutions, are all examples of methods for generating MOF thin films.⁵⁷

In cooperation with this work, surface coatings were prepared by liquid-phase epitaxy-based (LPE) thin film fabrication. When performing LPE, solutions of linker and metal components are used. MOF crystal layers are formed by iterative sequential deposition of the components on a self-assembled monolayer (SAM).⁵⁸ During this self-assembly process, the material grows with each iteration, called layer-by-layer (LBL) synthesis. These films, known as surface-mounted metal-organic frameworks (SURMOFs), were introduced by FISCHER and WÖLL in 2007.^{59, 60} SURMOFs have a thickness in the nanometer range but can be grown to achieve a thickness in the micrometer range when deposition cycles were repeated many times.^{61, 62}

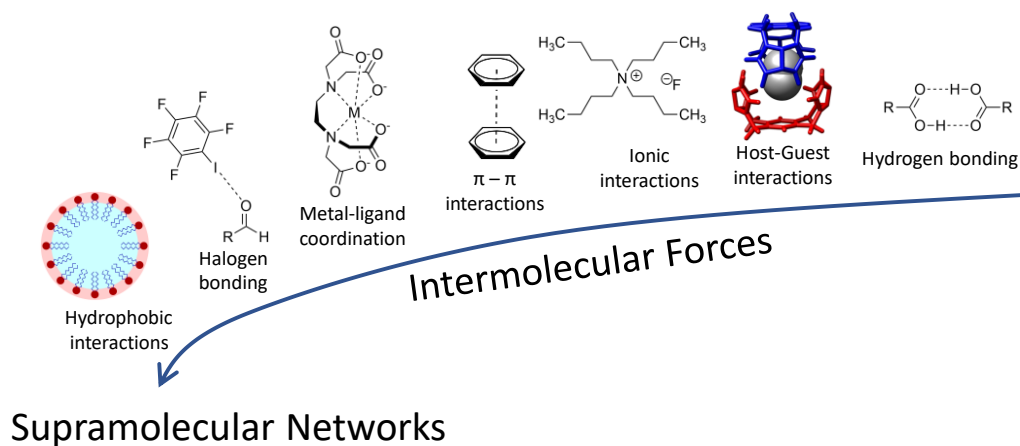


Figure 7. (a) Schematic SURMOF representation: MOF thin film is grown on top of an MHDA SAM on gold. (b) LBL growth of a SURMOF. Each repeated cycle adds a new SURMOF layer to the existing thin film.

The LPE-LBL-based SURMOFs are usually grown on functionalized surfaces. Gold-coated silicon wafers functionalized with a self-assembled monolayer (SAM) facilitate the binding of the initial reactants.⁶³ Native oxide substrates can also be used. In the case of a functionalized substrate, the linker molecules usually consist of a thiol head group that binds

to the gold surface and a binding group on the opposite side of the molecule, which can coordinate the metal component of the SURMOF. Common thiol reagents for SAMs are 16-mercaptopentadecanoic acid (MHDA), 11-mercaptopundecanol (MUD), 9-carboxy-10-(mercaptomethyl) triptycene (CMMT) or 4'-carboxyterphenyl-4-methanethiol (TPMTA) (Figure 7).

SBUs are added to anchor on top of the SAM. Subsequently, linkers are added to cross-link the metals and enable binding to the next layer of metal nodes. After each deposition cycle, the thin film gets rinsed with an appropriate solvent. If two specific linkers are used, pillar-layered SURMOFs can be achieved, resulting in cross-linked planar MOF structures (layers) of one kind and vertical connections (pillars) with linkers of another. WANNAPAIBOON *et al.* demonstrated this kind of SURMOF using H₂DE-bdc and DABCO linkers.⁶⁴

1.3.3 Metamaterials

The word metamaterial, whose prefix is derived from Greek and means “beyond”, originally arose in the early 21st century, with an example appearing in a study by SMITH *et al.* that explored a composite medium having simultaneously negative permeability and permittivity in the microwave area of the electromagnetic spectrum (Figure 8).^{65, 66} With advances in nanotechnology, it was possible to address shorter wavelengths, extending potential applications.

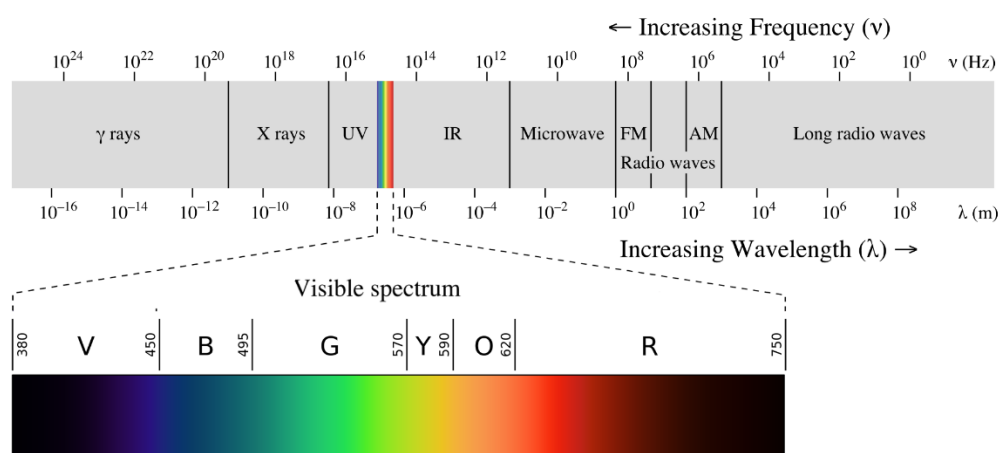


Figure 8. The electromagnetic spectrum is shown. Longer wavelengths come with increased energy. The visible spectrum ranges from $\sim 380 - 750$ nm.⁶⁷

The literal meaning of the word metamaterial suggests that material has properties further than those of normal materials. The features of metamaterials derive from the combination

of the materials' intrinsic characteristics and the pattern in which they are organized. They can be categorized into four main groups, depending on the wavelengths that they are designed for and operate on. These are mechanical, acoustic, structural, or nonlinear metamaterials.⁶⁸⁻⁷¹ While various applications exist for these materials, this work focused on synthesizing precursors for metamaterials having nonlinear properties.

1.3.4 Nonlinear Optical Materials

When light meets matter, things start to get more interesting. Materials can transmit, focus, absorb, reflect, or generate light. These are all important ways to control light in general. However, some materials respond nonlinearly with the optical properties upon radiation with intense light.

In general terms, the polarization of a molecule or material P depends linearly on the electric field strength E and is given by the following series

$$P = \alpha E + \beta E^2 + \gamma E^3 + \dots \quad (1)$$

where α is the linear polarizability, β the second-order hyperpolarizability, γ the third-order hyperpolarizability, and E is the applied electric field.⁷² For small electric fields, the higher-order hyperpolarizabilities can be disregarded. This means that the medium's polarization behaves proportionally to the strength of the applied electric field:

$$P \propto \alpha E \quad (2)$$

However, things change when an intense electric field is applied, *e.g.*, in the form of intense laser light. The higher-order hyperpolarizabilities become significant, and nonlinear optical properties can be observed.⁷³

The macroscopic polarization of a material is given by

$$P = \chi^{(1)}E + \chi^{(2)}E^2 + \chi^{(3)}E^3 + \dots \quad (3)$$

with χ being the susceptibility of any given material. $\chi^{(1)}$ is the linear, first-order susceptibility, whereas $\chi^{(2)}$ and $\chi^{(3)}$ are nonlinear second- and third-order susceptibilities. The field and polarization terms are vectors, and the susceptibility terms are tensors.

At the macroscopic level, a nonzero second-harmonic generation (SHG) ($\chi^{(2)}$ term) requires a non-centrosymmetric material, and large $\chi^{(2)}$ values necessitate a strong donor and/or

acceptor group bound to the molecule. For a large third-harmonic generation, an extended delocalized π -system is required.^{74, 75}



Figure 9. SHG process in an ammonium dihydrogen phosphate crystal. Reproduced from ref. [76] with permission from the Royal Society of Chemistry.

In the example of SHG, intense laser irradiation interacts with the nonlinear matter that produces radiation twice the incoming light's frequency. Figure 9 shows the SHG in an ammonium dihydrogen phosphate crystal. Two infrared laser lights combine into a visible blue light when shone through the crystal. Therefore, this effect is also known as frequency doubling.⁷⁷ With improvements in diode lasers' quality and output power in recent years, laser-based devices and systems have become increasingly prevalent, resulting in an increased demand for nonlinear optical materials.⁷⁸ They can be used in almost all scientific disciplines, such as biotechnology, telecommunication, medicine, and data processing; and until today, many useful devices have been realized, such as wavelength shifters⁷⁹, frequency doublers⁸⁰, switches⁸¹, modulators⁸², and many more.^{83, 84}

Compared to the two-photon fluorescence, SHG is a lossless process in which the incident radiation ω_{SHG} is transformed into radiation of twice the energy $2\omega_{\text{SHG}}$. Fluorescence processes lose energy during vibrational relaxation in the excited state. Therefore, the wavelength emitted during a one-photon fluorescence is shorter than that of the incident

radiation (Figure 11, page 19).⁸⁵ For further information on the fluorescence process, see chapter 1.4.1.

For many years, it has been known that certain kinds of organic materials have exceptionally large nonlinear optical effects. In the most effective organic materials, electronic nonlinearities are founded on molecular units with highly delocalized π -electrons and electron donor/acceptor groups on opposing sides of the molecule (Figure 10).⁸⁶ As a result, the most active molecules are strongly polarized. However, most polar compounds crystallize in a centrosymmetric form because they align in opposite directions, which cancels out the macroscopic polarization and, therefore, lacks the nonlinear optical effect.⁸⁵

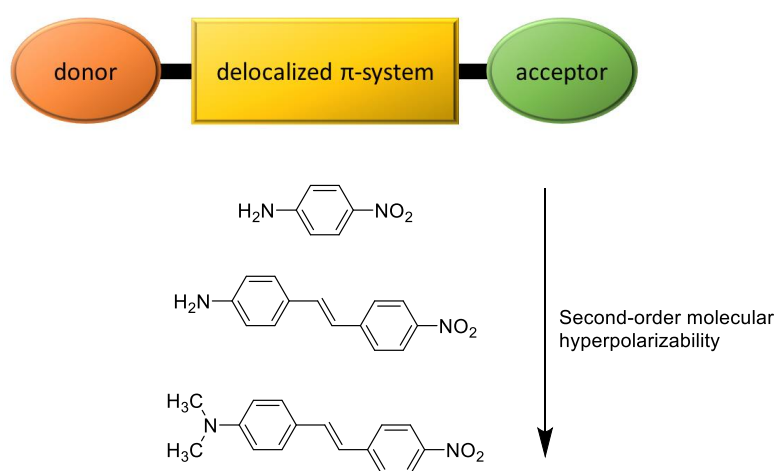


Figure 10. Molecular design of second-order molecular hyperpolarizability for large second-order nonlinear effects.

Therefore, the key challenge is to orient strong dipoles in a material. At the same time, organic molecules are versatile candidates for the design of strong dipoles, as organic chemistry offers a broad spectrum of modifications. With supramolecular chemistry, these dipoles could be anchored in a network that shows the desired nonlinear optical properties.

1.4 Fluorophores

The first small fluorophore was quinine sulfate, described by FREDRICK HERSCHEL in 1845 when he discovered a visible emission from quinine solution in water.⁸⁷ Seven years later, GEORGE STOKES stated that this emission, which he named “fluorescence”, was due to light absorption.⁸⁸ The effect was physically described by ALEXANDER JABŁOŃSKI in 1935, in which he also showed the popular energy diagram named after him.⁸⁹ Since then, new dyes and instrumentation have been invented, which ultimately led to the development of fluorescence microscopy, and is now one of the most common life-cell observation methods in biology. Just recently, in 2008, the Nobel prize was awarded for “the discovery and development of the green fluorescent protein, GFP”⁹⁰ and in 2014, “for the development of super-resolved fluorescence microscopy”⁹¹. This shows the fundamental role of fluorescence in chemistry, biology, and physics.

1.4.1 Introduction to Fluorescence

The JABŁOŃSKI diagram shows the photophysical processes which can occur during an excitation cycle (Figure 11). The numerous horizontal solid lines each constitute an energy level of the molecule. The singlet ground and electronically excited states are labeled S_0 , S_1 , S_2 , and S_n , respectively. A similar notation is used for the excited triplet states, which indicate T_1 , T_2 , etc. Each electronic state is further divided into the vibrational sublevels, represented by the grey lines.⁹²

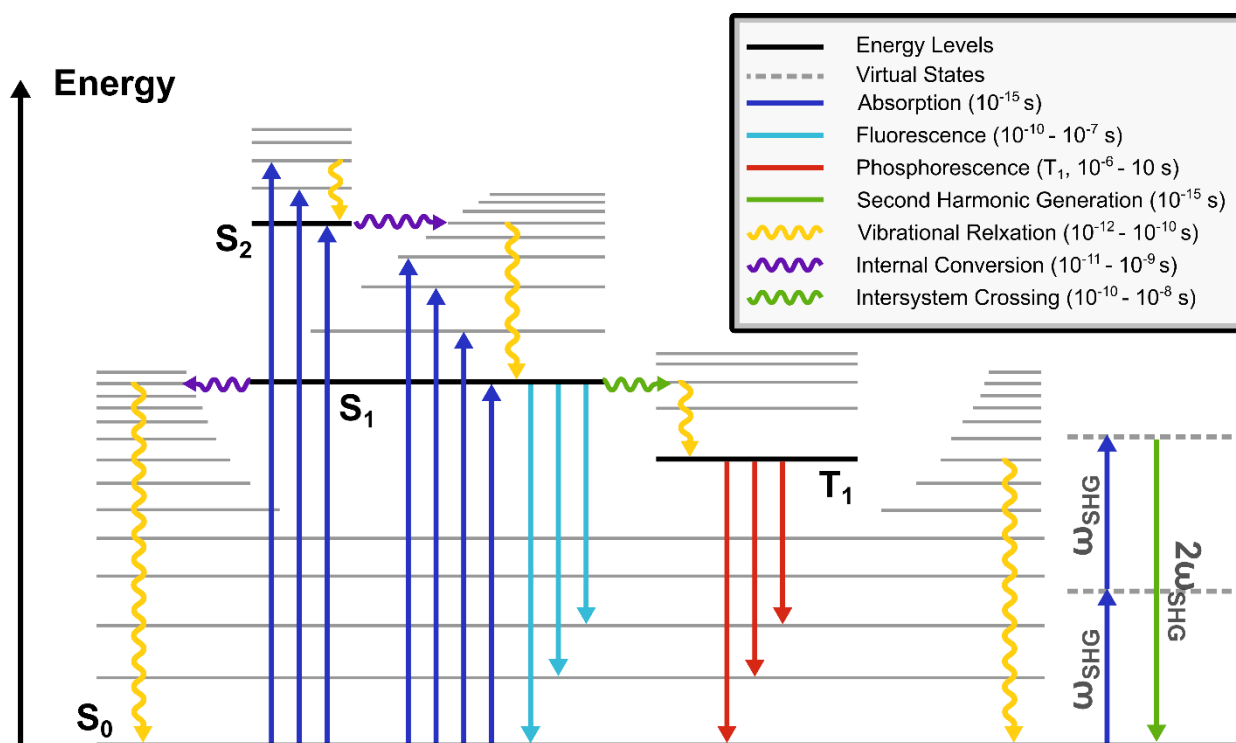


Figure 11. JABŁOŃSKI diagram of the fluorescence, phosphorescence processes versus SHG. (Lifetime values taken from ^{93, 94})

When a molecule absorbs a photon, it transitions to a higher excited electronic state and possibly to a higher vibrational state. It then relaxes by vibration to the ground vibrational level of the first excited singlet state S_1 . This process is known as internal conversion, and the relaxation within one excited state is called vibrational relaxation.⁹⁵ Non-radiative decay, in which the energy is transmitted into the vibration, rotation, and translation of the surrounding atoms or molecules, is the main mechanism through which excited, non-emitting molecules relax. As a result, the molecule loses its excitation energy as heat and settles back into its ground electronic state. It can also transmit its excitation energy through quenching or resonance energy transfer. Intersystem crossing, a non-radiative migration into the triplet state T_1 , can also occur for electrons in the excited singlet state S_1 . From there, the molecule can deactivate through non-radiative decay or radiative phosphorescence. If the deactivation from the S_1 state comes with the emission of a photon, this phenomenon is formally known as fluorescence.⁹² Because fluorescence occurs from the lowest vibrational level of the excited state S_1 , it generally does not depend on the excitation wavelength. Moreover, other processes, such as delayed fluorescence or triplet-triplet transitions can occur, but will not be further discussed in this work.

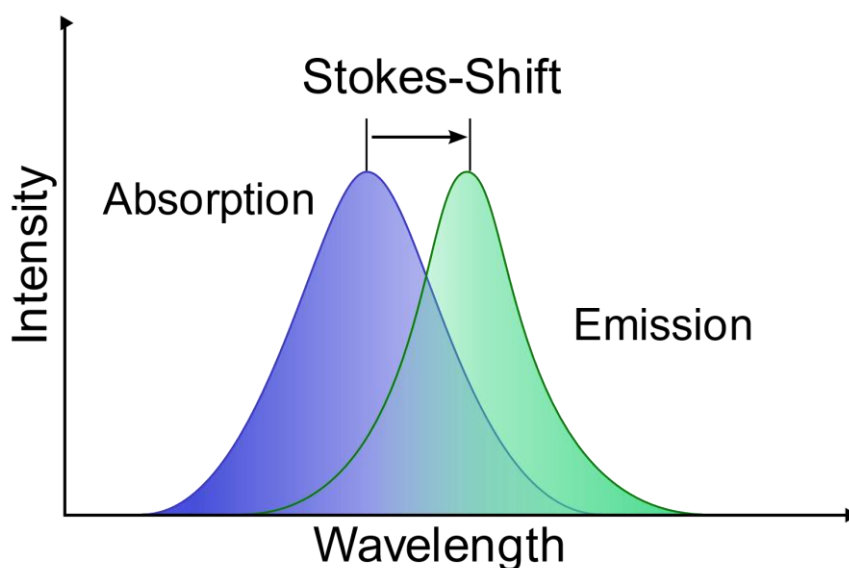


Figure 12. Simplified absorption/excitation and emission spectrum. The absorbed light is shifted towards longer wavelengths when emitted during fluorescence.

The energy difference between an absorbed and emitted photon during the fluorescence process results in a shift towards longer wavelengths, known as the STOKES shift, named after the beforementioned GEORGE STOKES.⁹⁶ It is of great importance for the sensitivity of the fluorescence emission signal because incoming excitation light can be filtered out. The effect can be easily observed when recording fluorophore's excitation and emission spectra (Figure 12).

As mentioned before, fluorophores play a fundamental role in chemical biology and find commercial applications in industry, for example, for constructing OLED devices.⁹⁷⁻⁹⁹ Most common organic fluorophores are based on only a few basic structures: coumarins, BODIPY dyes, fluoresceins, rhodamines, phenoxazines, and cyanines. All these structures have conjugated π systems to absorb UV or visible light. Upon excitation of a wavelength matching the HOMO/LUMO-gap between the π and π^* orbital, an electron is transferred between these orbitals resulting in an excited state of the molecule (Figure 13). Through internal conversion and vibrational relaxation, the energy gap ΔE_1 decreases to ΔE_2 ($\Delta E_1 > \Delta E_2$).¹⁰⁰ During the absorption, usually the lowest-lying transition $\pi \rightarrow \pi^*$ takes place, however, in compounds with heteroatoms $n \rightarrow \pi^*$ transitions might be the lowest-lying ones. This is usually the case for nitrogen-containing heterocycles such as pyridine.⁹³

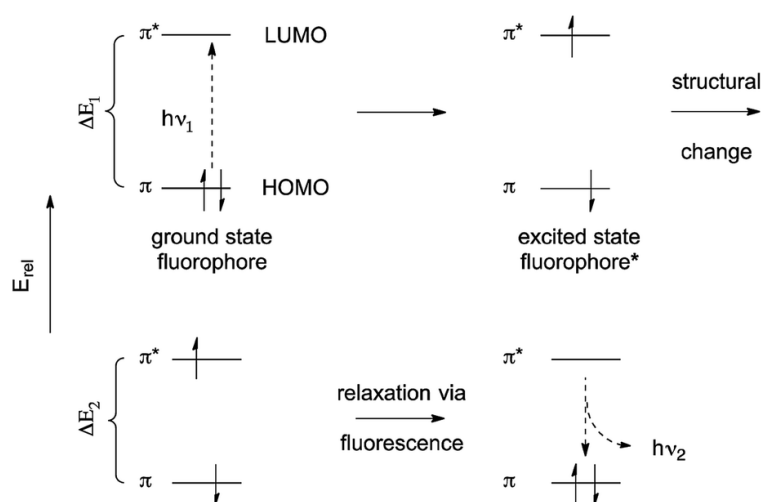


Figure 13. HOMO/LUMO diagram of a fluorophore. During the fluorescence process, a molecule absorbs the incident radiation of the wavelength $h\nu_1$. An electron from the π orbital is elevated and occupies the π^* orbital. The dipole moment changes due to the excited state, and solvent molecules reorganize to reach the ground level of the first excited singlet state. The fluorophore then emits radiation of wavelength $h\nu_2$ of lower energy than $h\nu_1$ due to the beforementioned relaxation. Reproduced from ref. [100] with permission from the Royal Society of Chemistry.

The fluorescence properties of a fluorophore are strongly dependent on its structure. With the tools of organic chemistry, it is possible to alter all the mentioned characteristics of a fluorophore. An increased π electron system, for example, results in a bathochromic absorption shift. Furthermore, fluorescence is often strongly dependent on the solvent used, especially if it is polar or nonpolar.⁹³

1.4.2 HINA as Small Fluorophore

Particularly interesting for biochemical investigations are small fluorophores. Many small organic fluorophores emit in the UV region and the smaller wavelengths, and are often based on one or two benzene rings. However, green-emitting dyes, such as fluorescein, acridine orange, BODIPY compounds, or Cy3B, are often much larger.^{100, 101} The investigations for novel small green fluorescent fluorophores are ongoing. Recently, in search for a small water-soluble fluorophore, KANG *et al.* demonstrated that 3-hydroxyisonicotinic acid (HINA) has good fluorescent properties.¹ Since today, it is the smallest green fluorescent dye with an emission wavelength of $\lambda_{\text{ex}} = 525$ nm for pH-values > 7.1 . Bearing only 14 atoms and a molar mass of 123 g/mol, it is much smaller than conventional green-emitting compounds.¹

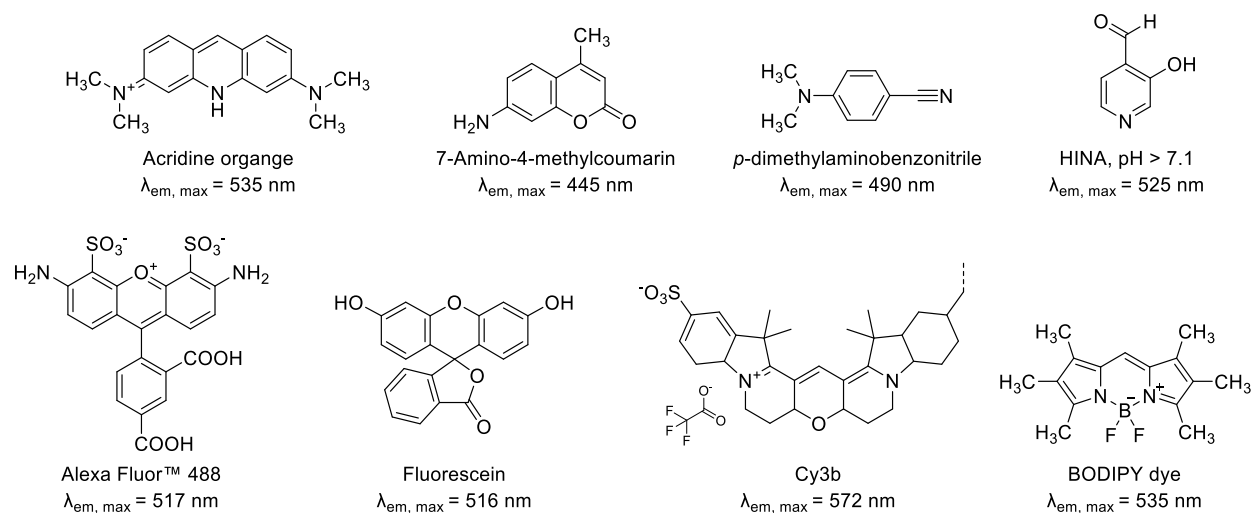


Figure 14. Dyes currently used for green emissions; the peak of the emission maximum ($\lambda_{em, max}$).¹⁰⁰⁻¹⁰⁴

There is still a constant need for improved organic fluorescent dyes, specifically fluorophores that emit in the red to the near-infrared region, which can be used for improved biomedical imaging (Figure 14).¹⁰⁵ Moreover, there is a constant need for fluorophores with tunable emission wavelengths. Therefore, synthetic efforts carried out in this work on HINA derivatives can contribute to this demand.

2 Objective

Within this thesis, two pyridine-based objectives should be investigated. On the one hand, there is a constant demand for new functional materials, which requires the development of new building blocks for material sciences. With this in mind, non-centrosymmetric 4,4'-bipyridines were synthesized to construct frameworks. On the other hand, pyridine-based isonicotinic acid (HINA) derivatives have strong green fluorescence properties. It is aimed to red-shift the emission properties by synthesizing different fluorinated HINA isomers.

4,4'-Bipyridine constitutes a rigid ditopic linker molecule, which is widely used in the construction of MOFs and SURMOFs, as well as in other supramolecular networks. However, commercially available unsubstituted bipyridine is typically used. To create functional materials, the intrinsic properties of the components can be designed and combined to create metamaterials. For this purpose, non-centrosymmetric 4,4'-bipyridines for the construction of frameworks should be synthesized (Figure 15, left, middle).

The scaffolds must meet certain requirements to be effective. The addition of push- and/or pull-substituents on the different pyridine rings creates a dipole moment, which allows for the directed self-assembly of SURMOF materials. Additionally, using photo-cleavable protection groups to control the growth of SURMOFs could make them 3D-printable. The use of photocleavable protection groups that exert a steric hindrance on one coordinating nitrogen of the bipyridine should also be investigated. To facilitate the synthesis of the scaffolds, well-known protecting groups from peptide chemistry should be used.

This work is part of the "3D Matter Made to Order" program of the Cluster of Excellence of Karlsruhe Institute of Technology (KIT) and Heidelberg University. In addition, strong cooperation with PROF. CHRISTOF WÖLL (Institute of Functional Interfaces, IFG) ensures the preparation and characterization of SURMOFs.

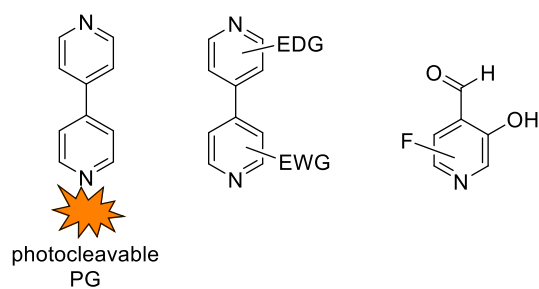


Figure 15. Main building blocks for preparing SURMOFs (left, middle) and fluorinated HINA derivatives (right).

In the second part of this work, three fluorinated HINA isomers should be prepared (Figure 15, right). These small electron-deficient heterocycles should be investigated and characterized in cooperation with DR. FRANK BIEDERMANN (Institute of Nanotechnology, INT), who will make the photophysical characterizations. The main objective is to obtain red-shifted fluorophores.

3 Main Section

The main section of this thesis is organized into several chapters. It starts with synthesizing non-centrosymmetric 4,4'-bipyridines, their characterization, and their application in materials. Subsequently, the synthesis of fluorinated HINA derivatives is reported, and the photophysical properties will be discussed.

3.1 Non-centrosymmetric 4,4'-Bipyridines for Materials Science

This part focuses on the preparation of non-centrosymmetric SURMOF structures, beginning with the synthesis of the linkers and possible protection strategies, and finally describes the synthesis and characterization of SURMOFs with the beforehand synthesized linkers.

3.1.1 Synthesis of Non-centrosymmetric 4,4'-Bipyridines

The LBL synthesis of the SURMOF-2 structure, which is used to prepare the thin films, relies on linear ditopic linkers. To synthesize them in a non-centrosymmetric fashion, the cross-coupling strategy was chosen. In the following subchapters, the synthesis strategy, relevant preliminary work, and the own results will be discussed.

Parts of the following chapter have been published in ChemPlusChem (WILEY-VCH): "Synthesis of Non-centrosymmetric Dipolar 4,4'-Bipyridines: Molecular Tectons for Programmed Assembly of Supramolecular Systems" by KÜHNER *et al.*, in which the synthesis and characterization of non-centrosymmetric 4,4'-bipyridines was presented.¹⁰⁶

3.1.1.1 General Synthesis Strategy - Cross-coupling of 4,4'-Bipyridines

For the C-C coupling between the two pyridine heterocycles, the SUZUKI-MIYAUURA cross-coupling was chosen to prepare various bipyridines. This palladium-catalyzed cross-coupling reaction between an organoboron compound (such as organoboronic acid, organoborane, organoboronate ester, or trifluoroborates) and a halide or pseudohalide was awarded the Nobel laureate to A. SUZUKI, in 2010, along with R. HECK and E. NEGISHI, who also

made important contributions to the field.¹⁰⁷ The reaction is known for its excellent regio- and chemoselectivity and typically proceeds under mild conditions, using less toxic boronic acids compared to similar coupling reactions that use organotin or organozinc reactants. The broad scope and ease of scalability and workup procedures have made this coupling popular and one of organic chemistry's most frequently used reactions. SUZUKI and MIYAURA first described the cross-coupling in 1986.¹⁰⁸ Similar to other cross-coupling reactions; this reaction typically involves an oxidative addition, transmetalation with the boron component, and reductive elimination to yield the cross-coupling product and the metal complex for further use in the subsequent catalytic cycle (Figure 16).¹⁰⁹⁻¹¹²

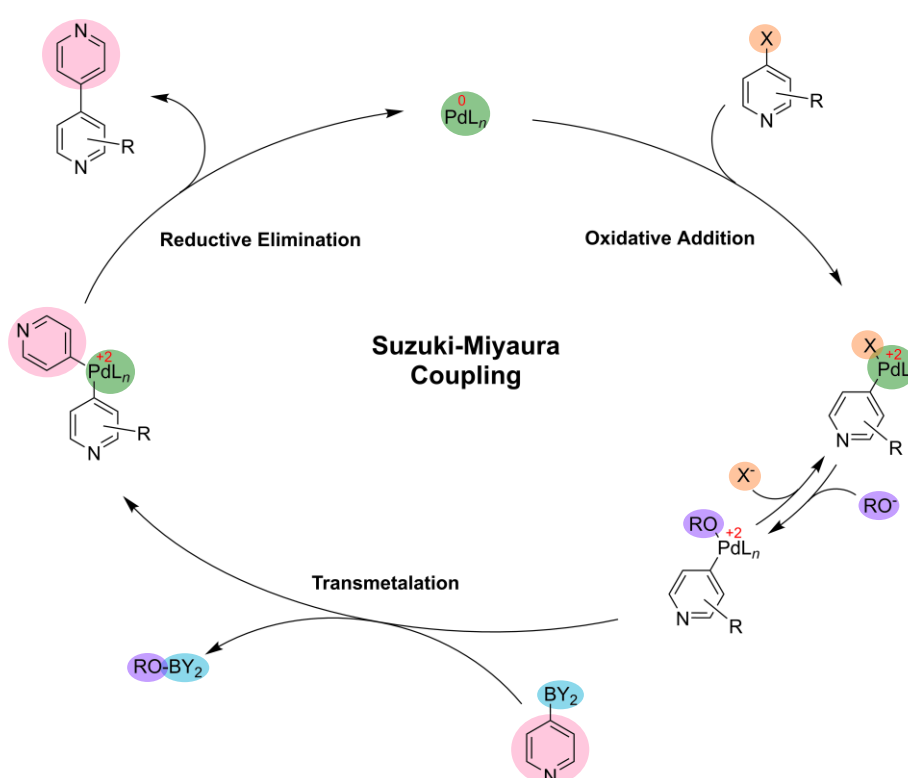


Figure 16. Palladacycle of the SUZUKI-MIYAURA cross-coupling. It undergoes oxidative addition, transmetalation, and reductive elimination before the palladium species can react again.

3.1.1.2 Preliminary Work on the Synthesis of Non-centrosymmetric 4,4'-Bipyridines

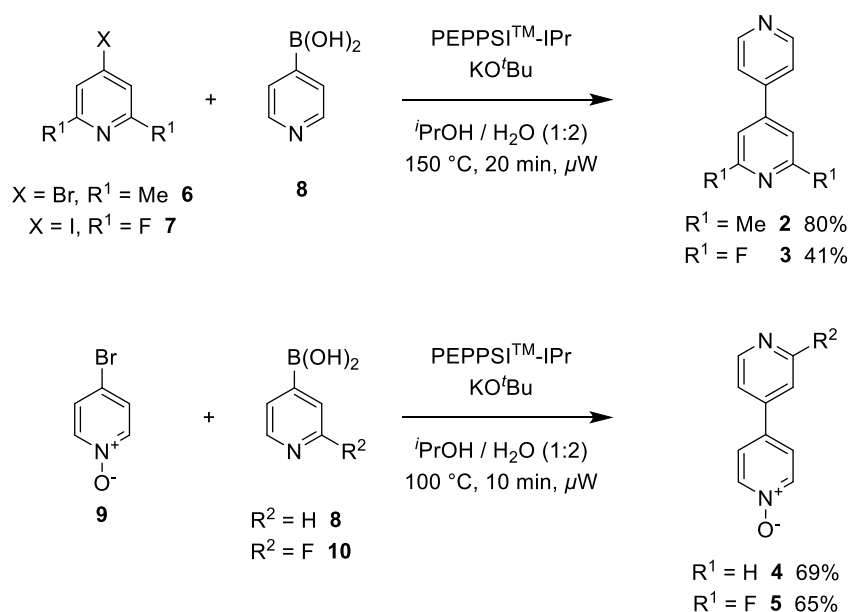
The synthesis of centrosymmetric 4,4'-bipyridines by homocoupling of pyridines is the most popular strategy to synthesize bipyridines for materials chemistry. However, a more determined strategy is needed to create a net dipole moment in the compounds.

Recently, GROSJEAN *et al.* showed that the bipyridine linker could vary in length by placing one to five benzene-based structures between pyridyl residues, using stepwise SUZUKI-MIYAJURA cross-coupling reactions to synthesize them.¹¹³ However, the molecules were centrosymmetric and contained benzene spacer groups between the pyridyl residues.

In 2015, OHMURA *et al.* published, to the best of the authors' knowledge, the only synthesis paper of non-centrosymmetric 4,4'-bipyridines using SUZUKI-MIYAJURA cross-coupling reactions.¹¹⁴ Non-centrosymmetric 4,4'-bipyridines were synthesized by them using Pd(OAc)₂ or Pd₂(dba)₃•CHCl₃ catalysts. Ligands such as PPh₃ or PCy₃ and potassium bases such as K₂CO₃ or potassium phosphate were used in the synthesis. The yields ranged from 34% to 74%, except for 2-methyl-4,4'-bipyridine (**1**), which had a very good yield of 91%.¹¹⁴

Further work was done in my own master's thesis, in which the successful synthesis of four non-centrosymmetric 4,4'-bipyridines, namely 2,6-dimethyl-4,4'-bipyridine (**2**), 2,6-difluoro-4,4'-bipyridine (**3**), as well as the two *N*-oxide containing 4,4'-bipyridines **4** and **5** were reported (Scheme 2).¹⁵ In contrast to the conditions used by OHMURA *et al.*, the reactions were conducted in a microwave reactor under pressure at elevated temperatures. Iodine or bromine-substituted pyridines **6** and **7** were reacted with 4-pyridylboronic acid (**8**), and for the *N*-oxides, 4-bromopyridine-*N*-oxide (**9**) and respective boronic acids **8** and **10** were used. The strong potassium base KO^tBu and the PEPPSITM-catalyst, based on an *N*-heterocyclic carbene (NHC) ligand, were also used. These harsh conditions enabled the synthesis of bipyridines with the *N*-oxide functional group.

Own Master's thesis:



Scheme 2. Non-centrosymmetric 4,4'-bipyridines that were prepared during my own master's thesis.¹⁵ A NHC-based PEPPSITM-catalyst was used in a microwave reaction.

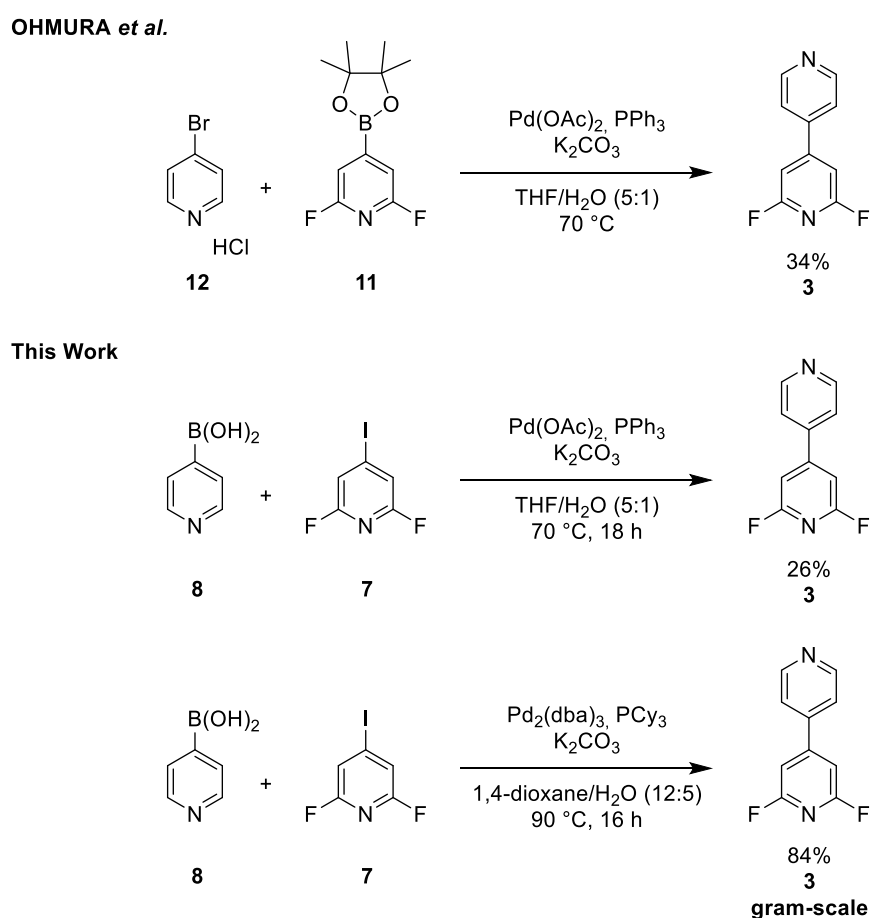
In this work, the conditions reported were used as the foundation for further optimizations of the conditions. The synthesis strategy and scope will be discussed in the following chapter.

3.1.1.3 Scope of Non-centrosymmetric 4,4'-Bipyridines

For the preparation and method development of new materials, larger amounts in the range of 100-1000 mg were needed, and efficient conditions for the linker synthesis had to be found. Moreover, for the SURMOF preparation, it was necessary to deliver a broad range of different bipyridines. Electron withdrawing and donating groups should be attached to one of the pyridine components to install a net dipole moment. Additionally, steric hindrance can play an important role during the coordination of a linker to a metal in a SURMOF. Therefore, functional groups should be attached to the 2- and/or 6-positions adjacent to the pyridyl nitrogen, and to the 3- and/or 5-positions. For fine-tuning or maximization of the dipole moment in a non-centrosymmetric 4,4'-bipyridine, push-/pull-bipyridines with electron donating and withdrawing groups on opposite pyridyls should be synthesized. Lastly, the synthesis of bipyridines with added functionality should be tried. These involved

the installation of an azo-functionality and the synthesis of an alkene-containing linker and a photocleavable linker.

Generally, electron-deficient substrates such as fluorinated aryls react poorly in the SUZUKI-MIYaura coupling, regardless of whether the electrophilic or the nucleophilic component is fluorinated.¹¹⁵ Because pyridine is an electron-deficient heterocycle (as mentioned in chapter 1.1), reactions involving pyridine give lower yields when compared to benzene derivatives. Because 2,6-difluoro-4,4'-bipyridine (**3**) could not be synthesized in good yields due to the electron withdrawing fluorine substituents, it was an ideal target for optimization.



Scheme 3. Improvements in the synthesis of 2,6-difluoro-4,4'-bipyridine (**3**).

A coupling reaction of 2,6-difluoro-4-iodopyridine (**7**) with unsubstituted 4-pyridylboronic acid (**8**) using Pd(OAc)₂, PPh₃ and K₂CO₃ carried out in a tetrahydrofuran/water mixture (5:1) at 70 °C only gave a poor yield of 26%. Protodeboronation of the boronic acid may have played a role, as unsubstituted pyridine was obtained after purification. OHMURA *et al.*

published a 34% yield for compound **3**. However, they used the fluorinated boronic ester **11** and an unsubstituted 4-bromopyridine **12** as the HCl salt. The conditions significantly improved in comparison with the literature and own previous experiments when Pd₂(dba)₃•CHCl₃ was used together with PCy₃ and potassium phosphate at an elevated temperature of 90 °C in a 1,4-dioxane/water (12:5) mixture, resulting in a very good yield of 84% when **3** was prepared on a gram-scale (Scheme 3).

Following these results, a library of non-centrosymmetric 4,4'-bipyridines was prepared (Figure 17). The yield of the fluorinated compounds **3**, **13**, and **14** was always lower than the yield of the methylated compounds **1**, **2**, and **15**, which were obtained in near-quantitative yields of >95%. No significant differences between organoboron functional groups were observed when boronic acids and boronic esters were used. The chlorinated bipyridines **16** and **17** were obtained in slightly lower yields than the other derivatives, which may be due to the larger atom radius of chlorine, especially in the synthesis of 3,5-dichloro-4,4'-bipyridine (**17**), where a steric hindrance of the halopyridine could impede oxidative addition during the cross-coupling.

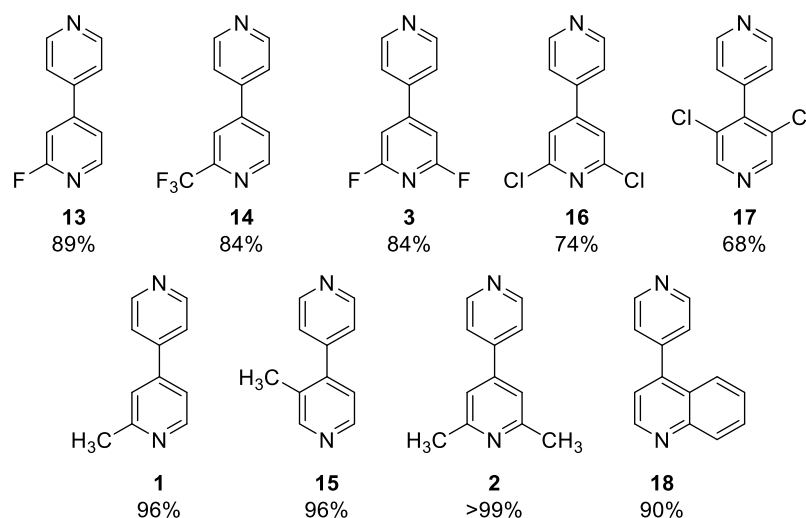
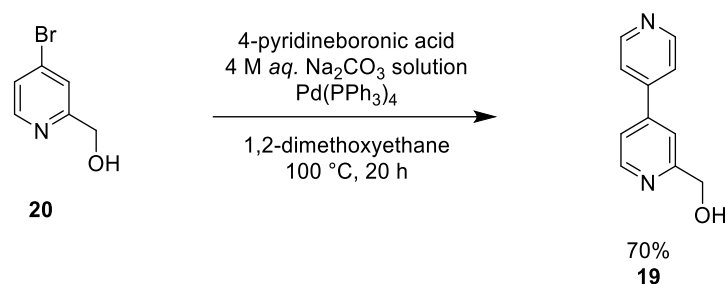


Figure 17. Scope of non-centrosymmetric bipyridines that were prepared following the improved conditions. For further details see the experimental section.

Overall, it was possible to introduce fluorine substituents on the 2- and 6- positions. Couplings with 3- and 5-fluorinated pyridines were unsuccessful. The trifluoromethyl group of **14** exhibits an electron withdrawing effect that is intermediate between fluorine and chlorine substituents. To study the steric effects of substituents, **16** and **17** with chlorine atoms at the 2,6- and 3,5-positions and **1** and **15** with methyl groups at the 2- and 3-position,

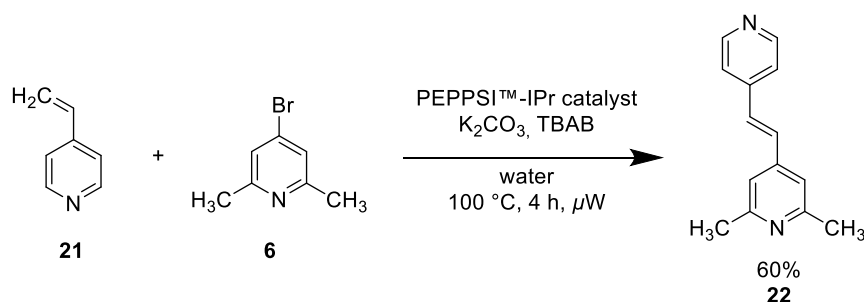
respectively, were synthesized. A linker with two electron donating groups, the dimethyl bipyridine **2**, and a naphthalene-containing linker **18** were successfully prepared. All efforts in synthesizing a push-/pull 4,4'-bipyridine with a methylated and a fluorinated pyridine ring were unsuccessful. In summary, a diverse set of novel non-centrosymmetric linkers could be synthesized in good to excellent yields. Next, added functionality should be implemented, starting with synthesizing a linker for a photocleavable bipyridine-protecting group (PG) conjugate.

For the attachment of PGs to a 4,4'-bipyridine, the synthesis of 2-methanol-4,4'-bipyridine (**19**) was carried out *via* cross-coupling conditions using an aqueous sodium carbonate solution and 1,2-dimethoxyethane as solvent system. The use of any additional phosphine ligands was redundant, and **19** could be synthesized in 70% yield from 2-methanol-4-bromopyridine (**20**) (Scheme 4). The methanol functional group in the 2-position will become useful in the attachment of protecting groups. Attempts to attach a protecting group directly to a 2-OH position were not conducted due to the 2-hydroxypyridine/2-pyridone tautomerism.¹¹⁶



Scheme 4. The synthesis of **19** from (4-bromopyridin-2-yl)methanol (**20**) was achieved in 70% yield.

SURMOFs could be post-synthetically modified *via* a [2+2] cycloaddition reaction if the linker bears a vinyl group. With an alkene, the linkers of a supramolecular network could be cross-linked in place upon irradiation with UV light. To synthesize such a linker, a HECK reaction of 4-bromo-2,6-dimethylpyridine (**6**) and 4-vinyl pyridine (**21**) was carried out using the PEPPSI™-IPr catalyst and tetra-*n*-butyl ammonium bromide (TBAB) as an additive. Literature indicated that this additive could improve the efficiency of the reaction.^{117, 118} The reaction was done in water in the microwave reactor following a procedure of BORAH *et al.*. After purification, the alkene **22** could be obtained in a yield of 60% (Scheme 5).¹¹⁹



Scheme 5. Synthesis of the non-centrosymmetric alkene-containing linker **22** using the HECK reaction.

3.1.1.4 Photoswitchable Azo-benzene Containing Non-centrosymmetric Linkers

The azobenzene functional group can alter its *cis/trans* isomeric structure upon irradiation with light of a suitable wavelength (Figure 18, a)). It is one of the most prominent photoswitchable groups applied in biology or materials chemistry. The potential of the azobenzene group was demonstrated by YU *et al.*, who used azobenzene dipyritylbenzene (AzoBiPyB) **23** in two different SURMOF structures (Figure 18, b) and c)). HEINKE *et al.* used azobenzene-containing compounds with BPDC-based linkers in a SURMOF to release 1,4-butanediol (BD) upon radiation with light.¹²⁰ They prepared 50 SURMOF layers with unfunctionalized BPDC as a base structure and grew 45 azobenzene-containing layers on top. The SURMOF was irradiated with appropriate light sources to trigger the azobenzene into the *cis* or *trans* form, which corresponds to an open or closed state. Afterward, the BD uptake was monitored using a quartz crystal microbalance (QCM), and it was found that the uptake of BD was 15 times faster when the top layer was in an open state compared to the closed state.

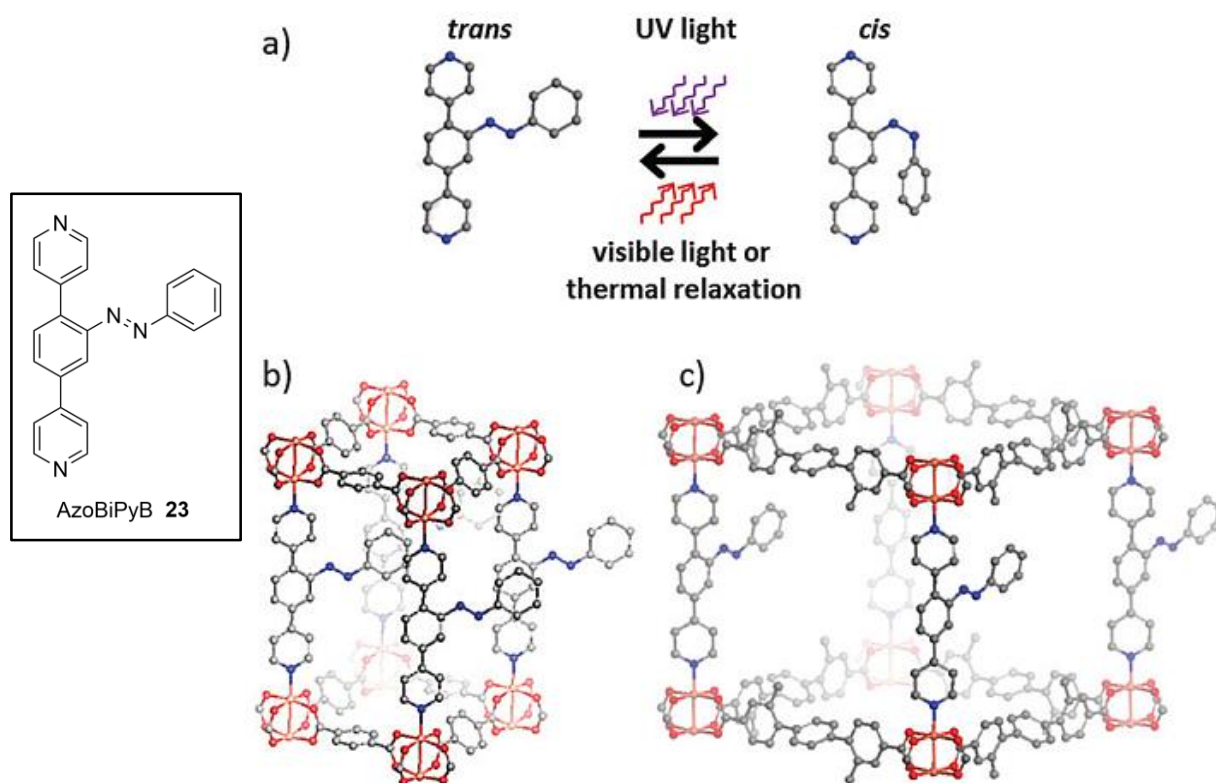
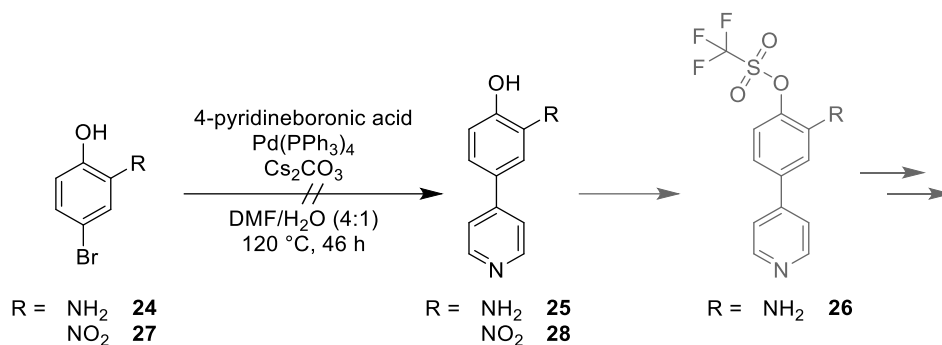


Figure 18. a) Structure of the *trans*- and *cis*-isomers of AzoBiPyB **23**. The configuration changes upon irradiation with a suitable light source; b) pillar-layered MOF structure of Cu₂(BDC)₂(AzoBiPyB); c) pillar-layered MOF structure of Cu₂(DMTPDC)₂(AzoBiPyB), reproduced from ref. [121] with permission from the PCCP Owner Societies.

To further explore the potential of these photo-triggered SURMOFs, the synthesis of non-centrosymmetric 4,4'-bipyridine-based linkers was planned. AzoBiPyB **23** is easily accessible *via* a double C-C cross-coupling to install the pyridine rings for coordination, but it has a few drawbacks. Firstly, it is longer than the small and rigid 4,4'-bipyridine structure, and secondly, it has no predefined orientation for implementation into the SURMOF, which might result in the azobenzene rings moving in opposite directions when shifting from the closed to the open state. The usage of non-centrosymmetric-based linkers could circumvent this issue since the orientation of linkers in the material could be controlled.

The synthesis of non-centrosymmetric dipyriddylenes was started with 2-amino-4-bromophenol (**24**). This starting material should enable a cross-coupling with a first pyridine moiety before the alcohol functional group of **25** could be converted to the triflate **26**, a pseudohalide that could subsequently be used as an electrophile in a second cross-coupling reaction.

However, the first C-C coupling reaction with unsubstituted 4-pyridylboronic acid (**8**) was unsuccessful; switching the starting material from the amine **24** to 2-nitro-4-bromophenol (**27**) did not give any product **28** (Scheme 6). The reasons for this failure may include unsuitable or harsh conditions, or the intolerance of the alcohol and nitrogen functional groups.

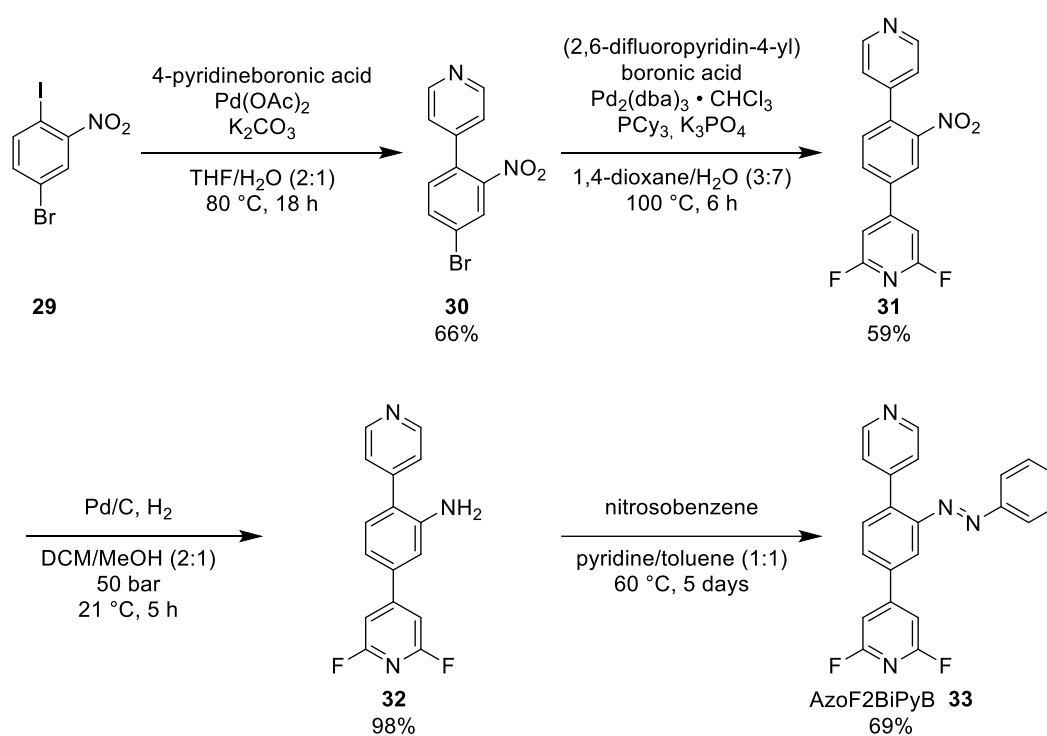


Scheme 6. Attempted synthesis of aryl triflate for second cross-coupling reaction.

Halogenides used in the SUZUKI-MIYAJURA cross-coupling can vary in reactivity. The oxidative addition is often the rate-determining step. The reactivity of the halogenide is influenced by the halogenide substituent and generally decreases in the following order: I > OTf > Br > Cl.¹¹⁶

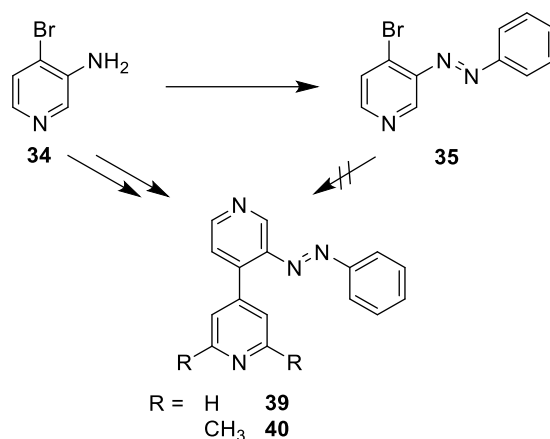
Instead of transforming the alcohol into a pseudohalogenide after the first cross-coupling, it was attempted to use halogens' different reactivity to address only one of two possible binding sites selectively. The synthesis was based on the commercially available 4-bromo-1-iodo-2-nitrobenzene (**29**), and the initial cross-coupling with 4-pyridylboronic acid (**8**) gave **30** in a yield of 66%. Conditions were mild, as it was tried to address the iodine position to react selectively. Mass spectrometry only showed the ion peaks $[\text{M} (^{81}\text{Br})]^+$ at m/z 280 and $[\text{M} (^{79}\text{Br})]^+$ at m/z 278 with the characteristic bromine pattern. Furthermore, the mass of the iodine-containing side product with m/z 326 was not observed. In a subsequent cross-coupling with the resulting bromine to reach the final bipyridinephenyl linker, the temperature was increased to 100 °C, as no conversion was observed at 80 °C, and finally **31** could be obtained in a good yield of 59% considering the deactivation of starting materials. The yield of the amine **32** was almost quantitative (98%) after reducing **31** in a pressure reactor with hydrogen at a pressure of 50 bar. The final azo coupling reaction was based on the BAEYER-MILLS reaction (or MILLS reaction) between aniline and a nitroso aryl, which was

discovered in the late 18th century.^{122, 123} Instead of acetic acid as part of the solvent system, which did not yield the desired molecule, pyridine and toluene were used. Finally, the AzoF2BiPyB linker **33** was successfully obtained in a yield of 69%, or 26%, over all four steps (Scheme 7).



Scheme 7. Synthesis of the AzoF2BiPyB **33** in four steps based on the starting material 4-bromo-1-iodo-2-nitrobenzene (**29**).

Two different approaches were tried in synthesizing short azobenzene-containing 4,4'-bipyridines. In the first approach, the MILLS reaction was conducted first, followed by the completion of the bipyridine in the subsequent step. The cross-coupling was conducted first in the second approach, followed by the azo coupling (Scheme 8).



Scheme 8. Two different strategies towards the AzoBiPys **39** and **40** were conducted.

The azo coupling of 4-bromo-3-aminopyridine (**34**) proved difficult, and under standard conditions with an acetic acid/toluene (1:1) solvent mixture, the product could not be detected *via* HPLC after three days. Instead, a MILLS reaction with tetramethylammonium hydroxide in pyridine was successful, but **35** was only obtained in a yield of 8%. Nevertheless, **35** was cross-coupled with 4-pyridylboronic acid (**8**), and the formation of a new species was monitored *via* TLC. However, due to the azo group, which might have changed its constitution during flash-column chromatography, the purification failed, and this synthesis strategy was not pursued further.

An initial cross-coupling of 4-bromo-3-aminopyridine (**34**) with similar conditions to those that were applied in the synthesis of AzoF2BiPyB **33**, using $\text{Pd}_2(\text{dba})_3 \cdot \text{CHCl}_3$ and tricyclohexyl phosphine as the catalytic system, gave 3-amino-4,4'-bipyridine (**36**) in a fair yield of 54%.

For the cross-coupling to get the methylated amine **37**, the respective boronic ester **38** had to be synthesized first. This MIYAUURA reaction was done with 4-bromo-2,6-dimethylpyridine (**6**), bis(pinacolato)diboron (B_2pin_2), $\text{Pd}(\text{OAc})_2$, PCy_3 and KOAc at 110 °C in 1,4-dioxane. After 18 hours, the reaction was finished, indicated by TLC, and the crude was filtered through a plug of Celite. Flash-column chromatography was unsuccessful in purifying the boronic ester **38**. Instead, it was noticed that the solid crystallized on the side of the round-bottom flask, indicating sublimation. As the sublimation took place at 21 °C, a sublimation apparatus had to be connected to a flow cooler, cooling an ethylene glycol/water

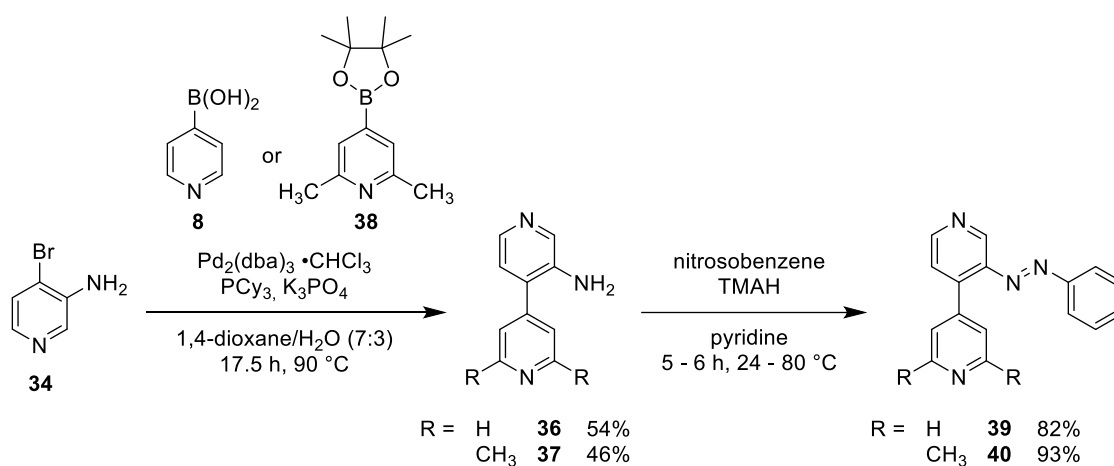
mixture to -10°C . By lowering the pressure using a vacuum pump, **38** could be obtained in a 64% yield as a colorless solid (Figure 19).



Figure 19. Sublimation of crude **38** in a sublimation apparatus under reduced pressure. The blue liquid is the cooling mixture being pumped through the apparatus.

The subsequent cross-coupling of **38** with 4-bromo-3-aminopyridine (**34**) gave **37** in a yield of 46%, slightly lower than for the coupling of unsubstituted **36**.

Surprisingly, in contrast to the preceding MILLS reaction on a pyridine, the azo couplings proceeded in very good yields of 82% and 93% for **39**, respectively, **40** after only a few hours of reaction time (Scheme 9).



Scheme 9. Synthesis AzoBiPy **39** and AzoMe₂BiPy **40** in two steps.

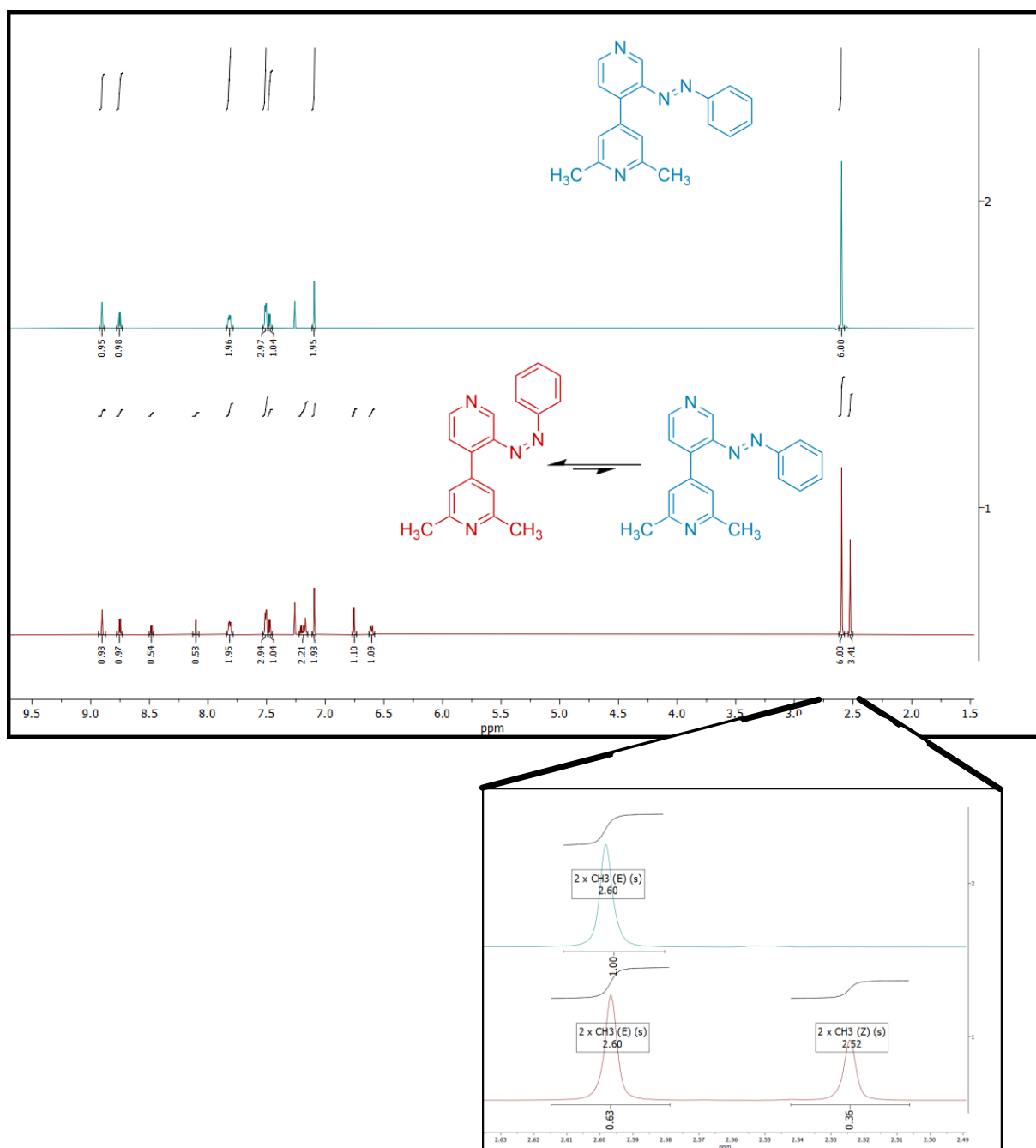


Figure 20. The azobenzene-containing linker AzoMe2BiPy **40** was investigated by ^1H NMR. The E -isomer (top) refers to the dark state. The PSS could be determined after irradiation with light at $\lambda = 365$ nm for 30 minutes, where a mixture of E - and Z -isomer was observed (bottom).

AzoMe2BiPy **40** was further characterized to verify its sensitivity to light. A 42 mM solution of **40** in deuterated methanol was prepared and measured using ^1H NMR. The sample was irradiated with a 10W LED light source at a wavelength of $\lambda = 365$ nm for 30, 60, 90, and 120 minutes and the measurements were taken again. Additionally, the dark state was

measured for comparison. The spectra showed new peaks which could be assigned to the *Z*-isomer of **40**, as evidenced by the shift of the CH_3 singlet at $\delta_{CH_3, Z\text{-isomer}} = 2.52$ ppm to the singlet of the *E*-isomer at $\delta_{CH_3, E\text{-isomer}} = 2.60$ ppm (Figure 20). The photo steady state (PSS) was reached after 30 minutes, as determined by the lack of significant change in the *Z*-/*E*-ratio as determined by the integration of the methyl peaks. The PSS for **40** was determined to be 63% of the *E*-isomer when irradiated at $\lambda = 365$ nm in deuterated methanol. The switching was also confirmed by HPLC analysis. A 0.50 mM solution of **40** in ACN reached the PSS after about 5 minutes upon irradiation (Figure 21). A slow thermal back-reaction to the *E*-isomer could be observed over time by the gently sloping curve due to the experimental setup. The samples were irradiated for different time intervals and then measured by HPLC. Because the measurements took about 25 minutes each, the sample taken after 30 minutes was standing in the vial holder of the HPLC for about five hours, during which some of the *Z*-isomers had already thermally switched back.

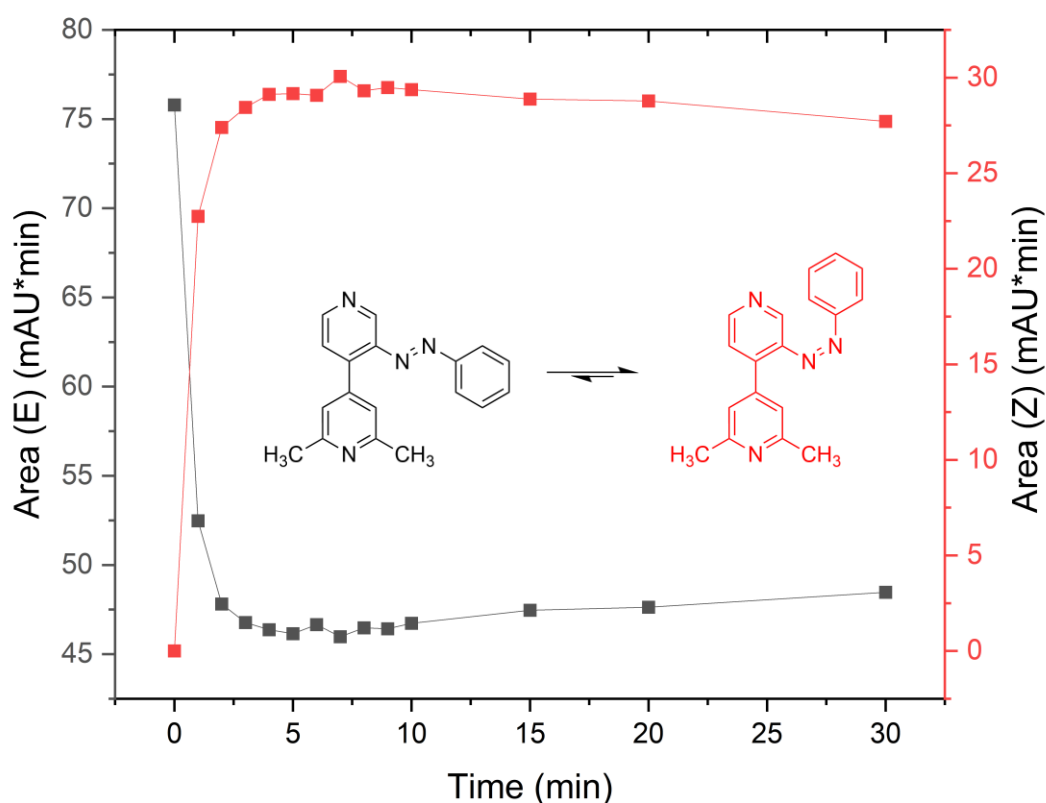


Figure 21. Diagram of the peak area corresponding to the *E*- and *Z*-isomer of **40** analyzed by HPLC after the samples were irradiated for different time intervals.

UV/vis spectra of **40** show the characteristic decrease in the absorption of the maximum of the PSS state compared to the dark state. The strong absorption in the dark state (*trans*-configuration) around $\lambda = 328$ nm results from $\pi \rightarrow \pi^*$ transitions. The *cis*-isomers of the PSS state absorb more light at the local maximum of $\lambda = 436$ nm due to $n \rightarrow \pi^*$ transitions (Figure 22).

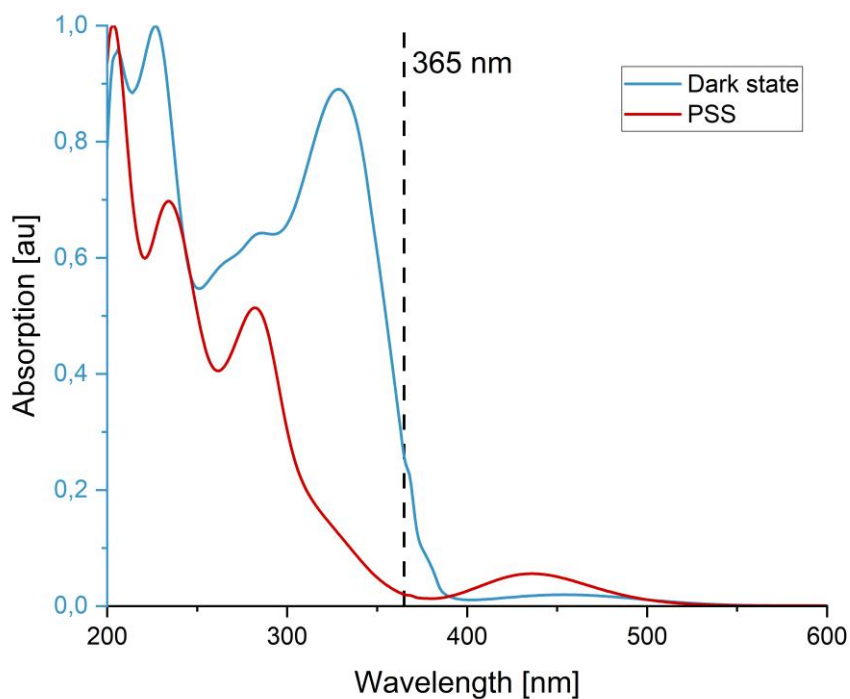


Figure 22. UV/vis-spectra of **40** in the dark state and PSS. The absorption was normalized. The wavelength of 365 nm is shown as a vertical straight line in the spectra.

3.1.1.5 Protection Strategy and Synthesis of SURMOF Linkers

To synthesize SHG SURMOF networks, non-centrosymmetric 4,4'-bipyridines must be constituted to enable a controlled material self-assembly. As the 4,4'-bipyridine is linear and ditopic, modifying it to favor the coordination of one nitrogen and/or making the coordination of one nitrogen more difficult would result in a predefined orientation during SURMOF growth under suitable conditions. This principle is explained in Figure 23, where the bipyridine should coordinate first on the green side. Therefore, all pyridine rings with the residue "X" would be facing toward the direction of the origin of the material.

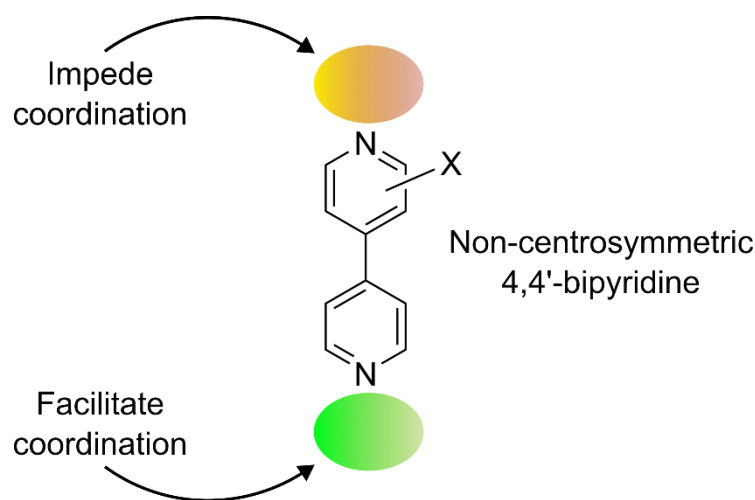


Figure 23. Schematic drawing of a non-centrosymmetric linker that can coordinate in principle on both nitrogen atoms. Techniques must be modified to facilitate coordination (green) on one side and/or impede coordination on the other. Residue "X" can be any atom except hydrogen.

Different approaches could be considered to achieve the desired properties. A chemical protection/deprotection approach would be the most straightforward strategy. However, during SURMOF synthesis, many reagents may interfere with the coordination of the unprotected pyridine and/or destroy existing SURMOF layers. Pyridine nitrogen is not a common target for protection/deprotection methods, as this approach originated from amino acid synthesis, which does not naturally feature pyridine scaffolds. Therefore, protocols for the deprotection of directly *N*-attached protecting groups would have to be investigated. During my master's thesis, it was demonstrated that despite mild "SURMOF-friendly" deprotection protocols, SURMOF growth was disturbed.¹⁵ Since the SURMOFs were prepared LBL, any defects in the structure may affect the next layers and continue throughout the SURMOF synthesis. Containing many defects, the reproducibility and

properties of the SURMOF may change. Because the chemical protection/deprotection strategy for SURMOF growth showed these disadvantages, this approach was not further investigated in this thesis.

In contrast to chemical deprotection, photocleavable protecting groups can remove the protection group during SURMOF synthesis by irradiating it with light, eliminating the need for potentially interfering deprotection reagents. This not only saves chemicals and reduces the number of steps in the SURMOF synthesis process, but also can enable the 3D printing of SURMOFs by selectively deprotecting certain parts of one layer. Many designs for photocleavable protecting groups (PPGs) are available in organic synthesis. The PPG chosen must have an excitation wavelength outside the linker molecules' excitation range. As 4,4'-bipyridine absorbs light below around 280 nm, the PPG should have an excitation maximum above 320 nm. Therefore, coumarin-based PPGs **41** and **42**, as well as the 6-nitroveratryloxycarbonyl (NVOC, **43**) were used. **43** has an absorption maximum of around 350 nm in DMSO¹²⁴, whereas that of the methoxy-substituted coumarin **41** has an excitation maximum at 323 nm in EtOH¹²⁵ and the diethylamino-substituted coumarin **42** has an excitation maximum at 390 nm in water¹²⁶. These mentioned PPGs fit the requirements and should be attached to a 4,4'-bipyridine (Figure 24).

Photocleavable Protection Groups:

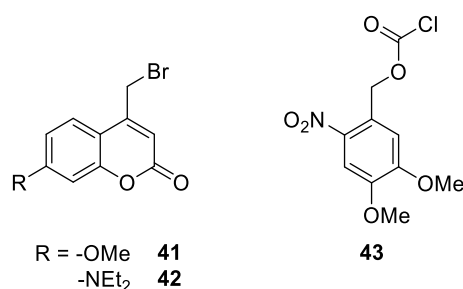
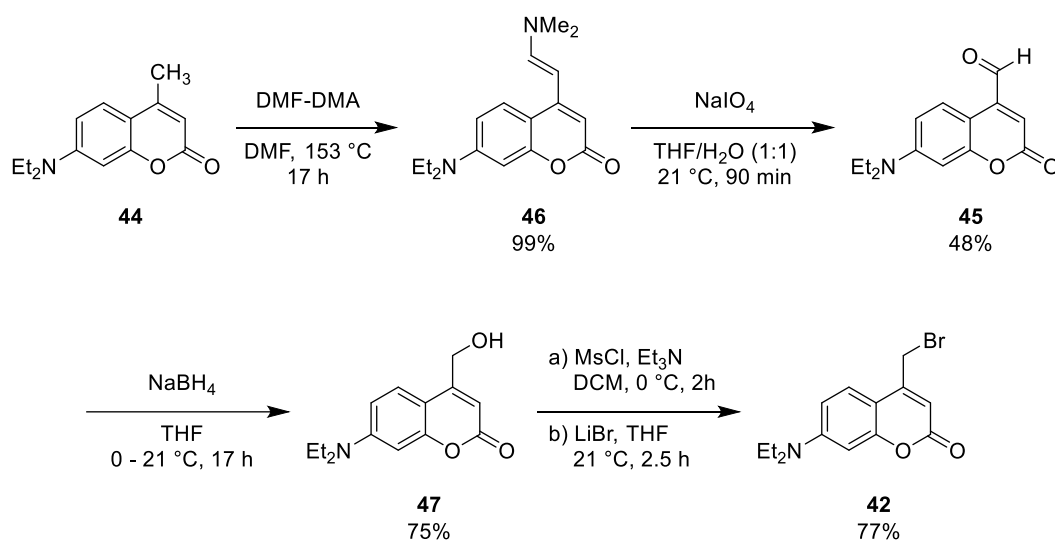


Figure 24. Suitable PPGs for the protection of the 4,4'-bipyridines: Coumarin PGs **41** and **42** and *ortho*-nitrobenzene-based NVOC-Cl **43**.

Methoxy coumarin **41** was readily available, while diethylamino coumarin **42** had to be prepared in four steps (Scheme 10). The synthesis was originally developed by SCHÖNLEBER *et al.*, who started the synthesis from commercially available **44**. Subsequently, they synthesized the aldehyde **45** using the Riley oxidation.¹²⁷ This step was tedious in purification, low yielding, and used very toxic selenium dioxide. WEINRICH *et al.* improved upon this synthesis by substituting the reaction with two consecutive steps.¹²⁸

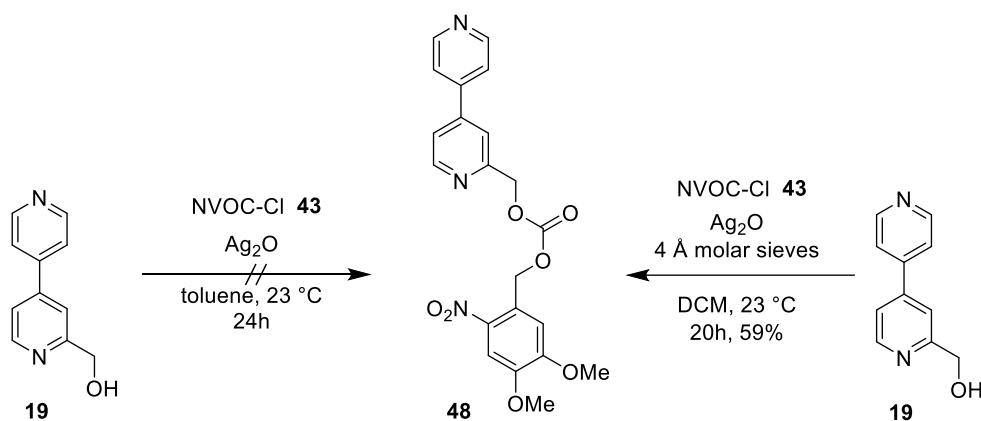
When the synthesis was carried out, the improved route *via* the enamine was chosen. The formylation was achieved through the construction of enamine **46** using DMF-DMA, and the enamine was then converted to aldehyde **45** through oxidative cleavage with sodium periodate. The yield over two steps was 48%, comparable to the yield obtained with selenium dioxide.¹²⁷ Reduction to the alcohol **47** and subsequent bromination gave coumarin **42**.



Scheme 10. Synthesis of diethylamino substituted coumarin PG **42** in four steps after a procedure of WEINRICH *et al.*¹²⁸

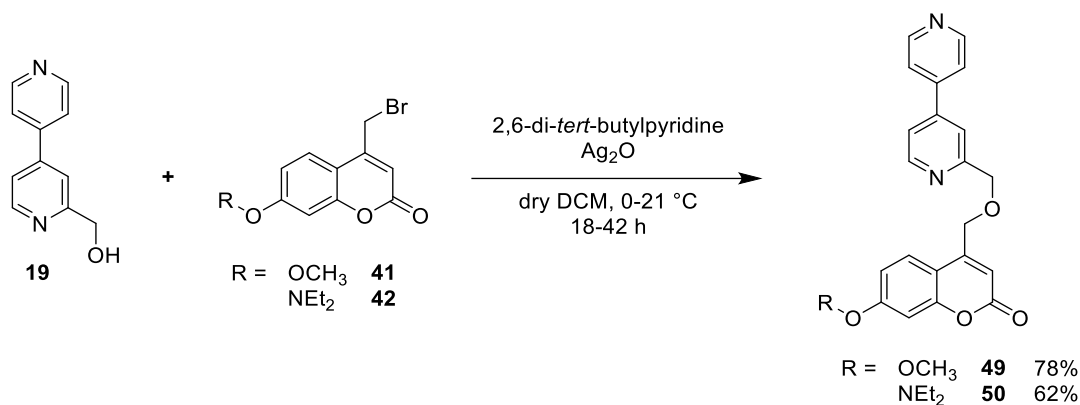
The synthesis of 2-methanol-4,4'-bipyridine **19** and the preparation of the PPGs **41-43** were successful. Next, the addition of the PPGs to the bipyridine was tried to get the desired PPG-bipyridine conjugates.

The reaction of NVOCl **43** with bipyridine alcohol **19** in dry toluene did not yield the desired product. However, when the same reaction was conducted in dry dichloromethane with the addition of 4 Å molar sieves, the final PPG linker **48** could be obtained in a good yield of 59% (Scheme 11).



Scheme 11. Synthesis of NVOC-bipyridine conjugate **48**.

Coupling of the coumarin PGs went smoothly under the same conditions but with an additional 3.00 equiv of 2,6-di-*tert*-butylpyridine and yielded OMe-coumarin-bipyridine conjugate **49** and NEt₂-coumarin-bipyridine conjugate **50** in good yields of 78%, respectively 62% (Scheme 12). The steric base was added to minimize coordination of the silver salt to the bipyridine's nitrogen.



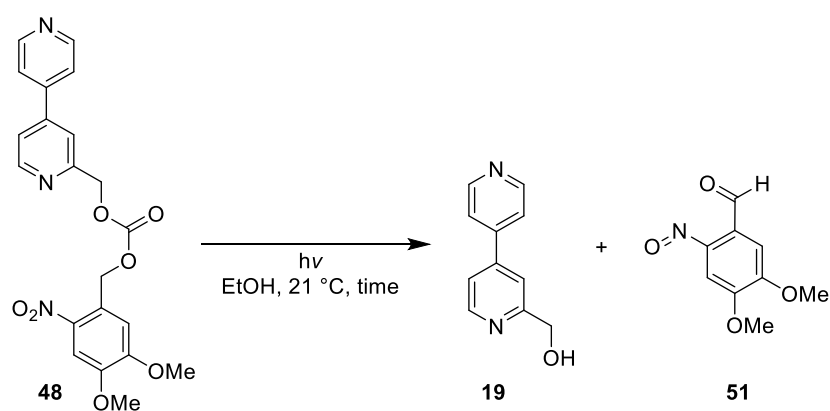
Scheme 12. Coumarin-bipyridine conjugates **49** and **50** were synthesized with the addition of 2,6-di-*tert*-butylpyridine.

The linker components have been successfully prepared at this point in the project. The next steps include the investigation of the cleavage reaction in the solution. After the deprotection conditions are sufficiently analyzed, SURMOF thin films can be prepared.

3.1.1.6 Photocleavage of PPG-bipyridine Conjugates

This chapter discusses the deprotection reaction of previously synthesized photocleavable bipyridine linkers in solution. The measurements were partly carried out by BENEDIKT SAPOTTA (AG WÖLL, IFG). The results are left for publication in this thesis and presented as an excerpt in this work (Figure 27).

Before SURMOF materials could be tested with the photocleavable linkers, the general deprotection upon irradiation with a suitable light source was tested. The photocleavage of the NVOC linker **48** was investigated first *via* HPLC chromatography and UV/vis absorption spectroscopy.



Scheme 13. The photocleavage reaction of the NVOC PG from **48**.

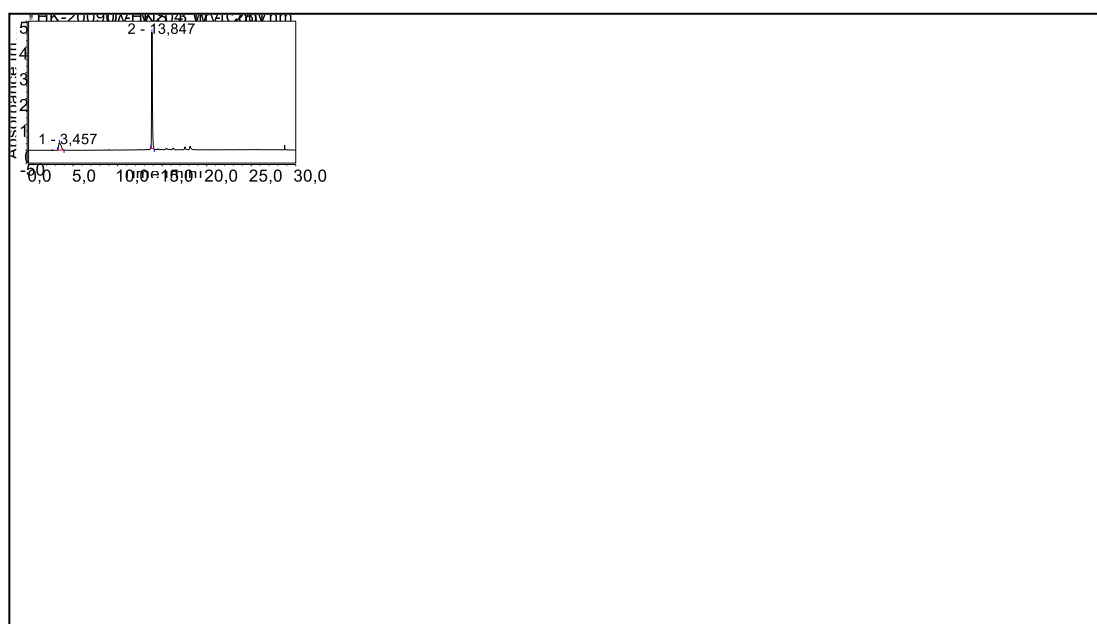


Figure 25. HPLC chromatogram of a mixture of **48** and **19**. The peak area at $t = 13.8$ min corresponds to **48**, and the peak at $t = 3.4$ min corresponds to 2-methanol-4,4'-bipyridine **19**.

For the HPLC analysis, **48** and **19** were analyzed separately to determine the retention time of the starting material and the expected 2-methanol- 4,4'-bipyridine **19** (Scheme 13 and Figure 25). The sample was dissolved in EtOH and irradiated with 4 × 8W LED light sources for defined time intervals, and an aliquot was taken after each period. It was then analyzed by HPLC, and the peak area corresponding to starting material and product was integrated and plotted in a diagram (Figure 26). It can be observed that while the integral of NVOC-bipyridine conjugate **48** vanishes, the integral of deprotected **19** increases, indicating that the photocleavage reaction proceeded successfully. To substantiate these findings, further UV/vis measurements of NVOC-bipyridine linker solution were carried out.

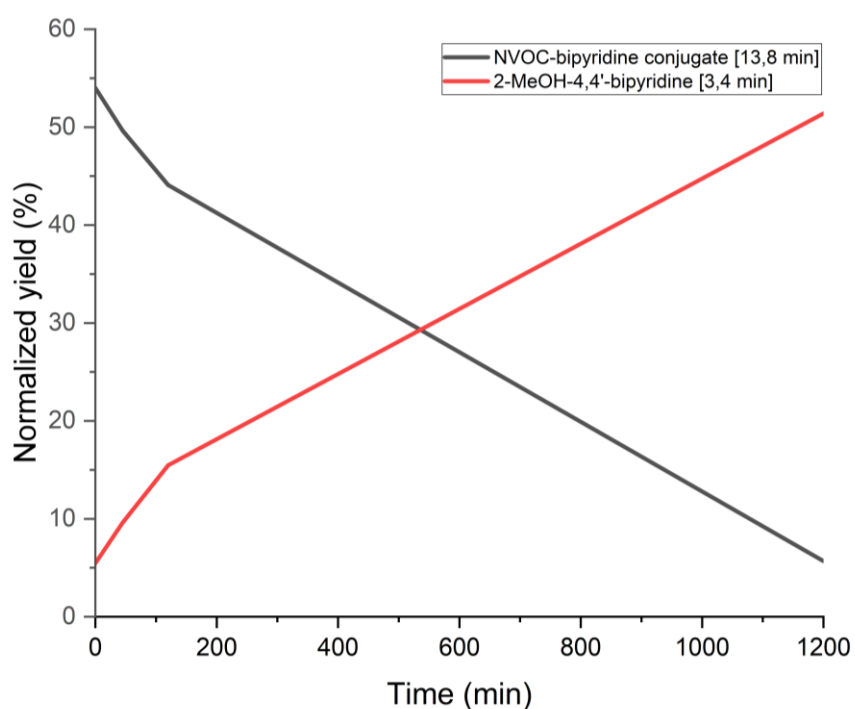


Figure 26. Deprotection of **48** was investigated by HPLC analysis after 0, 45, 120, and 1200 min. While the area of **48** decreased with time, the area of **19** increased roughly the same amount. The samples were irradiated with 4 × 8W LED light sources in a LUZCHEM photoreactor at $\lambda = 350$ nm.

The general experimental setup is shown in Figure 27, A); the ethanolic solution of **48** was irradiated with a light source whose power intensity could be ramped up to 50W. The light source was characterized by a peak wavelength of 368 nm at a corresponding full width at half maximum (FWHM) of 9 nm. Figure 27, B) depicts the UV/vis absorbance spectrum. The purple line shows the absorbance of the pristine linker **48** dissolved in ethanol. A maximum

absorption of around 345 nm could be observed, which correlates to that of the crude NVOC protecting group, which has a maximum absorption of around 350 nm in DMSO, referring to the literature.¹²⁴ The maximum of **48** completely vanished when irradiated for a few minutes, which indicates a decay of the photocleavable PG. The absorbance of nitroso side product **51** should weakly absorb around 410 nm and below 300 nm; however, because of unspecific absorption in this area, the formation could not be proven.¹²⁴

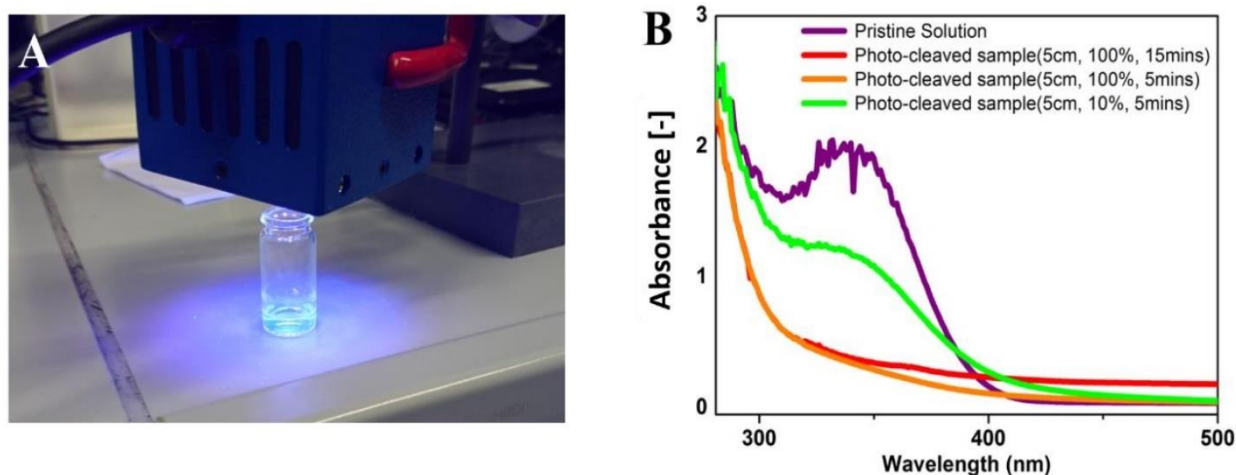


Figure 27. Photocleavage of NVOC-bipyridine linker **48** upon irradiation with 50W UV-A light of the wavelength $\lambda=365$ nm. A) general setup of photocleavage reaction, irradiation of the linker solution. B) UV absorbance of raw and irradiated linker solutions in ethanol. A power level of 10% corresponds to a flux density of roughly 10-20 mW/cm² received by the linker solution, which increases to 100% intensity corresponds to 100-200 mW/cm² at 100% power level.

In conclusion, successful photocleavage of the novel linker **48** was carried out and investigated, which is a prerequisite for the photochemical SURMOF deprotection. In the next chapters, this work focuses on the preparation and characterization of the bipyridine linkers.

3.1.2 SURMOF Preparation and Characterization

The synthesis and characterization of the individual linkers were shown in the previous chapters. The following chapter will discuss the preparation of SURMOFs with these linkers and the characterization of the network structures. It was divided into two sections; the first describes the SURMOF synthesis with photocleavable linkers, and the second is focused on SURMOFs with unprotected non-centrosymmetric bipyridine linkers.

3.1.2.1 SURMOF Preparation with PPG-linker Conjugate

This chapter discusses using previously prepared photocleavable bipyridine linkers (as described in Chapter 3.1.1.5) in synthesizing SURMOFs. I have been provided with unpublished data on QCM measurements of the photocleavable linker **48** by BENEDIKT SAPOTTA (AG WÖLL, IFG), which are included in this chapter to discuss the potential of the SURMOF linkers used (Figure 28).

To synthesize the SURMOFs, we used a LBL method in a fluidic cell on a self-assembled monolayer functionalized gold (Au) substrate. First, we functionalized the Au substrate with a MUD-terminated self-assembled monolayer. Then, we added a copper acetate solution in ethanol, followed by an ethanolic solution of BPDC and bipyridine. By repeating the process of adding metal and linker solutions, it is possible to control the thickness of the thin film. The reaction was carried out using automated pumps, and between each injection step, we rinsed the wafers with ethanol to remove any residual unreacted metal/linker or by-products.

For the photocleavable linker **48**, the synthesis was carried out on Si-OH terminated QCM sensor crystals. After each linker/metal solution cycle, the mass increase was computed from the shift in resonance frequency using the SAUERBREY equation.¹²⁹ Therefore, tracking the linker/mass ratio during the synthesis was possible. In the first experiment, a Cu-BPY-BPDC pillar-layered SURMOF was grown using only unsubstituted 4,4'-bipyridine for 75 cycles as a reference (Figure 28, a) and b)). In the second experiment, 40 cycles with 4,4'-bipyridine were grown, then the photocleavable linker **48** was used for 10 cycles, and finally, 9 cycles were added with unsubstituted 4,4'-bipyridine (Figure 28, c) and d)). The steady increase in the linker and metal mass, with a linker/metal mass ratio of approximately 2.0 after the first few layers, suggests that the SURMOF grew evenly. The

presence of the Cu-BPY-BPDC SURMOF structure on the QCM sensor surface could be confirmed by recording *out-of-plane* XRD with distinctive signals (Figure 28, b)).

The photocleavable linker experiment showed a sudden increase in the linker/metal mass ratio (Figure 28, c)), followed by a steep decline to the original ratio of around 2.4. This suggests that the structure continued to grow despite using the protected linkers. This could be due to either insufficient steric hindrance of the protecting groups or the formation and growth of the competing Cu-BPDC SURMOF 2 structure, which does not require the BPY pillar molecule.¹³⁰ Given the identical lattice spacing, the Cu-BPY-BPDC pillar-layer structure grown in [100] orientation cannot be differentiated from the Cu-BPDC SURMOF 2 structure by the out-of-plane XRD method. As the [100] peak is present in both Figure 28 b) and d), it cannot be ruled out that the sample produced might be a mixture of the Cu-BPY-BPDC pillar-layer structure and the Cu-BPDC SURMOF-2 crystalline phase. The growth of the SURMOF-2 crystalline phase is not expected to be influenced by the protected bipyridine linkers. Additionally, the signal-to-noise ratio for the protected SURMOF is much lower compared to the first experiment. This could be either due to interference of the protected linkers with existing SURMOF layers or the result of the deposition of XRD-amorphous layers with linkers on top of the crystalline SURMOF.

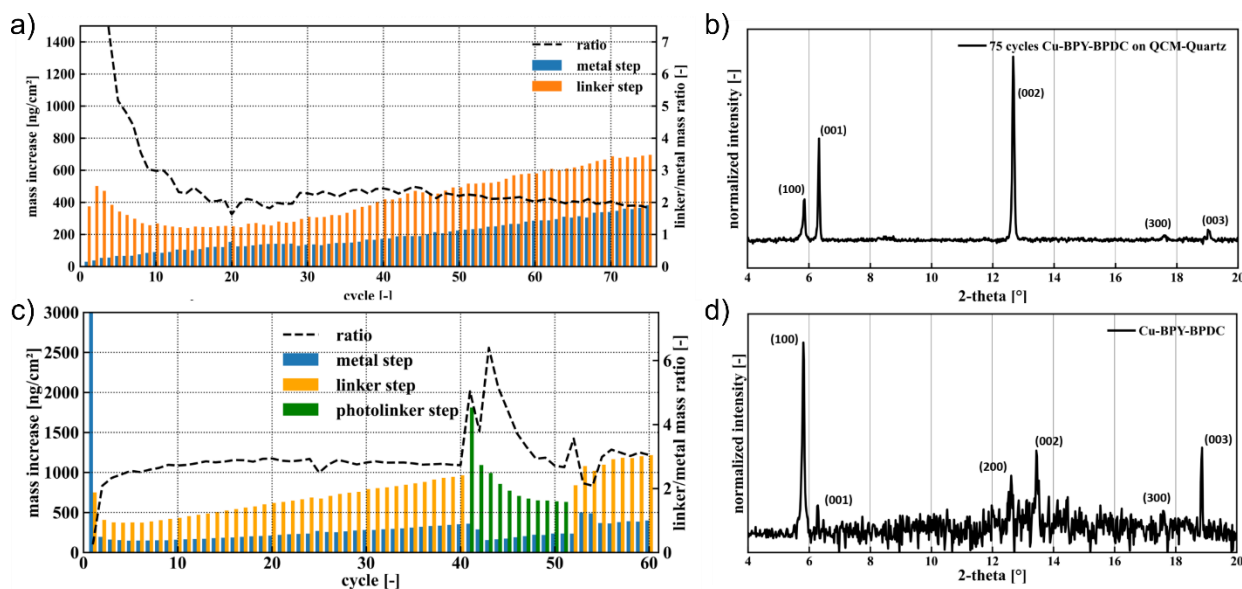


Figure 28. Results from the QCM experiment with linker **48**. a) mass increase and linker/metal mass ratio of the experiment using only unfunctionalized 4,4'-bipyridine. b) *out-of-plane* XRD of SURMOF without the photocleavable linker. c) mass increase and linker/metal mass ratio of the experiment using 4,4'-bipyridine and the photocleavable linker **48**. d) *out-of-plane* XRD of SURMOF with the photocleavable linker **48**.

In conclusion, further experimentation is necessary to evaluate the effectiveness of protected linkers in synthesizing SURMOFs. One possible approach to assess the efficiency of the protection provided by the novel linkers is to use monotopic linkers as a "blocking" end layer in place of protected linkers, with 4-phenyl pyridine as a suitable candidate for this experiment. Subsequently, the XRD and metal/linker mass ratio can be compared to our measured values. Additionally, it would be beneficial to conduct photoprotection experiments on SURMOFs further, to understand the properties and behavior of these materials.

3.1.2.2 SURMOF Preparation with Unprotected Non-centrosymmetric 4,4'-Bipyridines

In the following chapter, some previously synthesized non-centrosymmetric 4,4'-bipyridines (refer to chapter 3.1.1.2) were used to prepare SURMOFs. Parts of the following chapter have been published in *Advanced Materials* (WILEY-VCH): "Avoiding the Center-Symmetry Trap: Programmed Assembly of Dipolar Precursors into Porous, Crystalline Molecular Thin Films" by NEFEDOV *et al.*, in which the synthesis and characterization of the SURMOFs were carried out.¹³¹ The co-authors prepared and characterized the SURMOFs, and investigated their non-centrosymmetric properties. Since the results are original to the respective contributions from the collaborators, they are presented as an excerpt in this chapter (Figure 29).

Non-centrosymmetric solids lack spatial inversion symmetry and have various interesting properties, such as piezoelectricity and nonlinear optical effects, including SHG. While a small number of inorganic non-centrosymmetric materials occur naturally, artificial inorganic non-centrosymmetric compounds can be synthesized through advanced deposition techniques for thin films and coatings, which allow for the assembly of asymmetric (dipolar) subunits into non-centrosymmetric structures. In organic materials, chiral compounds can obtain non-centrosymmetric structures, but electrostatic forces often prevent the formation of macroscopic electric fields in dipolar building blocks. As a result, methods for creating non-centrosymmetric structures from asymmetric, achiral organic compounds are scarce. Previous attempts to create non-centrosymmetric SURMOFs with the LBL technique have not been successful due to the center-symmetry trap, which results in

the quenching of macroscopic electrostatic fields and prevents the formation of non-centrosymmetric structures.¹³²

While using chemical and photoremovable protecting groups proved challenging, a more straightforward approach, without the need for protection/deprotection steps, was developed to create SURMOFs with non-linear optical properties. In contrast to the protection strategy, which “forces” the coordination of one nitrogen of the bipyridine before the second coordination and propagation of the SURMOF growth, our strategy relied on the dipolar linkers holding different binding energies towards the metal clusters. Therefore, the functional groups in this study create a dipole moment, make the bipyridine asymmetric, and induce a charge redistribution that makes the two nitrogen atoms distinguishable concerning metal coordination. Of course, this approach requires a broad range of available linkers, which were prepared during the work of this thesis (chapter 3.1.1.2).

The SURMOF synthesis was attempted using 2,6-difluoro- (**3**) and 2,6-dimethyl-4,4'-bipyridine (**2**). Initial measurements showed that it was impossible to grow crystalline SURMOF structures with fluorinated linker **3**, which may be due to the electron withdrawing effect of the fluorine atoms, which could decrease the electron density and prevent the nitrogen from coordinating strongly enough with the metal node in the MOF. When **2** was used, crystalline SURMOF structures could be obtained, as shown by *in-plane* and *out-of-plane* XRD measurements (Figure 29, c)), which fit with the calculated values. As a reference, a SURMOF with non-functionalized 4,4'-bipyridine was grown. The general structure of the SURMOF is shown in Figure 29, a) and b).

It also investigated which side of the linker coordinates first with the metal node. DFT calculations showed that binding the copper paddlewheel complex to the non-functionalized side had a binding energy of 758 meV, while binding to the dipole side had a binding energy of 700 meV. Two major factors contribute to the orientation of the bipyridine in the SURMOF: the difference in electron density at the nitrogens and the steric hindrance of the methyl groups. Therefore, it can be concluded that the steric hindrance of the paddlewheel complex's carboxylates dominates the dipoles' orientation.

The non-centrosymmetric nature of the structure was confirmed by measuring the built-in electric field of the SURMOF using XPS core level shifts of Br marker atoms (Figure 29, d) and e)) and SHG spectroscopy of both SURMOFs (Figure 29, f)). In the SHG spectra, a strong SHG signal for the asymmetric SURMOF can be observed, while the symmetric SURMOF does

not show a pronounced SHG signal. To measure the core level binding energies of both SURMOFs, a top layer of tetrabromoterephthalic acid was added in the last step of the LBL synthesis. The XPS core level binding energy of the Br 3d signal for the symmetric SURMOF is 72.5 eV, while the asymmetric SURMOF showed a Br 3d signal that was shifted 0.9 eV to higher energies (Figure 29, d)).

However, it was found that the experimental binding energies were substantially lower than expected from simulations. It was concluded that the up/down ratio of the dipoles in the asymmetric SURMOF amounts to 1.07, meaning that 52% have an upward orientation and 48% have a downward orientation. This may be due to dipoles randomly binding with the substituted end first or dipoles re-orienting after synthesis while still in contact with the solvent, as the electrostatic interaction and the entropic effects favor a net charge distribution of 0.

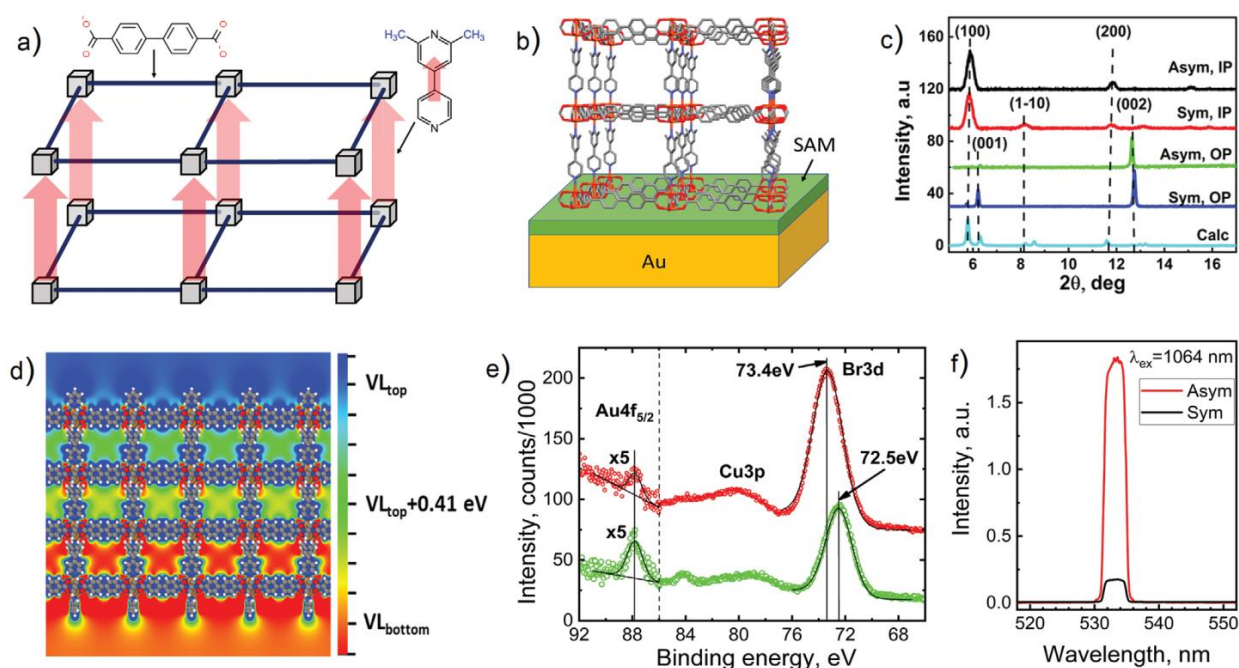


Figure 29. a) A schematic illustration of a non-centrosymmetric pillared-layer SURMOF design using the asymmetric pillar 2. b) Structure of Cu(BPDC)(Me₂-BPY) oriented along the [001] direction. c) Simulated (light blue curve) as well as experimental *in-plane* (IP) and *out-of-plane* (OP) XRD patterns of asymmetric (Asym) Cu(BPDC)(Me₂-BPY) and symmetric (Sym) Cu(BPDC)(BPY) SURMOFs. d) Shift in electrostatic energy for a Cu(BPDC)(Me₂BPY) thin film containing three polar Me₂BPY apical linker layers. The scale is aligned relative to the vacuum energy below the thin film and is specified relative to the overall change in the vacuum level (VL, calculated as -0.82 eV). e) XPS data recorded for symmetric Cu(BPDC)(BPY) (green circles) and asymmetric Cu(BPDC)(Me₂-BPY) (red circles) SURMOFs of 150 nm thickness. Both SURMOFs are coated with a Br₄-BDC-containing layer on top. The Gaussian fit of Au 4f_{5/2} and Br 3d peaks with the corresponding background is shown with black lines. f) SHG spectra of the asymmetric Cu(BPDC)(Me₂-BPY) and symmetric Cu(BPDC)(BPY) SURMOF were recorded with an excitation wavelength (λ_{ex}) of 1064 nm, reproduced from [131] with permission from WILEY-VCH.

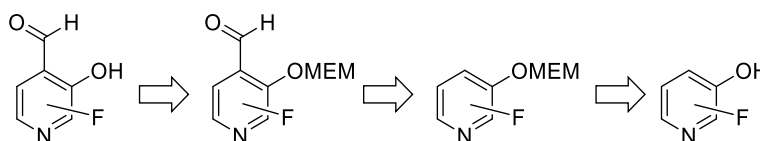
It was the first time non-linear optical effects were shown in SURMOFs with organic non-centrosymmetric linkers. While there is still room for improvement in the manufacturing of the SURMOFs and the general strategy, a wide range of bipyridine linker molecules can contribute to realizing asymmetric SURMOFs with even higher electrostatic potential shifts.

3.2 Synthesis and Characterization of Fluorinated HINA Derivatives

This thesis was not solely focused on synthesizing non-centrosymmetric bipyridine derivatives for materials but also on synthesizing fluorinated HINA derivatives. The significance of HINA as a small fluorophore was already discussed in the introduction (chapter 1.4.2). Firstly, the synthesis strategy will be described and discussed. Secondly, the derivatives will be photophysical characterized and discussed.

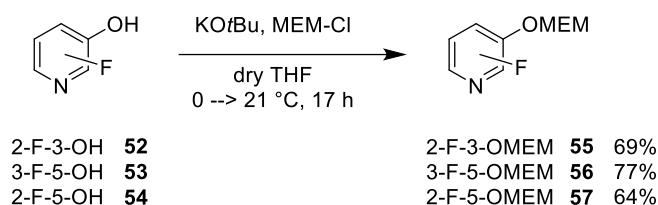
3.2.1 Synthesis of Fluorinated HINA Derivatives

A retrosynthetic analysis of the fluorinated HINA derivative can be started by installing the aldehyde through a lithiation reaction with the addition of *N,N*-dimethylformamide to the lithiated species (Scheme 14). To prevent the alcohol group from deprotonating during lithiation, it is necessary to protect this functional group. Converting the alcohol functional group to the methoxyethoxymethyl ether (MEM) not only protects the alcohol but also directs the lithiation to the *ortho* position. The directed *ortho* metalation (DoM) directs the lithium species *via* a complex-induced proximity effect, based on the hetero-atom coordination of the protecting group, into the *ortho* position relative to the protecting group (Scheme 16, top). The fluorinated pyridinols are commercially available, so the three regioisomeric fluorinated HINA derivatives should be synthesized in three consecutive reactions each.



Scheme 14. Retrosynthetic analysis of fluorinated HINA derivatives.

To install the MEM protecting group, the chlorinated protecting group MEM-Cl was stirred with the fluorinated pyridinols **52-54** in dry tetrahydrofuran overnight. The protection proceeded smoothly, with good yields ranging from 64 – 77% for **55-57** (Scheme 15).



Scheme 15. Protection of the alcohol with the MEM protecting group yielded **55-57**.

Lithiation of the MEM ether was first tried with 3-F-5-OMEM **56**. *N*-BuLi was used in dry tetrahydrofuran at -78 °C to activate the 4-position of the pyridine. After 60 minutes, an excess of *N,N*-dimethylformamide was added and quenched with sat. aq. ammonium chloride solution. In a ¹H NMR analysis of the crude after extraction, the desired aldehyde was visible as a doublet at $\delta = 10.44$ ppm. However, it seemed quite impure, and the ¹⁹F NMR indicated that more than three fluorinated species were obtained. After flash-column chromatography on silica in dichloromethane/methanol, it was impossible to get the desired aldehyde 3-F-4-CHO-5-OMEM **58**.

Initially, it was thought that the directing effect of the protecting group did not result in the regioselective formylation on the 4-position. Therefore, different DoM protecting groups were used, including methoxymethyl ether (MOM), 2-(trimethylsilyl)ethoxymethyl ether (SEM), benzyloxymethyl ether (BOM), *N,N*-diethylcarbamoyl ether, 2-tetrahydropyranyl (THP). While the protection of the pyridinols worked out with all the beforementioned protecting groups, the subsequent formylation was unsuccessful.

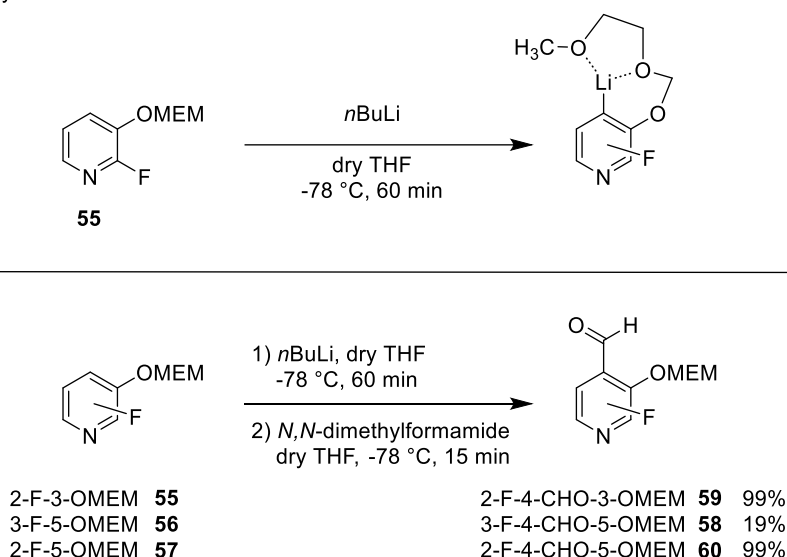
Therefore, the focus was placed again on purifying the MEM-protected aldehyde **58**, which was observed in the crude reaction mixture. An automated chromatography machine with an ELSD (evaporative light scattering detector) and fluorescence detector was used instead of manual flash-column chromatography. This had two advantages: first, the purification could be completed faster with higher pressure, which shortened the contact time of the aldehyde with acidic silica gel. Second, the column size could be reduced by about 50% because the detector works in real-time and only collects the fraction containing a detectable

compound. With these improvements, it was possible to isolate 3-F-4-CHO-5-OMEM **58** in a 19% yield using a mixture of CH/ethyl acetate (20:1 → 3:2).

Since prolonged contact times of the aldehydes with silica could make purification more difficult, a much more polar solvent mixture of dichloromethane with 1% to 5% methanol for the purification of 2-F-4-CHO-3-OMEM **59** was used, as the polar solvent would result in a shorter contact time of the aldehyde with silica. This allowed for the purification of **59** in a near-quantitative yield of 99%.

For the separation of 2-F-4-CHO-5-OMEM **60**, a diol-bonded silica column was used as the stationary phase, which enabled the aldehyde **60** to be obtained in a near-quantitative yield of 99% using a solvent mixture of CH/ethyl acetate (1:0 to 0:1) (Scheme 16, bottom).

DoM exemplary shown on 2-F-3-OMEM **55**



Scheme 16. Top: DoM of **55** shown with the MEM protecting group. Bottom: Formylation reaction of the ethers **55-57** to yield the aldehydes **58-60**.

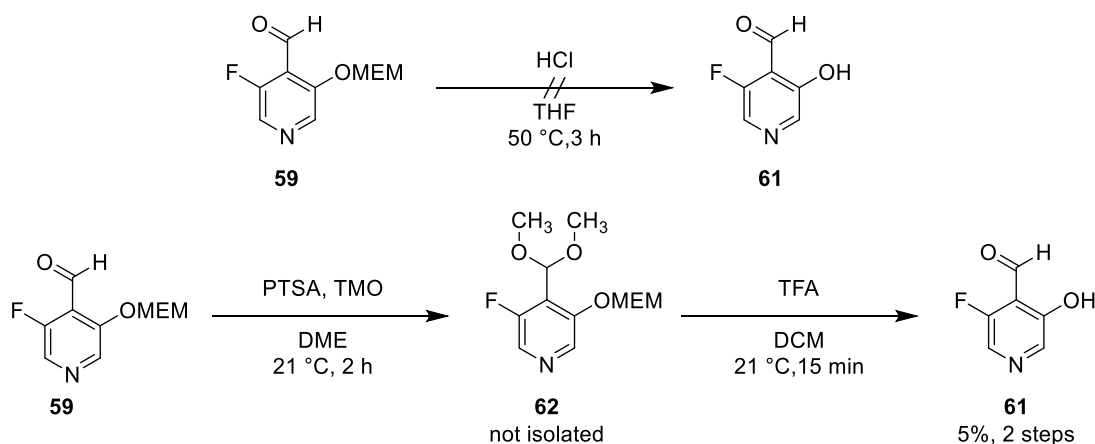
The deprotection reaction was expected to run smoothly under acidic conditions. When the deprotection of **58** was done with HCl in tetrahydrofuran, the deprotected species could not be observed. Instead, an inseparable mixture of many fluorinated species, indicated by ^{19}F NMR, was obtained.

The pyridine ring is extremely electron-deficient due to the nature of the pyridine and the electron withdrawing substituents. This can facilitate the formation and stabilize the hydrate form of the aldehyde. Usually, aldehyde hydrates can form under acidic conditions by adding a water molecule to the aldehyde resulting in a diol. The two forms exist in equilibrium, but

the aldehyde form is usually favored. However, electron withdrawing substituents stabilize the hydrate form, which causes 2,2,2-trichloroaldehyde to react readily with water to the chloral hydrate.

Therefore, the deprotection was attempted using water-free TFA in dry dichloromethane. This yielded solely the aldehyde form **61** observed in the crude ^1H NMR. A flash-column chromatography on diol-bonded silica gave the desired aldehyde. However, it was not possible to remove all the aliphatic impurities. Furthermore, the aldehyde formed the hydrate form during purification resulting in drastically reduced yields.

To circumvent the hydrate formation, it was tried to stir the protected aldehyde **59** with acidic *p*-toluenesulfonic acid (PTSA) and trimethyl orthoformate (TMO) in dry 1,2-dimethoxyethane (DME). However, methanol is formed during the water scavenging of TMO in this reaction. The presence of methanol formed a dimethyl acetal **62**, a protected form of the HINA **61** as indicated by ^1H NMR (Scheme 17).



Scheme 17. The successful synthesis of 3-F-5-OH HINA **61** via the dimethyl acetal **62**.

Theoretically, it should be possible to deprotect the alcohol and the acetal functional groups simultaneously using acidic conditions. Hence, the deprotection with TFA in dry dichloromethane was done. In the ^1H NMR of the crude, the aldehyde **61** and some minor impurities were detected. Because in the ^{19}F NMR, only one fluorinated species could be observed, it was expected that the impurities were of another kind than the fluorinated HINA **61**. During the purification, flash-column chromatography should be avoided. The HINAs should be water-soluble when being protonated at the nitrogen under acidic conditions or deprotonated at the alcohol under basic conditions. Therefore, the TFA acidic

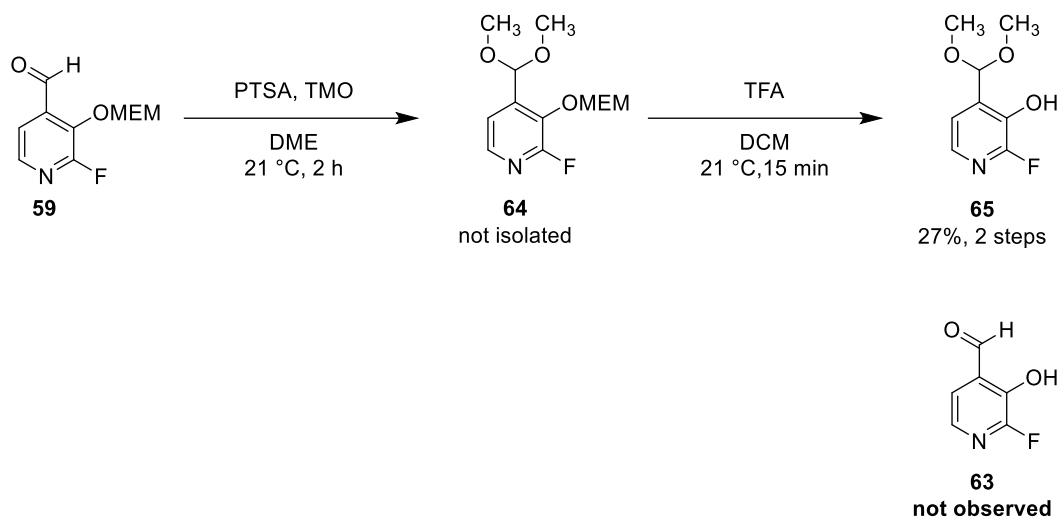
solution from the reaction was extracted with ethyl acetate to remove any side products. Afterward, the aqueous solution was made basic by adding 1 M NaOH solution until pH = 10-11 was reached. It was extracted with ethyl acetate again. Subsequently, it was possible to extract the highly fluorescent HINA derivative **61** at pH = 4-5 with a mixture of dichloromethane/*i*PrOH (4:1).



Figure 30. Successful extraction of the fluorinated HINA derivatives could be observed by irradiation with UV light.

By checking the organic phase for fluorescence when irradiated with a UV lamp at $\lambda = 365$ nm, it was possible to determine if the product could be extracted (Figure 30). The organic solvent was removed under reduced pressure, during which it was found that the small HINA derivative was quite volatile. After the residual solvent was removed, only 5% of **61** could be obtained (Scheme 17). Furthermore, even though the molecule was stored under an argon atmosphere at -18 °C, the compound decomposed within a few days.

During the synthesis of 2-F-3-OH HINA **63**, the previously installed dimethyl acetal **64** could not be cleaved by treatment with TFA in dichloromethane, and the dimethyl acetal **65** was obtained. (Scheme 18).



Scheme 18. Synthesis of 2-F-3-OH HINA **63** was not achieved during the deprotection reaction; the dimethyl acetal could not be removed.

Instead of the aldehyde signal, which was expected with a chemical shift of around $\delta = 9.0$ - 10.5 ppm, the acetal proton $4\text{-CCH}(\text{OCH}_3)_2$ could be observed at $\delta = 5.58$ ppm (Figure 31).

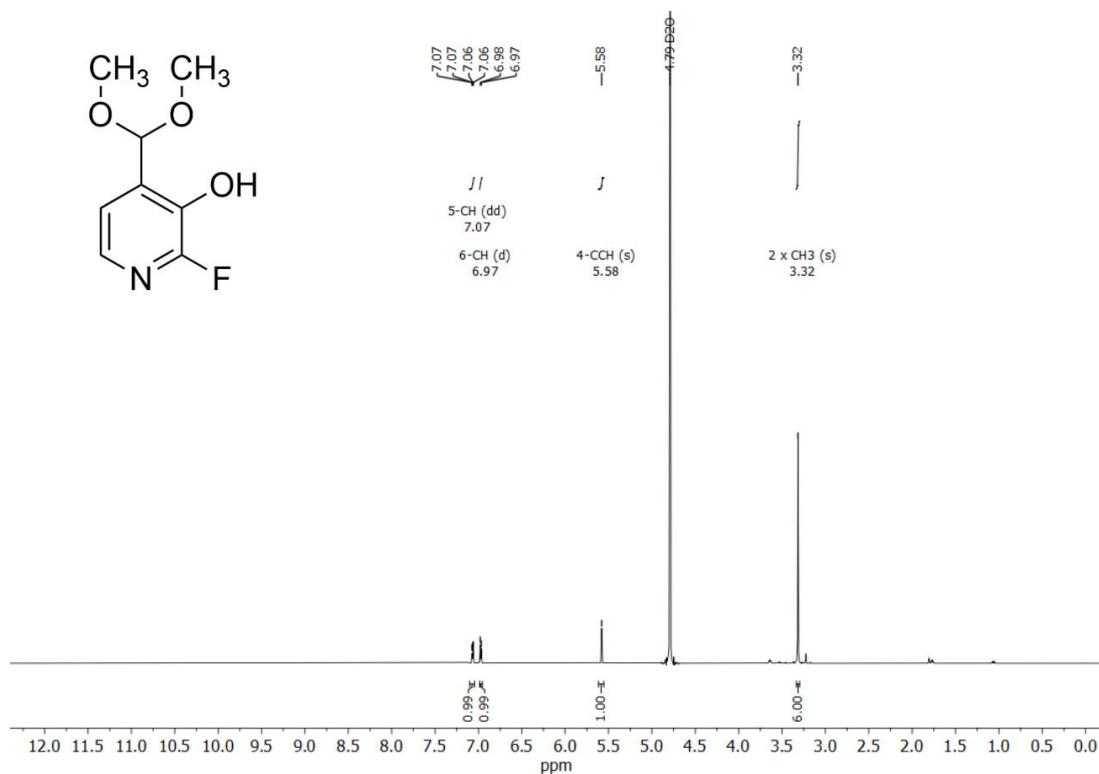
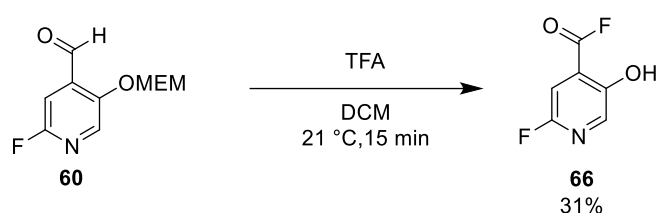


Figure 31. ^1H NMR of dimethyl acetal **65**.

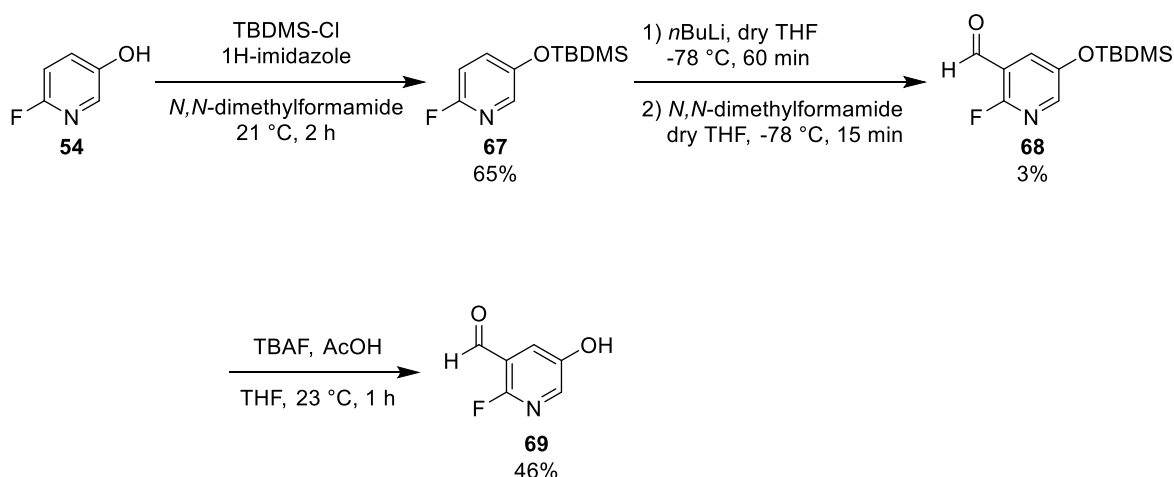
Additional tests of the deprotection reaction of **65** could not be done in the scope of this work, and it was impossible to characterize this compound due to its instability fully. Further experimentation would be necessary to confirm that the dimethyl acetal functional group of **65** cannot be cleaved with TFA in dichloromethane. It could also be possible that the desired HINA **63** was formed but could not be isolated because of its good water solubility or quick degradation.

Lastly, the deprotection of 2-F-5-OH HINA **65** was attempted directly with TFA in dry dichloromethane from the protected aldehyde **60**. It was possible to isolate the desired compound **66** in a yield of 31% (Scheme 19).



Scheme 19. Direct synthesis of HINA **66**.

While it was worked on the deprotection and extraction of the fluorinated HINA derivatives, the synthesis with a TBDMS PG was done in parallel (Scheme 20). This protecting group was chosen as it can be easily cleaved by fluoride reagents under mild conditions.



Scheme 20. Synthesis of 2-F-3-CHO nicotinaldehyde **69**.

The PG was introduced with TBDMS-Cl in the presence of imidazole and gave the protected alcohol **67** in a yield of 65%. The formylation reaction was done using the beforementioned

conditions and only gave 3% of an aldehyde-containing derivative after purification on silica. ^1H NMR analysis showed the typical aldehyde proton singlet at $\delta = 10.23$ ppm. However, a $^2J_{\text{CF}}$ coupling constant between the quaternary carbon next to the aldehyde to the fluorine atom of 25.1 Hz indicated the formation of protected 2-fluoro-5-hydroxynicotinaldehyde (**68**) (Figure 32). If the aldehyde functional group would be on the 4-position, then a $^3J_{\text{CF}}$ coupling constant should be around 8 Hz, whereas $^2J_{\text{CF}}$ coupling constants are commonly around 20 Hz, according to the literature.¹³³

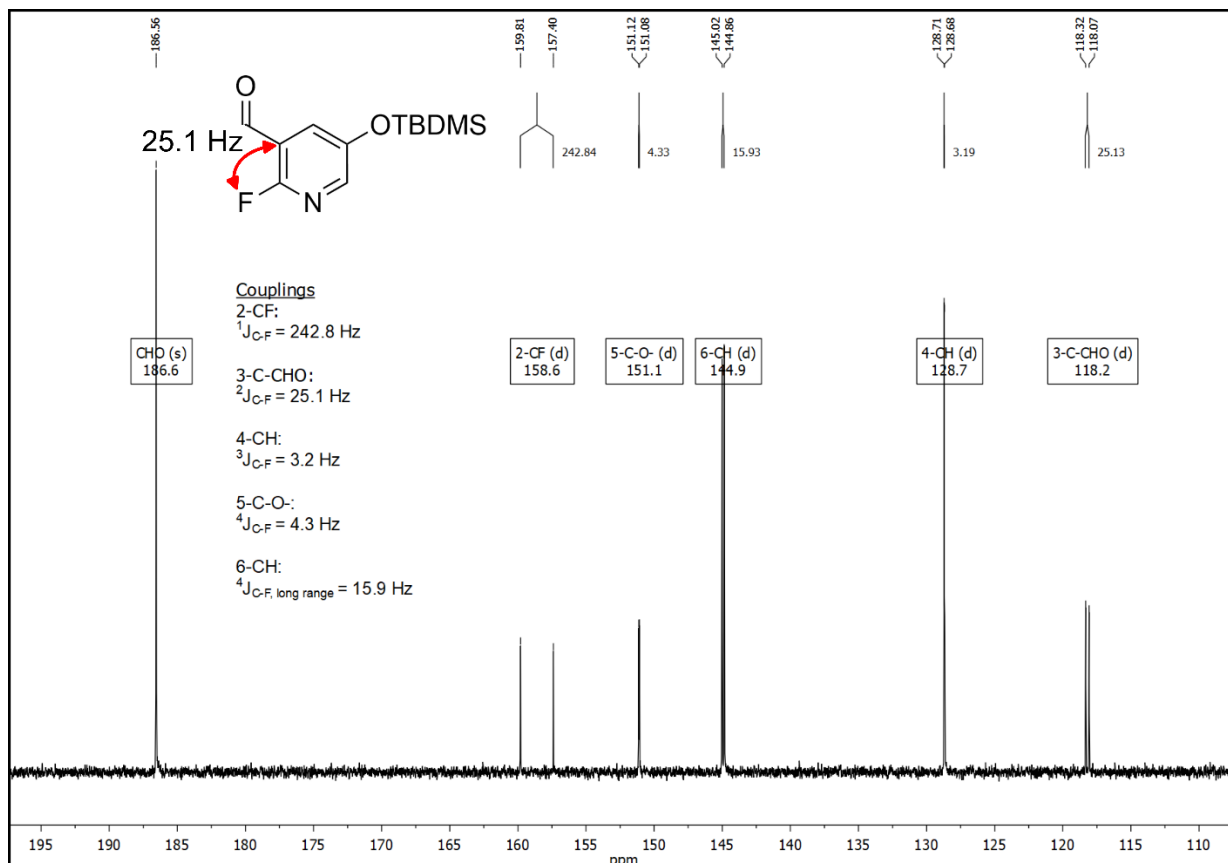


Figure 32. Cutout of the ^{13}C NMR spectrum of **68**. C-F coupling is depicted in red.

It was then deprotected using TBAF in an acetic acid/dichloromethane mixture, and **69** could be obtained in a 43% yield. The mass showed the expected $[\text{M}]^+$ peak at m/z 141. The two derivatives differ from the chemical shift. In the nicotinaldehyde **69**, a $^4J_{\text{HH}}$ coupling with a coupling constant of 3.2 Hz can be observed. The structure could further be verified by ^{13}C NMR. Only H-F couplings can be observed in the spectrum of HINA **66**, indicating a long distance between the protons in the *para* position to each other (Figure 33).

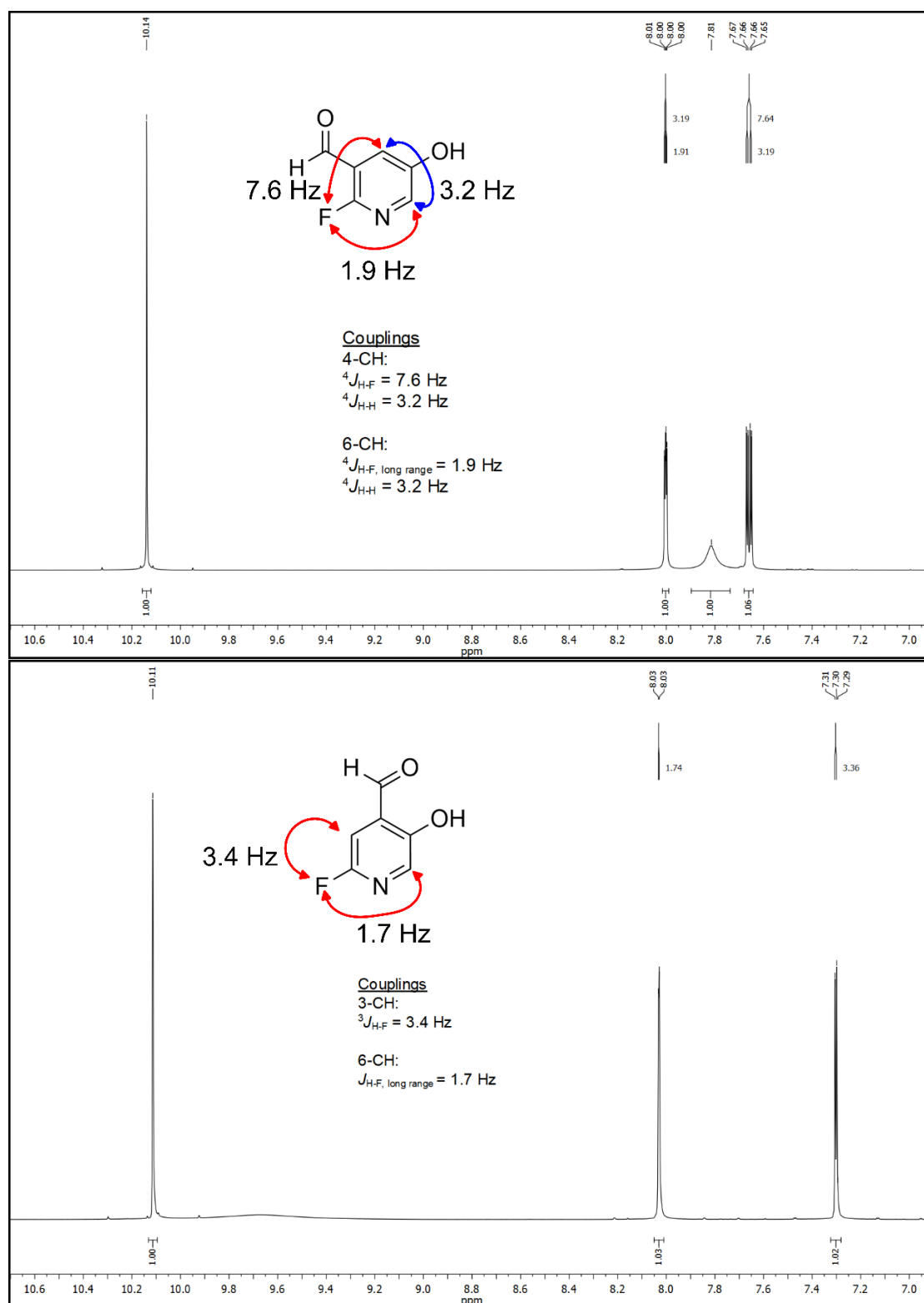


Figure 33. ¹H NMR analysis of nicotinaldehyde **69** (top) and isonicotinaldehyde **66** (bottom). H-F coupling is depicted in red, and H-H coupling is depicted in blue.

After some nicotinaldehydes were successfully synthesized, they were analyzed by UV/vis and fluorescence spectroscopy to characterize their potential as fluorophores.

3.2.2 UV/vis- and Fluorescence Spectroscopy of Nicotinaldehydes

This chapter contains unpublished data on UV/vis measurements of nicotinaldehydes. The measurements were prepared by RUI KANG (AG Biedermann, INT). The results are left for publication in this thesis and presented as an excerpt in this work (Figure 34 and Figure 35).

The previously synthesized 3-F-5-OH **61** and 2-F-5-OH **66** HINAs, as well as the 2-F-3-CHO nicotinaldehyde **69**, should be tested for their photophysical properties. Unfortunately, 3-F-5-OH **61** did not show the absorbance of a HINA derivative, and when another ^1H NMR was measured, it was found that the compound had already degraded and was not stable enough for further measurements. Therefore, the characterizations were carried out only with **66** and **69** and non-fluorinated HINA for comparison.

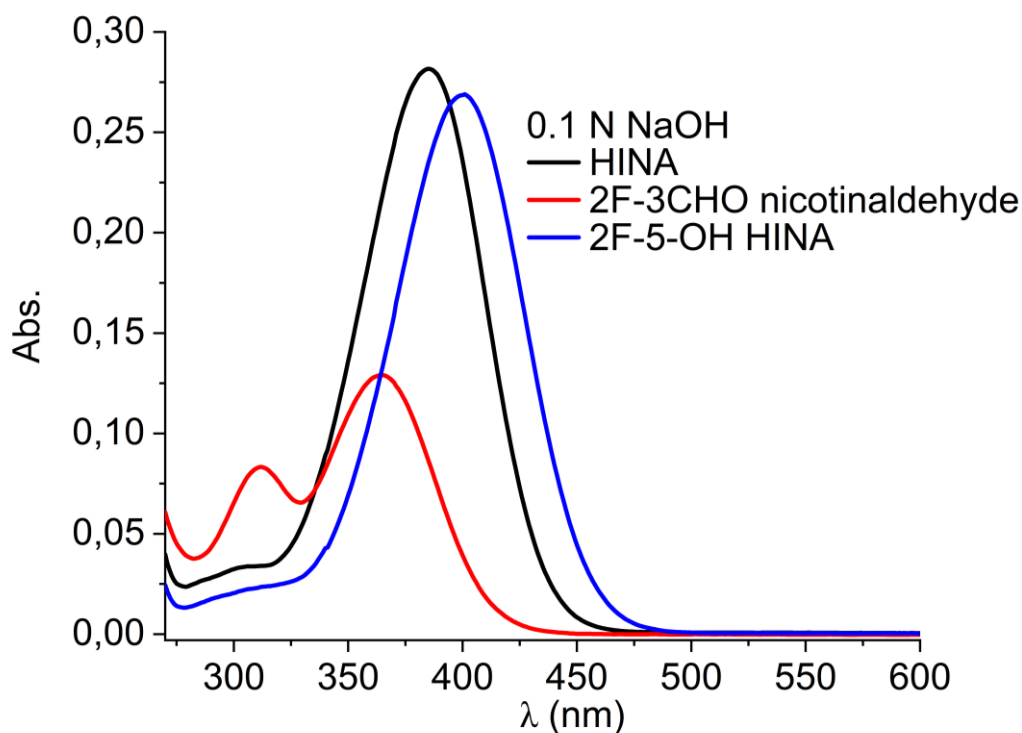


Figure 34. UV/vis absorbance spectroscopy of non-fluorinated HINA, 2-F-3-CHO **69** and 2-F-5-OH HINA **66**.

From the UV/vis absorbance spectrum in an aqueous NaOH solution, it can be observed that the native HINA and **66** with absorbance maxima at $\lambda = 385$ nm and $\lambda = 401$ nm show a very similar absorbance profile when compared to that of nicotinaldehyde **69** with a maximum absorbance at $\lambda = 364$ nm and with another local maximum at $\lambda = 312$ nm, which is not

present in the absorbance spectra of the HINA derivatives (Figure 34). Compared to the non-fluorinated HINA, the fluorinated derivative **66** shows a redshift of 16 nm.

Fluorescence measurements of 2-F-5-OH **66** and nicotinaldehyde **69** were done in different solvents with an excitation wavelength of $\lambda_{\text{ex}} = 420$ nm, respectively $\lambda_{\text{ex}} = 380$ nm. For the fluorinated HINA **66**, an emission maximum of around 550 nm could be observed, which is about 25 nm red-shifted compared to the non-fluorinated HINA (Figure 35).¹ Nicotinaldehyde **69** did not show strong fluorescence properties, and the emission strongly depended on the solvent used.

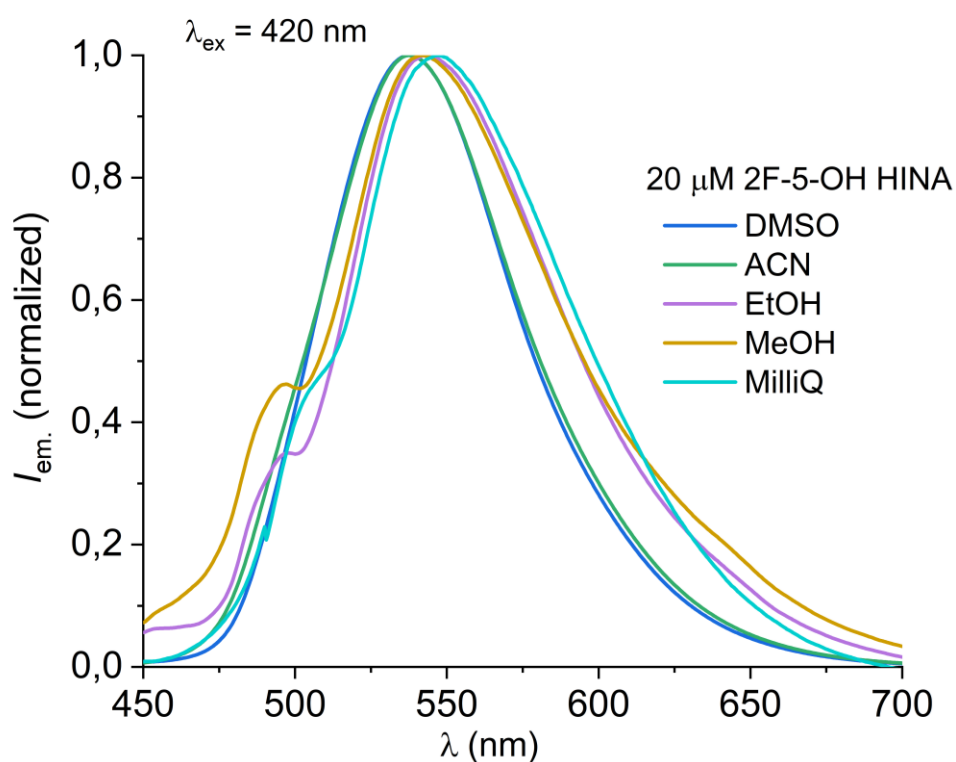


Figure 35. Emission spectroscopy of **66** in different solvents (excitation wavelength $\lambda_{\text{ex}} = 420$ nm).

In summary, it can be said that 2-F-5-OH **66** showed the desired redshift of 25 nm in fluorescence when compared to the small native HINA fluorophore. As expected, the regioisomeric 3-CHO nicotinaldehyde **69** did not exhibit strong emissive properties, probably due to the location of the aldehyde functional group. Despite the promising properties of fluorinated HINA derivatives, it can be said that the instability of the compounds and the elaborate synthesis prevent their applicability for biological applications. However, for specific purposes requiring small, strong-emissive,

pH-dependent fluorophores that can emit above 500 nm, HINA and fluorinated derivatives thereof are promising candidates.

4 Summary and Outlook

The following work was structured into two main parts. The first part presented contributions towards non-linear optical SURMOFs by investigating the synthesis and use of tailor-made linear linker molecules based on 4,4'-bipyridines. Different protection strategies of the SURMOF linkers had to be considered to create a net dipole moment in the resulting thin film structures. Furthermore, advances toward 3D-printable SURMOF structures were investigated. In the second part, the synthesis of fluorinated HINA derivatives, promising small fluorophores, was done, and the scaffolds were photophysical characterized.

4.1 Synthesis of Non-centrosymmetric 4,4'-Bipyridines for SURMOF Preparation

For the preparation and investigation of SURMOF structures with a net dipole moment, non-centrosymmetric 4,4'-bipyridines were synthesized in this work.

First, the synthesis of 4,4'-bipyridines using C-C cross-coupling reactions was investigated. While very good yields using a SUZUKI-MIYAJIMA cross-coupling have already been published, electron withdrawing substituents generally resulted in low yields. Therefore, conditions were improved, and the yield of 2,6-difluoro-4,4'-bipyridine (**3**) with two electron withdrawing fluorine substituents could be significantly improved to 84% on a gram-scale using the $\text{Pd}_2(\text{dba})_3 \cdot \text{CHCl}_3$ catalyst in a 1,4-dioxane/water solvent system. Subsequently, a variety of 4,4'-bipyridine-based non-centrosymmetric linkers were synthesized, having electron donating and withdrawing substituents attached to all four available positions of the pyridyl ring. Using the improved conditions, good to excellent yields ranging from 68-99% were obtained (Scheme 21, for further details, see Figure 17). The synthesis of electron donating (push) and electron withdrawing (pull) substituents on the different pyridyl rings resulting in a greater dipole moment of the linker, was not possible. Further investigations and optimizations must be made to fine-tune the resulting dipole moment of the linker.

On the way to SURMOFs with non-linear optical properties, different protection strategies for the SURMOF linkers were discussed. Different PPGs were considered, and three bipyridine-PPG conjugates were synthesized, of which two linkers used PPGs based on coumarins (**41** and **42**), and the last linker, **43**, was based on the NVOC PPG. The deprotection reaction of **43** was investigated in more detail using ^1H NMR, HPLC, and UV/vis. The results proved the cleavability of the PPG around 350-365 nm. Subsequently, SURMOF experiments using a QCM were carried out, and a mass increase analyzed the structures during the synthesis and *out-of-plane* XRD measurements. However, more experimentation is necessary to conclude the novel linkers' effectiveness safely.

Next, SURMOFs were grown with unprotected non-centrosymmetric linkers. The net dipole moment should be achieved by the different binding energies of the pyridyl nitrogens towards the metal clusters resulting from substitutions with electron withdrawing or donating groups on the pyridines. It was unsuccessful in preparing crystalline SURMOFs with 2,6-difluoro-4,4'-bipyridine (**3**); however, using the methyl-substituted correspondent **2**, SURMOFs could be grown, and the structures were further characterized. The crystalline nature of the resulting SURMOFs was confirmed through X-ray measurements. SHG spectroscopy showed a strong SHG signal for the asymmetric SURMOF, whereas when a SURMOF using unsubstituted bipyridine linkers was compared, no SHG signal could be observed. Subsequently, XPS core level shifts of Br marker atoms were measured and showed a built-in electric field of the asymmetric SURMOF. It was the first time non-linear optical effects could be shown in a SURMOF material using organic non-centrosymmetric linkers. However, it was also found that there is no perfect orientation of the linkers in the SURMOF, meaning that further advances are necessary to make competitive SHG SURMOFs in the future. An even more versatile linker design with push-/pull-functional groups based on molecules that have been calculated computationally could maximize the amount of perfectly oriented non-centrosymmetric linkers.

4.2 Synthesis and Characterization of Fluorinated HINA Derivatives

Based on recently published results that showed the potential of HINA as a small and potent fluorophore, it was decided to red-shift the absorbance and fluorescence properties by preparing fluorinated derivatives.

The synthesis was started with fluorinated hydroxypyridines (**52-54**), and the aldehydes should be obtained *via* the protection with DoM protecting groups. While it was possible to synthesize all three possible MEM-protected and formylated regioisomers (**58-60**), the deprotection and isolation of the fluorinated HINAs was difficult to achieve due to good water-solubility, volatility, and quick decomposition of the final products. 2-F-5-OH **66** and 3-F-5-OH **61** could be successfully prepared and were photophysical characterized (Figure 37). In parallel, nicotinaldehyde 2-F-3-CHO **69** was synthesized using a non-DoM PG. The different regioisomers were characterized, and the structure was discussed using ^1H and ^{13}C NMR spectroscopy.

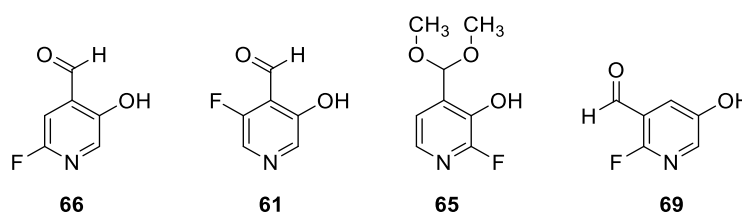


Figure 37 Synthesis of two fluorinated HINAs **66** and **61** was successful. For the 2-F-3-OH derivative, only the dimethyl ester **65** was obtained. When a non-DoM PG was used during the synthesis, **69** was obtained.

During the photophysical characterization, it was found that **61** was not stable enough for testing. Therefore, native HINA, 2-F-3-CHO **66**, and 2-F-3-CHO **69** were measured and compared. The fluorinated HINA **66** showed a redshift in the absorption maximum of 16 nm compared to the non-fluorinated correspondent. Furthermore, the fluorescence maximum was also shifted by 25 nm when comparing the two fluorophores. In contrast, 2-F-3-CHO **69** did not show the characteristics of the HINA derivatives when comparing the absorbance profiles.

In summary, a feasible synthesis route toward fluorinated HINA derivatives was shown. However, mostly low yields were obtained. Critical steps include the purification of

protected aldehydes and the extraction of the fluorinated HINA derivatives. Additionally, the volatility and instability of the compounds make the synthesis more difficult. Therefore, additional synthesis efforts must be made before these derivatives can be used for imaging applications.

5 Experimental Section

5.1 General Remarks

Materials and Methods

The starting materials, solvents, and reagents were purchased from ABCR, ACROS, ALFA AESAR, APOLLO SCIENTIFIC, CARBOLUTION, CHEMPUR, FLUKA, FLUOROCHEM, MERCK, RIEDEL-DE HAËN, SIGMA ALDRICH, STREM, TCI, or THERMO FISHER SCIENTIFIC and used without further purification unless stated otherwise.

Solvents of technical quality were purified with the MBRAUN solvent purification system MB SPS5 (acetonitrile, dichloromethane, diethyl ether, tetrahydrofuran, and toluene).

Solvents of *p.a.* quality were purchased from ACROS, FISHER SCIENTIFIC, SIGMA ALDRICH, ROTH, or RIEDEL-DE HAËN and were used without further purification. Other solvents were obtained from commercial suppliers: dry *N,N*-dimethylformamide (SIGMA ALDRICH, <0.005% water), dry 1,4-dioxane (SIGMA ALDRICH, <0.005% water), dry ethanol (SIGMA ALDRICH, <0.005% water), dry methanol (SIGMA ALDRICH, <0.005% water), dry methylene chloride (SIGMA ALDRICH, <0.005% water), 1,2-dimethoxyethane (SIGMA ALDRICH, <0.005% water).

Oxygen-free solvents were obtained by freeze-pump-thaw (three cycles) technique.

Air- and moisture-sensitive reactions were carried out under an argon atmosphere in oven-dried glassware using standard Schlenk techniques.

A BERGHOF BR100 pressure reactor was used for reaction setups under high pressure.

Flat-bottom crimp neck vials from CHROMAGLOBE with aluminum crimp caps were used for certain reactions.

Liquids were added with a stainless-steel cannula, and solids were added in a powdered shape.

Reactions at low temperatures were cooled using flat dewars produced by ISOTHERM (Karlsruhe) with water/ice or isopropanol/dry ice mixtures.

Solvents were evaporated under reduced pressure at 40 °C using a rotary evaporator. For solvent mixtures, each solvent was measured volumetrically.

Flash column chromatography was done using MERCK silica 60 (0.040 × 0.063 mm, 230–400 mesh ASTM) and quartz sand (glowed and purified with hydrochloric acid). Automated flash column chromatography was performed using a BUCHI PURE C-815 FLASH with UV and ELSD detector. FlashPure EcoFlex Silica cartridges from BUCHI in sizes 4 g to 120 g were used for normal-phase chromatography. The diol-modified columns used were PF-30DIOL columns in the sizes F0004-F0030 from INTERCHIM.

For the photocleavage reactions with LED UV light (350 nm, 8 × 8W), an LZC-ICH2 photoreactor from LUZCHEM was used. For the isomerization experiments, sample irradiation was done with a 10 W LED from LED ENGIN with an emission maximum of 365 nm. During the irradiation, the samples were placed in a metal cooling block that maintained a constant temperature of 22 ± 2 °C.

Analytical Balance

The analytical weight balance *AB204* of *METTLER TOLEDO* with an accuracy of 0.1 mg was used.

Reaction Monitoring

The reactions were monitored by thin-layer chromatography (TLC) using silica-coated aluminum plates (MERCK, silica 60, F254). UV active compounds were detected with a UV lamp at 254 nm and 365 nm excitation.

Melting point

Melting points were detected on an OptiMelt MPA100 device from STANFORD RESEARCH SYSTEM.

Nuclear Magnetic Resonance Spectroscopy (NMR)

NMR spectra were recorded on a BRUKER Avance 400 NMR instrument at 400 MHz for ^1H NMR, 101 MHz for ^{13}C NMR, and 376 MHz for ^{19}F NMR, or a BRUKER Avance 500 NMR instrument at 500 MHz for ^1H NMR, 126 MHz for ^{13}C NMR, and 470 MHz for ^{19}F NMR.

The NMR spectra were recorded at room temperature in deuterated solvents acquired from EURISOTOP, SIGMA ALDRICH, or DEUTERO. Chemical shifts δ were expressed in parts per million [ppm] and referenced to:

d_1 -chloroform (CDCl_3): 7.26 ppm for ^1H and 77.16 ppm for ^{13}C

d_4 -methanol (CD_3OD): 3.31 ppm for ^1H and 49.00 ppm for ^{13}C

d_3 -acetonitrile (CD_3CN): 1.94 ppm for ^1H and 118.26 ppm for ^{13}C

For the characterization of centrosymmetric signals, the signal's median point was chosen for multiplets in the signal range. The following abbreviations were used to describe the proton splitting pattern: d = doublet, t = triplet, m = multiplet, dd = doublet of the doublet, ddd = doublet of doublet of the doublet, dt = doublet of the triplet, q = quartet. Absolute values of the coupling constants " J " are given in Hertz [Hz] in absolute value and decreasing order. Signals of the ^{13}C spectrum were assigned by phase-edited heteronuclear single quantum coherence (HSQC). For assignments of complex structures, heteronuclear multiple bond correlation (HMBC) was measured and analyzed.

Infrared Spectroscopy (IR)

For solids, IR spectra were recorded on a BRUKER IFS 88 using ATR (attenuated total reflection). All spectroscopy samples were analyzed at room temperature. The position of the absorption is given in wave numbers $\bar{\nu}$ [cm^{-1}] and was measured in the range from 3600 cm^{-1} to 500 cm^{-1} .

Characterization of the absorption bands was done in dependence on the absorption strength with the following abbreviations: vs. (very strong, 0–9%), s (strong, 10–39%), m (medium, 40–69%), w (weak, 70–89%), vw (very weak, 90–100%).

Mass Spectrometry (MS)

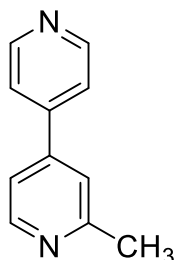
Electron ionization (EI) experiments were conducted using a FINNIGAN, MAT 90 (70 eV) instrument, with 3-nitrobenzyl alcohol (3-NBA) as matrix and reference for high resolution. For the interpretation of the mass spectra, the molecular ion $[M]^+$, peaks of pseudo molecules, such as $[M + H]^+$, and characteristic fragments are indicated as mass per charge ratio (m/z) and their intensity given in percent, relative to the main peak (100%). In the case of the high-resolution MS, the tolerated error is ± 5 ppm of the molecular mass.

ESI experiments were recorded on a Q-Exactive (Orbitrap) mass spectrometer (THERMO FISHER SCIENTIFIC) equipped with a HESI II probe to record high resolution. The tolerated error is ± 5 ppm of the molecular mass. The spectra were interpreted by molecular peaks $[M]^+$, peaks of protonated molecules $[M+H]^+$ and characteristic fragment peaks and indicated with their mass-to-charge ratio (m/z).

5.2 Characterization of Compounds

5.2.1 Bipyridines

2-Methyl-4,4'-bipyridine (1)



4-bromo-2-methylpyridine (500 mg, 2.91 mmol, 1.00 equiv), 4-pyridylboronic acid (429 mg, 3.49 mmol, 1.20 equiv), potassium phosphate (1.23 g, 5.81 mmol, 2.00 equiv), tricyclohexylphosphane (81.5 mg, 291 μ mol, 10 mol%) and tris(dibenzylideneacetone)dipalladium chloroform (150 mg, 145 μ mol, 5 mol%) were combined with a degassed mixture of 1,4-dioxane (14.0 mL) and water (6.00 mL). After stirring for

17.5 h at 90 °C, the mixture was cooled to 21 °C, extracted with dichloromethane, and washed with water and brine. The combined organic phase was dried over sodium sulfate and filtered, and the solvent was removed under reduced pressure. The crude product was purified *via* flash-chromatography on silica gel using dichloromethane with 2% to 5% methanol to yield the title compound (681 mg, 4.00 mmol, 99% yield) was obtained as a yellow solid.

m.p.: 91 °C

R_f = 0.26 (dichloromethane + 5% methanol)

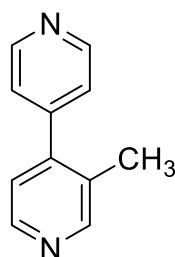
^1H NMR (500 MHz, CD_2Cl_2 , ppm) δ = 8.72–8.67 (m, 2H, 2'- and 6'-CH), 8.58 (dd, J = 5.2, 0.8 Hz, 1H, 6-CH), 7.58–7.49 (m, 2H, 3'- and 5'-CH), 7.41 (s, 1H, 3-CH), 7.35 (dd, J = 5.2, 2.0 Hz, 1H, 5-CH), 2.61 (s, 3H, CH_3).

^{13}C NMR (126 MHz, CD_2Cl_2 , ppm) δ = 160.0 (2-Cq), 151.0 (2'- and 6'-CH, 2C), 150.3 (6-CH), 146.1 (4'-Cq), 146.0 (4-Cq), 121.8 (3'- and 5'-CH, 2C), 121.2 (3-CH), 118.8 (5-CH), 24.7 (CH_3).

IR (ATR, cm^{-1}) $\tilde{\nu}$ = 3026 (m), 2979 (w), 2972 (w), 2963 (w), 2919 (m), 2884 (w), 2850 (w), 1592 (vs), 1536 (m), 1473 (m), 1459 (w), 1445 (m), 1419 (w), 1412 (w), 1392 (s), 1370 (w), 1290 (w), 1217 (w), 1211 (w), 986 (s), 858 (m), 815 (vs), 618 (vs), 601 (m), 552 (m), 528 (vs), 448 (s), 401 (vs).

MS (EI, 70 eV) m/z (%) = 171 (10) $[\text{M}+\text{H}]^+$, 170 (100) $[\text{M}]^+$, 169 (9) $[\text{M}-\text{H}]^+$.

HRMS (EI, $[\text{M}]^+$, $\text{C}_{11}\text{H}_{10}\text{N}_2$) calcd.: 170.0838, found: 170.0838.

3-Methyl-4,4'-bipyridine (15)

4-bromo-3-methylpyridine hydrochloride (834 mg, 4.00 mmol, 1.00 equiv), 4-pyridylboronic acid (590 mg, 4.80 mmol, 1.20 equiv), potassium phosphate (2.55 g, 12.0 mmol, 3.00 equiv), tricyclohexylphosphane (112 mg, 401 μ mol, 10 mol%) and tris(dibenzylideneacetone)dipalladium chloroform (207 mg, 200 μ mol, 5 mol%) were combined with a degassed mixture of 1,4-dioxane (14.0 mL) and water (6.00 mL). After stirring for 17.5 h at 90 °C, the mixture was cooled to 21 °C, extracted with dichloromethane, and washed with water and brine. The combined organic phase was dried over sodium sulfate and filtered, and the solvent was removed under reduced pressure. The crude product was purified *via* flash-chromatography on silica gel using dichloromethane with 2% to 5% methanol to yield the title compound (674 mg, 3.96 mmol, 99% yield) was obtained as an orange solid.

m.p.: 89 °C

R_f = 0.33 (dichloromethane + 5% methanol)

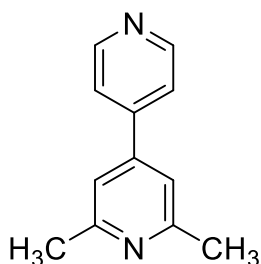
^1H NMR (500 MHz, CD_2Cl_2 , ppm) δ = 8.70–8.64 (m, 2H, 2'- and 6'-CH), 8.52 (s, 1H, 2-CH), 8.48 (d, J = 4.9 Hz, 1H, 6-CH), 7.29–7.24 (m, 2H, 3'- and 5'-CH), 7.14 (d, J = 4.9 Hz, 1H, 5-CH), 2.27 (s, 3H, CH_3).

^{13}C NMR (126 MHz, CD_2Cl_2 , ppm) δ = 152.0 (2-CH), 150.4 (2'- and 6'-CH, 2C), 148.0 (6-CH), 147.2 (4'- C_q), 146.7 (4- C_q), 130.6 (3- C_q), 123.8 (3'- and 5'-CH, 2C), 123.6 (5-CH), 17.2 (CH_3).

IR (ATR, cm^{-1}) $\tilde{\nu}$ = 2922 (m), 2849 (w), 1585 (s), 1557 (w), 1537 (w), 1480 (m), 1446 (m), 1407 (vs), 1378 (m), 1303 (w), 1215 (w), 1159 (m), 1079 (w), 1057 (w), 1040 (w), 989 (m), 856 (w), 829 (vs), 813 (s), 759 (w), 751 (w), 734 (w), 626 (s), 581 (vs), 534 (vs), 494 (w), 479 (w), 475 (w), 443 (w), 433 (m), 409 (w), 394 (m).

MS (EI, 70 eV) m/z (%) = 171 (13) $[\text{M}+\text{H}]^+$, 170 (100) $[\text{M}]^+$, 169 (53) $[\text{M}-\text{H}]^+$, 168 (7), 143 (31), 142 (17), 141 (5), 117 (5), 115 (12), 89 (5).

HRMS (EI, $[\text{M}]^+$, $\text{C}_{11}\text{H}_{10}\text{N}_2$) calcd.: 170.0838, found: 170.0840.

2,6-Dimethyl-4-pyridin-4-ylpyridine (2)

4-bromo-2,6-dimethylpyridine (501 mg, 2.69 mmol, 1.00 equiv), 4-pyridylboronic acid (397 mg, 3.23 mmol, 1.20 equiv), potassium phosphate (1.14 g, 5.39 mmol, 2.00 equiv), tricyclohexylphosphane (75.5 mg, 269 μ mol, 10 mol%) and tris(dibenzylideneacetone)-dipalladium chloroform (139 mg, 134 μ mol, 5 mol%) were combined with a degassed mixture of 1,4-dioxane (7.00 mL) and water (3.00 mL). After stirring for 17.5 h at 90 °C, the mixture was cooled to 21 °C, extracted with dichloromethane, and washed with water and brine. The combined organic phase was dried over sodium sulfate and filtered, and the solvent was removed under reduced pressure. The crude product was purified *via* flash-chromatography on silica gel using dichloromethane with 2% to 5% methanol to yield the title compound (496 mg, 2.69 mmol, quant.) as an orange hygroscopic solid.

m.p.: 56 °C

R_f = 0.27 (dichloromethane 5% methanol)

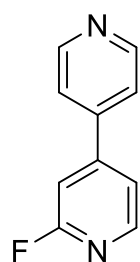
^1H NMR (500 MHz, CDCl_3 , ppm) δ = 8.73–8.67 (m, 2H, 2'- and 6'-CH), 7.53–7.47 (m, 2H, 3'- and 5'-CH), 7.19 (s, 2H, 3- and 5-CH), 2.61 (s, 6H, 2- and 6- CH_3).

^{13}C NMR (126 MHz, CDCl_3 , ppm) δ = 158.9 (2- and 6- C_q), 150.7 (2'- and 6'-CH), 146.3–146.3 (4- and 4'- C_q), 121.6 (3'- and 5'-CH), 118.2 (3- and 5-CH), 24.8 (2- and 6- CH_3).

IR (ATR, cm^{-1}) $\tilde{\nu}$ = 3027 (w), 2980 (w), 2921 (m), 2851 (w), 1595 (vs), 1572 (s), 1541 (vs), 1395 (s), 1215 (m), 989 (m), 819 (vs), 647 (vs), 561 (s), 459 (s).

MS (EI, 70 eV) m/z (%) = 185 (15) $[\text{M}+\text{H}]^+$, 184 (100) $[\text{M}]^+$, 183 (6) $[\text{M}-\text{H}]^+$, 168 (4), 142 (4), 115 (6).

HRMS (EI, $[\text{M}]^+$, $\text{C}_{12}\text{H}_{12}\text{N}_2$) calcd.: 184.0995, found: 184.0995.

2-Fluoro-4,4'-bipyridine (13)

2-fluoro-4-iodopyridine (1.11 g, 5.00 mmol, 1.00 equiv), 4-pyridylboronic acid (738 mg, 6.00 mmol, 1.20 equiv), tris(dibenzylideneacetone)dipalladium chloroform (25.9 mg, 25.0 μ mol, 5 mol%), tricyclohexylphosphane (16.8 mg, 60.0 μ mol, 12 mol%) and potassium phosphate (2.12 g, 10.0 mmol, 2.00 equiv) were combined with a degassed mixture of 1,4-dioxane (12.0 mL) and water (5.00 mL). After stirring for 16 h at 110 °C, the mixture was cooled to 21 °C, extracted with ethyl acetate, and washed with water and brine. The combined organic phase was dried over sodium sulfate and filtered, and the solvent was removed under reduced pressure. The crude product was purified *via* flash-chromatography on silica gel using dichloromethane with 5% methanol to yield the title compound (779 mg, 4.47 mmol, 89% yield) as a colorless solid.

m.p.: 212 °C

R_f = 0.45 (dichloromethane + 5% methanol)

^1H NMR (400 MHz, CDCl_3 , ppm) δ = 8.79–8.73 (m, 2H), 8.35 (d, J = 5.3 Hz, 1H), 7.55–7.49 (m, 2H), 7.43 (ddd, J = 5.2, 1.7, J = 1.7 Hz, 1H), 7.19–7.14 (m, 1H).

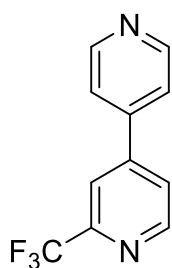
^{13}C NMR (101 MHz, CDCl_3 , ppm) δ = 164.7 (d, J = 239.4 Hz), 151.4 (d, J = 8.0 Hz), 151.0 (2C), 148.8 (d, J = 15.3 Hz), 144.5 (d, J = 3.3 Hz), 121.5 (2C), 119.5 (d, J = 4.2 Hz), 107.6 (d, J = 38.5 Hz).

^{19}F NMR (376 MHz, CDCl_3 , ppm) δ = -66.8 (2-CF).

IR (ATR, cm^{-1}) $\tilde{\nu}$ = 3070 (w), 3044 (w), 3023 (w), 2965 (w), 2945 (w), 2927 (w), 2887 (w), 2863 (w), 1619 (w), 1609 (w), 1596 (vs), 1574 (w), 1537 (m), 1475 (m), 1417 (w), 1398 (vs), 1346 (w), 1336 (w), 1317 (m), 1289 (w), 1247 (w), 1221 (w), 1200 (s), 1126 (w), 1096 (w), 1078 (w), 1058 (w), 990 (m), 966 (w), 894 (s), 857 (m), 815 (vs), 737 (m), 667 (w), 640 (w), 616 (vs), 558 (s), 535 (vs), 497 (w), 482 (w), 469 (w), 439 (vs), 381 (w).

MS (EI, 70 eV), m/z (%): 293 (17), 281 (29), 262 (34), 243 (28), 231 (31), 181 (58), 175 (11) $[\text{M}+\text{H}]^+$, 174 (100) $[\text{M}]^+$, 173 (25), 162 (5), 147 (8), 134 (6), 131 (14), 121 (6).

HRMS (EI, $[\text{M}]^+$, $\text{C}_{10}\text{H}_7\text{N}_2\text{F}$) calcd.: 174.0588, found: 174.0589.

2-Trifluoromethyl-4,4'-bipyridine (14)

4-iodopyridine (471 mg, 2.30 mmol, 1.00 equiv), 4-(4,4,5,5-tetramethyl-1,3,2-dioxaborolan-2-yl)-2-(trifluoromethyl)pyridine (691 mg, 2.53 mmol, 1.10 equiv), potassium carbonate (795 mg, 5.75 mmol, 2.50 equiv), triphenylphosphine (60.3 mg, 230 μ mol, 10 mol%) and palladium(II) acetate (25.8 mg, 115 μ mol, 5 mol%) were combined with a degassed mixture of tetrahydrofuran (10.0 mL) and water (2.00 mL). After stirring for 20 h at 70 °C, the mixture was cooled to 21 °C, extracted with dichloromethane, and washed with water and brine. The combined organic phase was dried over sodium sulfate and filtered, and the solvent was removed under reduced pressure. The crude product was purified *via* flash-chromatography on silica gel using dichloromethane with 2% to 10% methanol to yield the title compound (434 mg, 1.93 mmol, 84% yield) as a colorless solid.

m.p.: 86 °C

R_f = 0.08 (dichloromethane + 5% methanol)

^1H NMR (500 MHz, CDCl_3 , ppm) δ = 8.84 (d, J = 5.1 Hz, 1H, 6-CH), 8.80–8.75 (m, 2H, 2'- and 6'-CH), 7.90 (d, J = 1.7 Hz, 1H, 3-CH), 7.72 (dd, J = 5.1, 1.7 Hz, 1H, 5-CH), 7.57–7.53 (d, J = 4.6 Hz, 2H, 3'- and 5'-CH).

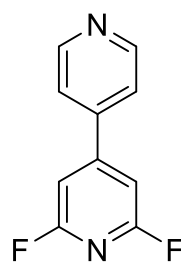
^{13}C NMR (126 MHz, CDCl_3 , ppm) δ = 151.1 (d, J = 5.9 Hz, 2C, 2'- and 6'-CH), 149.5 (q, J = 34.9 Hz, 2- $\text{C}_q\text{-CF}_3$), 147.6 (4- C_q), 144.3 (4'- C_q), 132.7 (d, J = 104.0 Hz), 124.2 (5-CH), 121.5 (2C, 3'- and 5'-CH), 121.5 (q, J = 274.5 Hz, 2- CCF_3), 118.5 (q, J = 2.8 Hz, 3-CH).

^{19}F NMR (376 MHz, CDCl_3 , ppm) δ = -68.0 (2- CF_3).

IR (ATR, cm^{-1}) $\tilde{\nu}$ = 3210 (w), 3197 (w), 3163 (w), 3098 (w), 3085 (w), 3061 (w), 3044 (w), 2951 (w), 2922 (w), 2866 (w), 1741 (vw), 1595 (m), 1540 (w), 1426 (m), 1409 (m), 1341 (m), 1327 (s), 1305 (w), 1269 (m), 1237 (w), 1224 (m), 1186 (vs), 1120 (vs), 1109 (vs), 1086 (vs), 1054 (vs), 1028 (m), 987 (m), 969 (w), 905 (m), 873 (m), 850 (w), 836 (m), 819 (vs), 755 (w), 745 (m), 721 (m), 696 (m), 686 (vs), 654 (m), 613 (vs), 584 (m), 552 (m), 540 (s), 518 (vs), 462 (w), 433 (w), 418 (m), 402 (w).

MS (EI, 70 eV) m/z (%) = 225 (11) $[\text{M}+\text{H}]^+$, 224 (100) $[\text{M}]^+$, 223 (3) $[\text{M}-\text{H}]^+$, 205 (3), 203 (4), 156 (3), 155 (25), 128 (4), 102 (4), 101 (3), 51 (3).

HRMS (EI, $[\text{M}]^+$, $\text{C}_{11}\text{H}_7\text{N}_2\text{F}_3$) calcd.: 224.0556, found: 224.0555.

2,6-Difluoro-4,4'-bipyridine (3)¹⁵

2,6-Difluoro-4-iodopyridine (1.10 g, 4.56 mmol, 1.00 equiv), 4-pyridylboronic acid (673 mg, 5.48 mmol, 1.20 equiv), potassium carbonate (1.94 g, 9.13 mmol, 2.00 equiv), tricyclohexylphosphane (128 mg, 456 μ mol, 10 mol%) and tris(dibenzylideneacetone)dipalladium chloroform (236 mg, 228 μ mol, 5 mol%) were combined with a degassed mixture of tetrahydrofuran (20.0 mL) and water (4.00 mL). After stirring for 18 h at 90 °C, the mixture was cooled to 21 °C, extracted with dichloromethane, and washed with water and brine. The combined organic phase was dried over sodium sulfate and filtered, and the solvent was removed under reduced pressure. The crude product was purified *via* flash-chromatography on silica gel using dichloromethane with 2% to 5% methanol to yield the title compound (736 mg, 3.83 mmol, 84% yield) as a colorless solid.

m.p.: 205 °C

R_f = 0.54 (chloroform/acetone/methanol/ NH_3 , 150:40:9:1)

^1H NMR (500 MHz, CDCl_3 , ppm) δ = 8.69–8.66 (m, 2H, 2'- and 6'-CH), 7.52–7.47 (m, 2H, 3- and 5-CH), 7.04 (s, 2H, 3- and 5-CH).

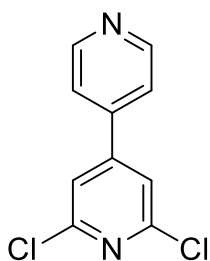
^{13}C NMR (126 MHz, CDCl_3 , ppm) δ = 162.4 (dd, J = 248 Hz, J = 15.8 Hz, 2C, 2- and 6-CF), 155.4 (dd, J = 8.0 Hz, 4'-C_q), 150.5 (2C, 2'-CH and 6'-CH), 144.0 (dd, J = 3.2 Hz, 4-C_q), 121.6 (2C, 3'-CH and 5'-CH), 104.5–104.1 (m, 2C, 3- and 5-CH).

^{19}F NMR (376 MHz, CDCl_3 , ppm) δ = -66.8 (2- and 6-CF).

IR (ATR, cm^{-1}) $\tilde{\nu}$ = 3072, 3027, 2959, 2922, 2898, 2851, 1945, 1625, 1598, 1575, 1551, 1531, 1506, 1439, 1425, 1404, 1361, 1336, 1266, 1220, 1210, 1128, 1078, 1027, 992, 967, 877, 822, 650, 642, 608, 551, 479.

MS (EI, 70 eV) m/z (%) = 193 (12%) $[\text{M}+\text{H}]^+$, 192 (100%) $[\text{M}]^+$, 191 (23%) $[\text{M}-\text{H}]^+$, 190 (31%), 181 (17%), 162 (16%).

HRMS (EI, $[\text{M}]^+$, $\text{C}_{10}\text{H}_6\text{F}_2\text{N}_2$) calcd.: 192.0499, found: 192.0500.

2,6-Dichloro-4,4'-bipyridine (16)

2,6-dichloro-4-iodopyridine (500 mg, 1.83 mmol, 1.00 equiv), 4-pyridylboronic acid (270 mg, 2.20 mmol, 1.20 equiv), tricyclohexylphosphane (61.4 mg, 219 μ mol, 12 mol%), potassium phosphate (775 mg, 3.65 mmol, 2.00 equiv) and tris(dibenzylideneacetone)dipalladium chloroform (18.9 mg, 18.3 μ mol, 10 mol%) were combined with a degassed mixture of 1,4-dioxane (8.00 mL) and water (3.00 mL). After stirring for 18 h at 90 °C, the mixture was cooled to 21 °C, extracted with dichloromethane, and washed with water and brine. The combined organic phase was dried over sodium sulfate and filtered, and the solvent was removed under reduced pressure. The crude product was purified *via* automatic flash-chromatography on silica gel using dichloromethane with 1% to 11% methanol to yield the title compound (305 mg, 1.36 mmol, 74%) as a yellow solid.

m.p.: 184 °C

R_f = 0.52 (dichloromethane + 5% methanol)

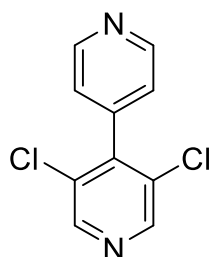
^1H NMR (500 MHz, CDCl_3 , ppm) δ = 8.81–8.75 (m, 2H, 2'- and 6'-CH), 7.50 (s, 2H, 3- and 5-CH), 7.49–7.47 (m, 2H, 3'- and 5'-CH).

^{13}C NMR (126 MHz, CDCl_3 , ppm) δ = 151.7 (2- and 6- C_q), 151.2 (4- C_q), 151.2 (2'- and 6'-CH), 143.2 (4'- C_q), 121.4 (3- and 5-CH), 121.0 (3'- and 5'-CH).

IR (ATR, cm^{-1}) $\tilde{\nu}$ = 3041 (ν -C-H, w), 2928 (w), 1943 (vw), 1578 (vs), 1519 (s), 1366 (vs), 1171 (s), 1125 (s), 982 (w), 881 (w), 809 (vs), 628 (vs), 547 (m), 462 (w), 432 (m).

MS (EI, 70 eV, 20 °C, %) m/z = 228 (11) [M ($^{37}\text{Cl}_2$) $^+$], 227 (7), 226 (62) [M ($^{37}\text{Cl}^{35}\text{Cl}$) $^+$], 225 (12), 224 (100) [M ($^{35}\text{Cl}_2$) $^+$], 191 (15) [$\text{M}-\text{Cl}$] $^+$, 190 (6), 189 (44) [$\text{M}-\text{Cl}$] $^+$, 127 (16), 126 (9), 51 (13).

HRMS (EI, [M] $^+$, $\text{C}_{10}\text{H}_6\text{N}_2^{35}\text{Cl}_2$) calcd.: 223.9903, found: 223.9904.

3,5-Dichloro-4,4'-bipyridine (17)

3,5-dichloro-4-iodopyridine (500 mg, 1.83 mmol, 1.00 equiv), 4-pyridylboronic acid (270 mg, 2.19 mmol, 1.20 equiv), tris(dibenzylideneacetone)dipalladium chloroform (94.8 mg, 91.6 μmol , 5 mol%), tricyclohexylphosphane (61.7 mg, 220 μmol , 12 mol%) and potassium carbonate (776 mg, 3.65 mmol, 2.00 equiv) were combined with a degassed mixture of 1,4-dioxane (8.00 mL) and water (3.00 mL). After stirring for 18 h at 90 °C, the mixture was cooled to 21 °C, extracted with dichloromethane, and washed with water and brine. The combined organic phase was dried over sodium sulfate and filtered, and the solvent was removed under reduced pressure. The crude product was purified *via* flash-chromatography on silica gel using dichloromethane with 2% to 5% methanol to yield the title compound (284 mg, 1.26 mmol, 69% yield) as yellow crystals.

m.p.: 109 °C

R_f = 0.60 (dichloromethane + 5% methanol)

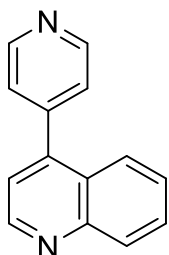
^1H NMR (500 MHz, CDCl_3 , ppm) δ = 8.80–8.77 (m, 2H, 2'- and 6'-CH), 8.62 (s, 2H, 2- and 6-CH), 7.24–7.21 (m, 2H, 3'- and 5'-CH).

^{13}C NMR (126 MHz, CDCl_3 , ppm) δ = 150.3 (2C, 2'- and 6'- C_q), 148.0 (2C, 2- and 6- C_q), 144.0 (4- C_q), 141.8 (4'- C_q), 131.2 (2C, 3- and 5- C_q), 123.6 (2C, 3' and 5'-CH).

IR (ATR, cm^{-1}) $\tilde{\nu}$ = 3070 (vw), 3026 (vw), 2925 (w), 2850 (w), 1963 (vw), 1868 (vw), 1817 (w), 1718 (vw), 1601 (w), 1544 (m), 1412 (m), 1401 (m), 1384 (s), 1218 (s), 1205 (s), 884 (m), 800 (vs), 748 (s), 632 (s), 581 (vs).

MS (EI, 70 eV) m/z (%) = 228 (10) $[\text{M} (^{37}\text{Cl}_2)]^+$, 227 (6), 226 (59) $[\text{M} (^{37}\text{Cl}^{35}\text{Cl})]^+$, 225 (12), 224 (100) $[\text{M} (^{35}\text{Cl}_2)]^+$, 191 (6) $[\text{M}-\text{Cl}]^+$, 189 (20) $[\text{M}-\text{Cl}]^+$, 162 (8), 153 (12), 127 (9), 126 (9), 99 (11), 74 (11), 51 (7).

HRMS (EI, $[\text{M}]^+$, $\text{C}_{10}\text{H}_6\text{N}_2^{35}\text{Cl}_2$) calcd.: 223.9903, found: 223.9902.

4-(Pyridin-4-yl)quinoline (18)

4-bromoquinoline (500 mg, 2.88 mmol, 1.00 equiv), 4-pyridylboronic acid (355 mg, 2.88 mmol, 1.20 equiv), tris(dibenzylideneacetone)dipalladium chloroform (149 mg, 144 μ mol, 5 mol% equiv), tricyclohexylphosphane (80.9 mg, 288 μ mol, 0.100 equiv) and potassium carbonate (1.02 g, 4.81 mmol, 2.00 equiv) were combined with a degassed mixture of 1,4-dioxane (7.00 mL) and water (3.00 mL). After stirring for 18 h at 90 °C, the mixture was cooled to 21 °C, extracted with dichloromethane, and washed with water and brine. The combined organic phase was dried over sodium sulfate and filtered, and the solvent was removed under reduced pressure. The crude product was purified *via* flash-chromatography on silica gel using dichloromethane with 2% to 5% methanol to yield the title compound (448 mg, 2.17 mmol, 90% yield) as a yellow hygroscopic solid.

m.p.: 88 °C

R_f = 0.29 (dichloromethane + 5% methanol)

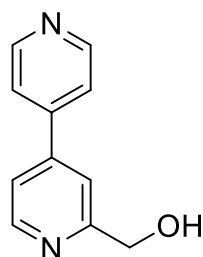
^1H NMR (500 MHz, CDCl_3 , ppm) δ = 8.98 (d, J = 4.4 Hz, 1H, CH), 8.82–8.75 (m, 2H, CH), 8.20 (d, J = 8.4 Hz, 1H, CH), 7.81 (dd, J = 8.4, 1.8 Hz, 1H, CH), 7.76 (ddd, J = 8.4, 6.9, 1.4 Hz, 1H, CH), 7.54 (ddd, J = 8.4, 6.9 Hz, 1.4 Hz, 1H, CH), 7.46–7.41 (m, 2H, CH), 7.32 (d, J = 4.3 Hz, 1H, CH). The spectrum contains traces of grease.

^{13}C NMR (126 MHz, CDCl_3 , ppm) δ = 150.3 (2C, $2^{\text{Py}}, 6^{\text{Py}}\text{-CH}$), 150.1 (1C, 2-CH), 148.8 (1C, 8a- C_q), 146.0 (1C, 4^{Py}-C_q), 145.6 (1C, 4- C_q), 130.3 (1C, 8-CH), 129.9 (1C, 7-CH), 127.4 (1C, 6-CH), 125.9 (1C, 4a- C_q), 125.1 (1C, 5-CH), 124.4 (2C, $3^{\text{Py}}, 5^{\text{Py}}\text{-CH}$), 121.1 (1C, 3-CH). The spectrum contains traces of grease.

IR (ATR, cm^{-1}) $\tilde{\nu}$ = 3068 (w), 3031 (w), 2999 (w), 2925 (w), 2850 (w), 1935 (vw), 1581 (s), 1407 (m), 833 (s), 815 (s), 776 (vs), 609 (vs), 568 (vs), 414 (s).

MS (EI, 70 eV) m/z (%) = 207 (13) $[\text{M}+\text{H}]^+$, 206 (100) $[\text{M}]^+$, 205 (65) $[\text{M}-\text{H}]^+$, 179 (7), 178 (11), 152 (5), 151 (11), 58 (6).

HRMS (EI, $[\text{M}]^+$, $\text{C}_{14}\text{H}_{10}\text{N}_2$) calcd.: 206.0838, found: 206.0839.

[4,4'-Bipyridin]-2-ylmethanol (19)

(4-Bromopyridin-2-yl)methanol (230 mg, 1.22 mmol, 1.00 equiv), 4-pyridylboronic acid (226 mg, 1.83 mmol, 1.50 equiv), 4 M aqueous solution of sodium carbonate (972 mg, 9.17 mmol, 7.50 equiv) and tetrakis(triphenylphosphane)palladium(0) (141 mg, 122 μ mol, 10 mol%) were combined with degassed 1,2-dimethoxyethane (5.00 mL). After stirring for 20 h at 100 $^{\circ}$ C, the reaction mixture was cooled to 21 $^{\circ}$ C, extracted with ethyl acetate, and washed with water and brine. The combined organic phase was dried over sodium sulfate and filtered, and the solvent was removed under reduced pressure. The crude product was purified *via* flash-chromatography on silica gel using dichloromethane with 5% methanol to yield the title compound (158 mg, 851 μ mol, 70% yield) as a colorless solid.

m.p.: 91 $^{\circ}$ C

R_f = 0.35 (cyclohexane/ethyl acetate, 1:1)

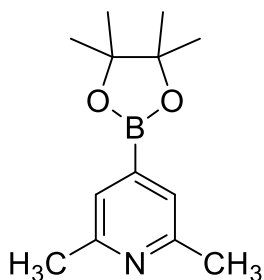
^1H NMR (400 MHz, CDCl_3 , ppm) δ = 8.78–8.71 (m, 2H, 2'- and 6'-CH), 8.68 (dd, J = 5.2, 0.9 Hz, 1H, 6-CH), 7.56–7.53 (m, 2H, 3'- and 5'-CH), 7.53–7.51 (m, 1H, 3-CH), 7.47–7.43 (m, 1H, 5-CH), 4.87 (s, 2H, CH_2), 3.62 (s, 1H, OH).

^{13}C NMR (101 MHz, CDCl_3 , ppm) δ = 160.5 (2- C_q), 150.9 (2C, 2'- and 6'-CH), 149.6 (6-CH), 146.6 (4- C_q), 145.7 (4'- C_q), 121.6 (2C, 3'- and 5'-CH), 120.4 (5-CH), 118.3 (3-CH), 64.5 (CH_2).

IR (ATR, cm^{-1}) $\tilde{\nu}$ = 3123 (m), 3047 (m), 3030 (m), 2969 (w), 2945 (w), 2919 (w), 2866 (w), 2829 (m), 2825 (m), 2715 (w), 2645 (w), 2639 (w), 1608 (w), 1592 (vs), 1567 (m), 1536 (s), 1499 (w), 1479 (w), 1442 (w), 1421 (w), 1401 (vs), 1364 (s), 1332 (w), 1303 (m), 1241 (w), 1215 (w), 1207 (w), 1118 (w), 1078 (w), 1065 (w), 1033 (vs), 1006 (m), 989 (m), 973 (m), 912 (m), 877 (w), 863 (m), 822 (vs), 745 (s), 732 (s), 674 (w), 660 (w), 618 (vs), 575 (vs), 540 (vs), 518 (m), 463 (vs), 428 (w), 405 (m), 382 (w).

MS (EI, 70 eV) m/z (%) = 281 (12), 269 (17), 231 (15), 219 (22), 187 (11) $[\text{M}+\text{H}]^+$, 186 (86) $[\text{M}]^+$, 185 (100) $[\text{M}-\text{H}]^+$, 181 (27), 169 (31), 157 (41), 156 (21), 155 (26), 131 (27), 119 (27), 100 (6), 77 (6), 69 (85), 51 (6).

HRMS (EI, $[\text{M}]^+$, $\text{C}_{11}\text{H}_{10}\text{N}_2\text{O}$) calcd.: 186.0788, found: 186.0786.

2,6-Dimethyl-4-(4,4,5,5-tetramethyl-1,3,2-dioxaborolan-2-yl)pyridine (38)

4-Bromo-2,6-dimethyl-pyridine (1.00 g, 5.37 mmol, 1.00 equiv), B₂Pin₂ (1.50 g, 5.91 mmol, 1.10 equiv), palladium(II) acetate (60.3 mg, 269 μmol, 5 mol% equiv), tricyclohexylphosphane (151 mg, 537 μmol, 10 mol%) and potassium acetate (1.32 g, 13.4 mmol, 2.50 equiv) were combined with degassed 1,4-dioxane (20.0 ml). After stirring for 18 h at 110 °C, the mixture was cooled to 21 °C and filtered through a short

plug of Celite® with dichloromethane. The solvent was removed under reduced pressure, and the crude was redissolved in chloroform. It was washed with water, dried over sodium sulfate, and suspended over activated charcoal (2.0 g) for two hours. It was filtered, and the solvent was removed under reduced pressure. The crude product was purified *via* sublimation at 0.100 mbar and 65 °C to yield the title compound (804 mg, 3.45 mmol, 64% yield) as white hygroscopic crystals.

$R_f = 0.14$ (dichloromethane/methanol, 4:1)

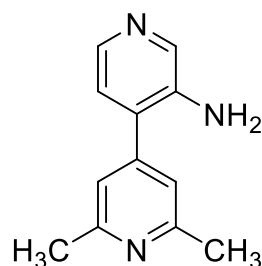
¹H NMR (500 MHz, CDCl₃, ppm) $\delta = 7.30$ (s, 2H, 3- and 5-CH), 2.52 (s, 6H, 2- and 6-CH₃), 1.34 (s, 12H, 4 × CH₃).

¹³C NMR (126 MHz, CDCl₃, ppm) $\delta = 157.2$ (2C, 2- and 6-C_q), 125.4 (2C, 3- and 5-CH), 84.5 (2C, 2 × C_q(CH₃)₂), 25.0 (4C, 4 × CH₃), 24.3 (2C, 2- and 6-CH₃). 4-C_q is not visible due to boron.

IR (ATR, cm⁻¹) $\tilde{\nu} = 3048$ (vw), 2978 (m), 2928 (w), 1632 (w), 1548 (w), 1519 (w), 1473 (w), 1452 (w), 1390 (vs), 1371 (vs), 1358 (vs), 1322 (vs), 1249 (s), 1213 (m), 1163 (m), 1142 (vs), 1116 (vs), 1007 (w), 983 (w), 963 (m), 891 (m), 871 (w), 849 (vs), 734 (m), 694 (w), 674 (vs), 578 (w), 562 (w), 523 (w), 449 (w), 414 (w).

MS (EI, 70 eV) m/z (%) = 234 (10), 233 (70) [M(¹¹B) +H]⁺, 232 (18) [M(¹¹B)]⁺, 231 (8) [M(¹⁰B)]⁺, 218 (33), 217 (8), 181 (41), 176 (8), 148 (13), 147 (100), 134 (33), 133 (37), 132 (11), 131 (43), 129 (13), 119 (8), 100 (9), 69 (78), 59 (14), 58 (13).

HRMS (EI, [M]⁺, C₁₃H₂₀O₂N¹¹B) calcd.: 233.1582, found: 233.1581.

2',6'-Dimethyl-[4,4'-bipyridin]-3-amine (37)

4-bromopyridin-3-amine (215 mg, 1.24 mmol, 1.00 equiv), 2,6-dimethyl-4-(4,4,5,5-tetramethyl-1,3,2-dioxaborolan-2-yl)pyridine (**38**) (348 mg, 1.49 mmol, 1.20 equiv), potassium phosphate (527 mg, 2.48 mmol, 2.00 equiv), tricyclohexylphosphane (34.8 mg, 124 μ mol, 10 mol%) and tris(dibenzylideneacetone)dipalladium chloroform (64.2 mg, 62.0 μ mol, 5 mol%) were combined with a degassed mixture of 1,4-dioxane (5.00 mL) and water (2.10 mL). After stirring for 17.5 h at 90 °C, the mixture was cooled to 21 °C, extracted with dichloromethane, and washed with water and brine. The combined organic phase was dried over sodium sulfate and filtered, and the solvent was removed under reduced pressure. The crude product was purified *via* flash-chromatography on silica gel using dichloromethane with 2% to 5% methanol to yield the title compound (115 mg, 577 μ mol, 46% yield) as an orange solid.

m.p.: 168 °C

R_f = 0.24 (dichloromethane + 5% methanol)

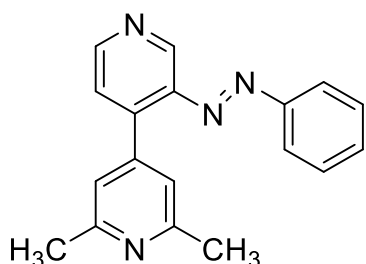
^1H NMR (500 MHz, CDCl_3 , ppm) δ = 8.18 (s, 1H, 2-CH), 8.08 (d, J = 4.9 Hz, 1H, 6-CH), 7.06 (s, 2H, 3'- and 5'-CH), 7.00 (d, J = 4.9 Hz, 1H, 5-CH), 3.80 (s, 2H, NH_2), 2.59 (s, 6H, 2'- and 6'- CH_3).

^{13}C NMR (126 MHz, CDCl_3 , ppm) δ = 159.0 (2C, 2'- and 6'- C_q), 145.6 (C_q), 140.4 (6-CH), 139.5 (C_q), 138.6 (2-CH), 131.2, 123.6 (5-CH), 119.7 (2C, 3'- and 5'-CH), 24.8 (2C, 2'- and 6'- CH_3).

IR (ATR, cm^{-1}) $\tilde{\nu}$ = 3336 (m), 3160 (s), 2921 (w), 2850 (w), 1738 (vw), 1656 (w), 1608 (s), 1588 (s), 1565 (vs), 1541 (s), 1500 (m), 1422 (vs), 1400 (vs), 1374 (m), 1324 (s), 1295 (m), 1238 (s), 1220 (s), 1064 (s), 1028 (m), 870 (m), 815 (vs), 759 (m), 735 (m), 664 (m), 653 (vs), 626 (s), 596 (m), 572 (s), 551 (s), 540 (vs), 518 (s), 480 (s), 463 (m), 449 (s), 409 (m), 394 (m).

MS (EI, 70 eV) m/z (%) = 200 (14) $[\text{M}+\text{H}]^+$, 199 (100) $[\text{M}]^+$, 198 (15) $[\text{M}-\text{H}]^+$, 184 (10), 169 (5), 158 (6), 157 (8), 69 (13).

HRMS (EI, $[\text{M}]^+$, $\text{C}_{12}\text{H}_{13}\text{N}_3$) calcd.: 199.1104, found: 199.1104.

(E)-2,6-dimethyl-3'-(phenyldiazenyl)-4,4'-bipyridine (40)

2',6'-dimethyl-[4,4'-bipyridin]-3-amine (**37**) (73.0 mg, 366 μ mol, 1.00 equiv) was combined with pyridine (1.00 mL), and tetramethylammonium hydroxide (1.07 g, 1.07 mL, 2.93 mmol, 8.00 equiv) solution was added. It was heated up to 80 °C, and a solution of nitrosobenzene (58.9 mg, 57.7 μ L,

550 μ mol, 1.50 equiv) in pyridine (1.50 mL) was slowly added over 60 minutes *via* a syringe pump. After stirring for another 4 hours at 80 °C it was extracted with ethyl acetate and washed with water and brine. The combined organic phase was dried over sodium sulfate and filtered, and the solvent was removed under reduced pressure. The crude product was purified *via* flash-chromatography on silica gel using dichloromethane with 2% to 6% methanol in darkness to yield the title compound (98.4 mg, 341 μ mol, 93% yield) as a purple solid.

m.p.: 143 °C

R_f = 0.33 (dichloromethane + 5% methanol)

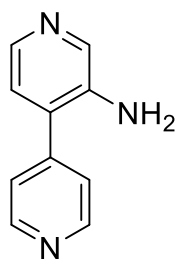
^1H NMR (500 MHz, CDCl_3 , ppm) δ = 8.90 (s, 1H, 2'-CH), 8.75 (d, J = 5.1 Hz, 1H, 6'-CH), 7.85–7.78 (m, 2H, 2 \times phenyl-CH), 7.53–7.49 (m, 3H, 3 \times phenyl-CH), 7.48 (d, J = 5.1 Hz, 1H, 5'-CH), 7.09 (s, 2H, 3- and 5-CH), 2.60 (s, 6H, 2 \times CH_3).

^{13}C NMR (126 MHz, CDCl_3 , ppm) δ = 157.8 (2C, 2- and 6- C_q), 152.8 (phenyl- C_q), 151.4 (6'-CH), 144.8, 144.7 (2C), 138.8 (2'-CH), 132.1 (phenyl-CH), 129.4 (2C, 2 \times phenyl-CH), 124.1 (5'-CH), 123.5 (2C, 2 \times phenyl-CH), 121.7 (2C, 3- and 5-CH), 24.7 (2C, 2- and 6- CH_3).

IR (ATR, cm^{-1}) $\tilde{\nu}$ = 3036 (w), 3004 (w), 2918 (w), 1606 (w), 1582 (s), 1568 (m), 1536 (s), 1489 (w), 1468 (w), 1458 (w), 1445 (w), 1409 (w), 1390 (m), 1303 (w), 1227 (w), 1207 (w), 1186 (w), 1149 (w), 1055 (w), 1030 (w), 1021 (w), 999 (w), 980 (w), 933 (w), 873 (w), 837 (vs), 810 (w), 778 (m), 755 (vs), 731 (w), 690 (vs), 647 (s), 622 (w), 613 (w), 584 (m), 567 (m), 537 (vs), 514 (vs), 470 (m), 435 (w), 409 (w).

MS (EI, 70 eV) m/z (%) = 316 (8), 315 (10), 289 (21) $[\text{M}+\text{H}]^+$, 288 (100) $[\text{M}]^+$, 273 (24), 184 (7), 183 (35), 168 (13), 167 (10), 121 (14), 115 (7), 105 (39), 77 (87), 69 (12), 58 (9).

HRMS (EI, $[\text{M}]^+$, $\text{C}_{18}\text{H}_{16}\text{N}_4$) calcd.: 288.1369, found: 288.1371.

3-Amino-4,4'-bipyridine (36)

4-bromopyridin-3-amine (200 mg, 1.16 mmol, 1.00 equiv), 4-pyridylboronic acid (171 mg, 1.39 mmol, 1.20 equiv), potassium phosphate (490 mg, 2.31 mmol, 2.00 equiv), tricyclohexylphosphane (32.4 mg, 116 μ mol, 10 mol%) and tris(dibenzylideneacetone)dipalladium chloroform (59.7 mg, 57.7 μ mol, 5 mol%) were combined with a degassed mixture of 1,4-dioxane (3.00 mL) and water (1.30 mL). After stirring for 17.5 h at 90 °C, the mixture was cooled to 21 °C, extracted with dichloromethane, and washed with water and brine. The combined organic phase was dried over sodium sulfate and filtered, and the solvent was removed under reduced pressure. The crude product was purified *via* flash-chromatography on silica gel using dichloromethane with 2% to 5% methanol to yield the title compound (107 mg, 626 μ mol, 54% yield) was obtained as an orange, hygroscopic solid.

R_f = 0.89 (dichloromethane + 5% methanol)

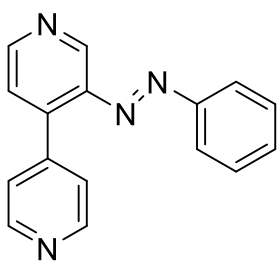
^1H NMR (500 MHz, CDCl_3 , ppm) δ = 8.77–8.71 (m, 2H, 2'- and 6'-CH), 8.19 (s, 1H, 2-CH), 8.10 (d, J = 4.9 Hz, 1H, 6-CH), 7.44–7.39 (m, 2H, 3'- and 5'-CH), 7.02 (d, J = 4.9 Hz, 1H, 5-CH), 3.83 (s, 2H, NH_2).

^{13}C NMR (126 MHz, CDCl_3 , ppm) δ = 150.9 (2C, 2'- and 6'- C_q), 145.0 (C_q), 140.5 (6-CH), 139.4 (C_q), 138.8 (2-CH), 130.5 (C_q), 123.6 (5-CH), 123.3 (2C, 3'- and 5'-CH).

IR (ATR, cm^{-1}) $\tilde{\nu}$ = 3381 (w), 3322 (w), 3163 (m), 3067 (w), 3058 (w), 3036 (w), 1942 (vw), 1655 (w), 1599 (w), 1585 (m), 1557 (s), 1534 (w), 1504 (w), 1479 (m), 1419 (m), 1404 (vs), 1333 (w), 1317 (m), 1296 (w), 1279 (w), 1238 (m), 1214 (w), 1061 (m), 1031 (w), 993 (w), 858 (w), 832 (w), 812 (vs), 744 (m), 735 (m), 673 (s), 660 (s), 626 (vs), 581 (vs), 530 (vs), 497 (s), 486 (s), 448 (s), 441 (s), 409 (m).

MS (EI, 70 eV) m/z (%) = 172 (13) $[\text{M}+\text{H}]^+$, 171 (100) $[\text{M}]^+$, 170 (24) $[\text{M}-\text{H}]^+$, 144 (18), 143 (9), 117 (5), 116 (6), 89 (5).

HRMS (EI, $[\text{M}]^+$, $\text{C}_{10}\text{H}_9\text{N}_3$) calcd.: 206.0838, found: 206.0839.

(E)-3-(phenyldiazenyl)-4,4'-bipyridine (39)

3-Amino-4,4'-bipyridine (**36**) (100 mg, 584 μmol , 1.00 equiv) was combined with pyridine (1.00 mL), and tetramethylammonium hydroxide (1.70 g, 1.70 mL, 4.67 mmol, 8.00 equiv) solution was added. It was heated up to 80 °C, and a solution of nitrosobenzene (93.8 mg, 92.0 μL , 876 μmol , 1.50 equiv) in pyridine (1.50 mL) was slowly added over 60 minutes *via* a syringe pump. After stirring for another 4 hours at 80 °C it was extracted with ethyl acetate and washed with water and brine. The combined organic phase was dried over sodium sulfate and filtered, and the solvent was removed under reduced pressure. The crude product was purified *via* flash-chromatography on silica gel using dichloromethane with 3% to 5% methanol in darkness to yield the title compound (125 mg, 480 μmol , 82% yield) as a purple solid.

m.p.: 122 °C

R_f = 0.29 (dichloromethane + 5% methanol)

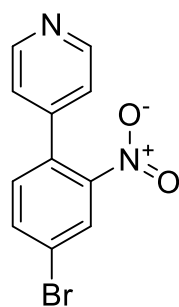
^1H NMR (500 MHz, CDCl_3 , ppm) δ = 8.93 (s, 1H, 2-CH), 8.79 (d, J = 5.1 Hz, 1H, 6-CH), 8.75–8.72 (m, 2H, 2'- and 6'-CH), 7.84–7.79 (m, 2H, 3-ph- and 5-ph-CH), 7.53–7.48 (m, 4H, 5-CH and 2-ph-, 4-ph- and 6-ph-CH), 7.45–7.42 (m, 2H, 3'- and 5'-CH).

^{13}C NMR (126 MHz, CDCl_3 , ppm) δ = 152.7 (C_q), 151.6 (6-CH), 149.8 (2C, 2'- and 6'-CH), 144.5 (C_q), 144.2 (C_q), 144.2 (C_q), 139.0 (2-CH), 132.2 (4-ph-CH), 129.5 (2C, 2-ph- and 6-ph-CH), 125.0 (2C, 3'- and 5'-CH.), 124.0 (5-CH), 123.6 (2C, 3-ph- and 5-ph-CH).

IR (ATR, cm^{-1}) $\tilde{\nu}$ = 3041 (w), 3014 (w), 1582 (s), 1530 (w), 1483 (w), 1468 (w), 1397 (m), 1190 (m), 1139 (m), 1062 (w), 1035 (w), 990 (w), 925 (w), 851 (w), 837 (m), 817 (vs), 772 (m), 752 (vs), 737 (s), 683 (vs), 615 (vs), 588 (m), 575 (s), 537 (vs), 497 (vs), 456 (w), 384 (m).

MS (EI, 70 eV) m/z (%) = 261 (19) $[\text{M}+\text{H}]^+$, 260 (100) $[\text{M}]^+$, 259 (6) $[\text{M}-\text{H}]^+$, 231 (4), 156 (5), 155 (26), 128 (6), 105 (27), 101 (8), 78 (6), 77 (82), 75 (4), 51 (10).

HRMS (EI, $[\text{M}]^+$, $\text{C}_{16}\text{H}_{12}\text{N}_4$) calcd.: 260.1056, found: 260.1058.

4-(4-Bromo-2-nitrophenyl)pyridine (30)

4-Bromo-1-iodo-2-nitrobenzene (328 mg, 1.00 mmol, 1.00 equiv), 4-pyridylboronic acid (123 mg, 1.00 mmol, 1.00 equiv), potassium carbonate (276 mg, 2.00 mmol, 2.00 equiv), triphenylphosphine (26.2 mg, 100 μ mol, 10 mol%) and palladium(II) acetate (33.7 mg, 150 μ mol, 15 mol%) were combined with a degassed mixture of tetrahydrofuran (20.0 mL) and water (10.0 mL). After stirring for 18h at 80 °C, the reaction mixture was cooled to 21 °C, extracted with dichloromethane, and washed with water and brine. The combined organic phase was dried over sodium sulfate and filtered, and the solvent was removed under reduced pressure. The crude product was purified *via* flash-chromatography on silica gel using cyclohexane and ethyl acetate (20:1 to 0:1) to yield the title compound (184 mg, 659 μ mol, 66% yield) as a colorless solid.

m.p.: 158 °C

R_f = 0.17 (cyclohexane/ethyl acetate, 2:1)

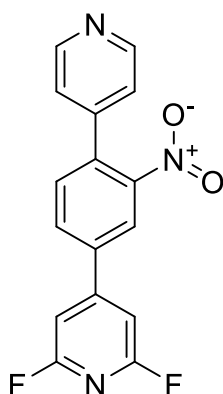
^1H NMR (400 MHz, CDCl_3 , ppm) δ = 8.74–8.63 (m, 2H, 2- and 6-CH), 8.13 (d, J = 2.0 Hz, 1H, 3-ph-CH), 7.82 (dd, J = 8.2, 2.0 Hz, 1H, 5-ph-CH), 7.30 (d, J = 8.2 Hz, 1H, 6-ph-CH), 7.23–7.19 (m, 2H, 3- and 5-CH).

^{13}C NMR (101 MHz, CDCl_3 , ppm) δ = 150.3 (2C, 3- and 5-CH), 149.0 (2-ph- $\text{C}_q\text{-NO}_2$), 144.8 (4- C_q), 136.1 (5-ph-CH), 133.0 (1-ph- C_q), 132.9 (6-ph-CH), 127.8 (3-ph-CH), 123.1 (4-ph-CBr), 122.7 (2C, 3- and 5-CH).

IR (ATR, cm^{-1}) $\tilde{\nu}$ = 3031 (w), 2995 (w), 2966 (w), 2931 (w), 2854 (w), 1599 (m), 1520 (vs), 1472 (s), 1408 (s), 1353 (vs), 1327 (m), 1295 (m), 1268 (m), 1217 (s), 1152 (m), 1095 (m), 1069 (m), 1021 (w), 994 (m), 967 (w), 928 (s), 871 (s), 841 (m), 823 (m), 810 (vs), 768 (vs), 761 (vs), 720 (m), 674 (m), 666 (m), 642 (m), 603 (s), 555 (s), 526 (vs), 458 (w), 436 (vs), 415 (s), 388 (m).

MS (EI, 70 eV) m/z (%) = 281 (15) [$\text{M} (^{81}\text{Br})+\text{H}$] $^+$, 280 (77) [$\text{M} (^{81}\text{Br})$] $^+$, 278 (78) [$\text{M} (^{79}\text{Br})$] $^+$, 253 (14), 252 (100), 251 (22), 250 (94), 225 (24), 224 (15), 223 (31), 222 (14), 197 (15), 195 (21), 169 (14), 153 (17), 126 (42), 116 (21).

HRMS (EI, [M] $^+$, $\text{C}_{11}\text{H}_7^{79}\text{BrN}_2\text{O}_2$) calcd.: 277.9685, found: 277.9684.

2,6-Difluoro-4-(3-nitro-4-(pyridin-4-yl)phenyl)pyridine (31)

4-(4-Bromo-2-nitrophenyl)pyridine (**30**) (278 mg, 996 μmol , 1.00 equiv), (2,6-difluoropyridin-4-yl)boronic acid (174 mg, 1.10 mmol, 1.10 equiv), potassium phosphate (423 mg, 1.99 mmol, 2.00 equiv) tricyclohexylphosphane (33.5 mg, 120 μmol , 12 mol%) and tris(dibenzylideneacetone)dipalladium chloroform (51.6 mg, 49.8 μmol , 5 mol%) were combined with a degassed mixture of 1,4-dioxane (3.00 mL) and water (7.00 mL). After stirring for 18 h at 100 $^{\circ}\text{C}$, the mixture was cooled to 21 $^{\circ}\text{C}$, extracted with dichloromethane, and

washed with water and brine. The combined organic phase was dried over sodium sulfate and filtered, and the solvent was removed under reduced pressure. The crude product was purified *via* flash-chromatography on silica gel using dichloromethane with 2% to 5% methanol to yield the title compound (183 mg, 584 μmol , 59% yield) as a yellow hygroscopic solid.

m.p.: 204 $^{\circ}\text{C}$

R_f = 0.32 (cyclohexane/ethyl acetate, 2:1)

^1H NMR (500 MHz, CDCl_3 , ppm) δ = 8.73 (d, J = 5.2 Hz, 2H, 2'- and 6'-CH), 8.23 (d, J = 1.9 Hz, 1H, 2-ph-CH), 7.93 (dd, J = 8.0, 1.9 Hz, 1H, 6-ph-CH), 7.60 (d, J = 7.9 Hz, 1H, 5-ph-CH), 7.29–7.27 (m, 2H, 3'- and 5'-CH), 7.11 (s, 2H, 3- and 5-CH).

^{13}C NMR (126 MHz, CDCl_3 , ppm) δ = 162.7 (dd, J = 247.7, 16.1 Hz, 2C, 2- and 6-CF), 154.9 (dd, J = 8.2 Hz, 4-C_q), 150.4 (2C, 2'- and 6'-CH), 149.3 (3-ph-C_q-NO₂), 144.7 (4-C_q), 137.9 (dd, J = 3.4 Hz, 1-ph-C_q), 135.6 (4-ph-C_q), 132.9 (5-ph-CH), 131.2 (6-ph-CH), 123.4 (2-ph-CH), 122.7 (2C, 3'- and 5'-CH), 105.4–103.5 (m, 2C, 3- and 5-CH).

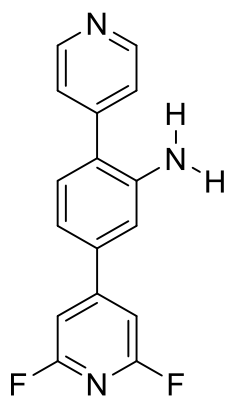
^{19}F NMR (471 MHz, CDCl_3 , ppm) δ = -66.3 (2- and 6-CF).

IR (ATR, cm^{-1}) $\tilde{\nu}$ = 3036 (w), 1618 (vs), 1596 (s), 1572 (w), 1555 (m), 1536 (vs), 1492 (w), 1462 (w), 1422 (vs), 1398 (w), 1375 (m), 1361 (vs), 1262 (w), 1218 (m), 1200 (w), 1163 (w), 1072 (w), 1030 (m), 997 (w), 936 (w), 895 (w), 877 (w), 864 (w), 851 (m), 833 (m), 823 (vs), 765 (m), 752 (s), 722 (w), 683 (w), 666 (w), 635 (w), 594 (w), 561 (w), 538 (w), 514 (m), 435 (w), 419 (w).

MS (EI, 70 eV) m/z (%) = 319 (30), 313 (39) [M]⁺, 285 (44), 281 (18), 269 (36), 239 (19), 231 (23), 230 (27), 219 (46), 181 (27), 169 (55), 131 (29), 119 (33), 69 (100).

HRMS (EI, $[M]^+$, $C_{16}H_9O_2N_3 F_2$) calcd.: 313.0657, found: 313.0655.

5-(2,6-difluoropyridin-4-yl)-2-(pyridin-4-yl) benzeneamine (**32**)



2,6-Difluoro-4-(3-nitro-4-(pyridin-4-yl)phenyl)pyridine (**31**) (507 mg, 1.62 mmol, 1.00 equiv) was dissolved in a solution of dichloromethane (20.0 mL), and methanol (10.0 mL) and 10% palladium on charcoal (170 mg, 160 μ mol, 10 mol%) was added. The reaction was stirred for 5 hours at 21 °C in the high-pressure reactor under an H_2 atmosphere at a pressure of 50 bar. The crude product was filtered through a plug of Celite® with dichloromethane and methanol. The solvent was removed under reduced pressure, and the crude product was purified *via* flash-

chromatography on silica gel using dichloromethane with 2% to 15% methanol to yield the title compound (451 mg, 1.59 mmol, 98% yield) as a yellow solid.

m.p.: 135 °C

R_f = 0.24 (dichloromethane + 5% methanol)

1H NMR (500 MHz, $CDCl_3$, ppm) δ = 8.75–8.69 (m, 2H, 2'- and 6'-CH), 7.46–7.42 (m, 2H, 3'- and 5'-CH), 7.25 (d, 1H, J = 7.8 Hz, 5-ph-CH), 7.07 (dd, 1H, J = 7.9, 1.8 Hz, 6-ph-CH), 7.02 (s, 2H, 3- and 5-CH), 7.00 (d, 1H, J = 1.8 Hz, 2-ph-CH), 4.01 (br s, 2H, NH_2).

^{13}C NMR (126 MHz, $CDCl_3$, ppm) δ = 162.4 (dd, J = 245.8, 16.4 Hz, 2C, 2- and 6-CF), 159.1 (dd, J = 8.1, 4- C_q) 150.7 (2C, 2'- and 6'-CH), 146.6 (4-ph- C_q), 144.3 (3-ph- C_q-NH_2), 137.8 (dd, J = 3.2 Hz, 1-ph- C_q), 131.2 (5-ph-CH), 126.2 (4'- C_q), 123.8 (2C, 3'- and 5'-CH), 117.5 (6-ph-CH), 114.3 (2-ph-CH), 104.5–103.4 (m, 2C, 3- and 5-CH).

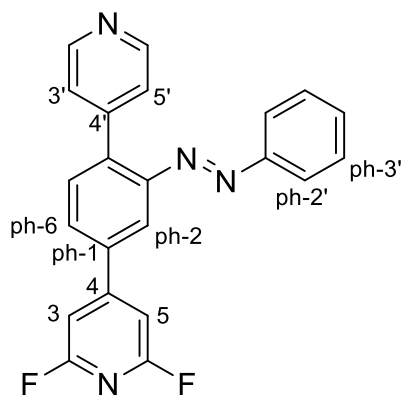
^{19}F NMR (471 MHz, $CDCl_3$, ppm) δ = -68.5 (2- and 6-CF).

IR (ATR, cm^{-1}) $\tilde{\nu}$ = 3353 (w), 3336 (w), 3330 (w), 3320 (w), 3216 (w), 1616 (vs), 1596 (vs), 1550 (vs), 1520 (m), 1462 (m), 1434 (m), 1398 (vs), 1361 (m), 1327 (m), 1310 (m), 1296 (s), 1266 (m), 1204 (s), 1187 (s), 1164 (m), 1119 (w), 1108 (w), 1091 (w), 1068 (w), 1026 (vs), 994 (s), 966 (m), 881 (w), 871 (m), 849 (vs), 833 (m), 802 (vs), 758 (s), 747 (s), 728 (vs), 718 (s), 698 (s), 671 (s), 652 (s), 643 (s), 616 (s), 588 (vs), 568 (vs), 541 (s), 533 (vs), 496 (s), 483 (s), 462 (vs), 432 (s), 416 (s), 409 (s), 399 (s), 388 (s), 382 (s), 375 (s).

MS (EI, 70 eV) m/z (%) = 381 (6), 369 (6), 331 (6), 319 (11), 284 (19), 283 (100), 282 (20), 281 (9), 269 (14), 256 (11), 231 (11), 219 (20), 181 (16), 169 (28), 131 (16), 119 (20), 69 (62).

HRMS (EI, $[M]^+$, $C_{16}H_{11}F_2N_3$) calcd.: 283.0916, found: 283.0917.

(E)-2,6-Difluoro-4-(3-(phenyldiazenyl)-4-(pyridin-4-yl)phenyl)pyridine (33)



5-(2,6-difluoropyridin-4-yl)-2-(pyridin-4-yl)benzeneamine (**32**) (120 mg, 424 μ mol, 1.00 equiv) was combined with a mixture of pyridine (5.00 mL) and toluene (5.00 mL) before nitrosobenzene (90.7 mg, 89.0 μ L, 847 μ mol, 2.00 equiv) was added. It was heated up to 60 $^{\circ}$ C for 4 days before adding more nitrosobenzene (90.7 mg, 89.0 μ L, 847 μ mol, 2.00 equiv). After stirring for another 18 hours at 80 $^{\circ}$ C it was extracted with ethyl acetate and washed with water and

brine. The combined organic phase was dried over sodium sulfate and filtered, and the solvent was removed under reduced pressure. The crude product was purified *via* flash-chromatography on silica gel using dichloromethane with 3% to 5% methanol in darkness to yield the title compound (109 mg, 292 μ mol, 69% yield) as a purple solid.

m.p.: 182 $^{\circ}$ C

R_f = 0.38 (dichloromethane + 5% methanol)

1H NMR (500 MHz, $CDCl_3$, ppm) δ = 8.75–8.70 (m, 2H, 2'- and 6'-CH), 8.07 (d, 1H, J = 1.9 Hz, 2-ph-CH), 7.86–7.80 (m, 3H, 2'-ph-CH, 6'-ph-CH and 6-ph-CH), 7.74 (d, 1H, J = 8.0 Hz, 5-ph-CH), 7.54–7.49 (m, 3H, 3'-ph-CH, 5'-ph-CH and 4'-ph-CH), 7.46–7.43 (m, 2H, 3'- and 5'-CH), 7.16 (s, 2H, 3- and 5-CH).

^{13}C NMR (126 MHz, $CDCl_3$, ppm) δ = 157.2 (), 125.4, 84.5, 25.0, 24.3.

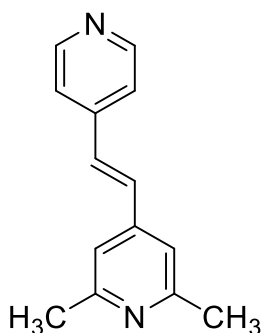
^{19}F NMR (471 MHz, $CDCl_3$, ppm) δ = -67.7 (2- and 6-CF).

IR (ATR, cm^{-1}) $\tilde{\nu}$ = 3043 (w), 2924 (w), 1625 (vs), 1595 (vs), 1572 (m), 1555 (vs), 1536 (w), 1516 (w), 1489 (w), 1459 (m), 1446 (w), 1421 (vs), 1385 (s), 1366 (s), 1309 (w), 1283 (w), 1269 (w), 1254 (w), 1231 (w), 1194 (m), 1163 (w), 1150 (w), 1122 (w), 1071 (w), 1026 (vs), 994 (m), 975 (w), 919 (w), 888 (w), 861 (m), 847 (m), 806 (vs), 765 (m), 748 (vs), 732 (s),

686 (vs), 656 (w), 640 (w), 628 (w), 591 (m), 565 (m), 538 (s), 499 (vs), 467 (w), 455 (w), 443 (w), 429 (w), 416 (m), 398 (w), 384 (w), 375 (w).

MS (EI, 70 eV) m/z (%) = 481 (9), 431 (10), 381 (12), 373 (24), 372 (100), 371 (23), 369 (12), 331 (11), 319 (22), 281 (15), 269 (24), 268 (9), 267 (43), 239 (13), 231 (14), 219 (28), 181 (17), 169 (35), 131 (17), 119 (22), 105 (24), 77 (77), 69 (70), 58 (8).

HRMS (EI, $[M]^+$, $C_{22}H_{14}F_2N_4$) calcd.: 372.1181, found: 372.1183.

2,6-Dimethyl-4-(2-(pyridin-4-yl)vinyl)pyridine (22)

4-Vinylpyridine (158 mg, 160 μ L, 1.50 mmol, 1.50 equiv), 4-bromo-2,6-dimethyl-pyridine (186 mg, 1.00 mmol, 1.00 equiv), PEPPSI-IPr catalyst (68.1 mg, 100 μ mol, 10 mol%), tetrabutylammonium bromide (484 mg, 1.50 mmol, 1.50 equiv) and potassium carbonate (415 mg, 3.00 mmol, 3.00 equiv) were suspended in degassed water (3.00 mL). After stirring for 4 hours at 100 °C in a microwave reactor, the mixture was cooled to 21 °C, extracted with ethyl acetate, and washed with

water and brine. The combined organic phase was dried over sodium sulfate and filtered, and the solvent was removed under reduced pressure. The crude product was purified *via* automated flash-chromatography on silica gel using dichloromethane with 1% to 10% methanol to yield the title compound (126 mg, 598 μ mol, 60% yield) as a yellow solid.

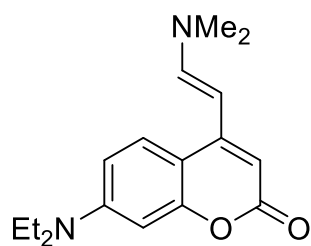
^1H NMR (500 MHz, CDCl_3 , ppm) δ = 8.64–8.60 (m, 2H, 2'- and 6'-CH), 7.40–7.35 (m, 2H, 3'- and 5'-CH), 7.17 (d, J = 2.5 Hz, 2H, 2 \times vinyl-CH), 7.08 (s, 2H, 3- and 5-CH), 2.56 (s, 6H, 2- and 6- CH_3).

^{13}C NMR (126 MHz, CDCl_3 , ppm) δ = 158.6 (2C, 2- and 6- CCH_3), 150.5 (2C, 2'- and 6'-CH), 144.1 (4- or 4'- C_q), 143.8 (4- or 4'- C_q), 131.2 (vinyl-CH), 129.9 (vinyl-CH), 121.2 (2C, 3'- and 5'-CH), 118.0 (2C, 3- and 5-CH), 24.7 (2C, 2 \times CH_3).

IR (ATR, cm^{-1}) $\tilde{\nu}$ = 3068 (w), 3031 (w), 2999 (w), 2925 (w), 2850 (w), 1935 (vw), 1581 (s), 1407 (m), 833 (s), 815 (s), 776 (vs), 609 (vs), 568 (vs), 414 (s).

MS (EI, 70 eV) m/z (%) = 211 (16) $[\text{M}+\text{H}]^+$, 210 (100) $[\text{M}]^+$, 209 (32) $[\text{M}-\text{H}]^+$, 195 (21), 168 (17).

HRMS (EI, $[\text{M}]^+$, $\text{C}_{14}\text{H}_{14}\text{N}_2$) calcd.: 210.1152, found: 210.1150.

(E)-7-(Diethylamino)-4-[2-(dimethylamino)vinyl]-2H-chromen-2-one (46)¹²⁸

To a stirred solution of 7-(diethylamino)-4-methyl-coumarin (2.50 g, 10.8 mmol, 1.00 equiv) in dry N,N-dimethylformamide (75.0 mL), DMF-DMA (2.58 g, 2.88 mL, 21.6 mmol, 2.00 equiv) was added. After stirring for 17h at 153 °C, the reaction mixture was cooled to 21 °C, extracted with dichloromethane, and washed with

sat. aq. sodium hydrogen carbonate solution and brine. The combined organic phase was dried over sodium sulfate and filtered, and the solvent was removed under reduced pressure. The crude title compound (3.07 g, 10.7 mmol, 99% yield) was obtained as a brown solid, which proved pure without further purification.

m.p.: 178 °C

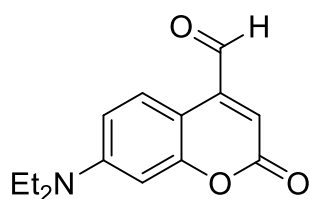
R_f = 0.19 (dichloromethane)

¹H NMR (500 MHz, CDCl₃, ppm) δ = 7.52 (d, J = 9.0 Hz, 1H, 5-*H*), 7.21 (d, J = 13.0 Hz, 1H, CHCHN), 6.54 (dd, J = 9.0, 2.6 Hz, 1H, 6-*H*), 6.48 (d, J = 2.6 Hz, 1H, 8-*H*), 5.84 (s, 1H, 3-*H*), 5.21 (d, J = 13.0 Hz, 1H, CHCHN), 3.39 (q, J = 7.1 Hz, 4H, 2 × CH₂CH₃), 2.98 (s, 6H, N(CH₃)₂), 1.19 (t, J = 7.1 Hz, 6H, 2 × CH₂CH₃).

¹³C NMR (126 MHz, CDCl₃, ppm) δ = 163.5, 156.5, 152.4, 150.2, 146.7, 124.9, 108.2, 108.0, 98.2, 93.6, 87.6, 44.8, 12.6.

IR (ATR, cm⁻¹) $\tilde{\nu}$ = 2968 (m), 2927 (m), 2894 (m), 2870 (m), 2812 (w), 2673 (w), 1674 (s), 1604 (vs), 1565 (vs), 1513 (vs), 1418 (vs), 1404 (s), 1374 (vs), 1358 (vs), 1329 (vs), 1306 (vs), 1283 (vs), 1232 (vs), 1196 (vs), 1164 (s), 1139 (s), 1112 (vs), 1057 (vs), 1016 (vs), 977 (vs), 904 (vs), 832 (vs), 816 (vs), 792 (vs), 771 (vs), 734 (s), 713 (vs), 666 (s), 650 (s), 628 (vs), 613 (s), 584 (s), 503 (s), 475 (s), 436 (vs), 416 (s).

HRMS (ESI, [M+H]⁺, C₁₇H₂₃N₂O₂) calcd.: 287.1754, found: 287.1750.

7-(Diethylamino)-2-oxo-2H-chromene-4-carbaldehyde (45)¹²⁸

Sodium periodate (3.41 g, 15.9 mmol, 1.59 equiv) was added to a solution of (E)-7-(Diethylamino)-4-[2-(dimethylamino)vinyl]-2H-chromen-2-one (**46**) (2.86 g, 9.99 mmol, 1.00 equiv) in a mixture of tetrahydrofuran (25.0 mL) and water (25.0 mL). A cloudy red precipitate immediately formed. After stirring for 90 min at 21 °C, the precipitate was filtered off and washed with ethyl acetate. Sat. aq. sodium hydrogen carbonate solution was added, and the aqueous layer was extracted with dichloromethane. The combined organic phase was dried over sodium sulfate and filtered, and the solvent was removed under reduced pressure. The crude product was purified via flash-chromatography on silica gel using a mixture of ethyl acetate/cyclohexane (1:1) to yield the title compound (1.17 g, 4.78 mmol, 48% yield) as a red solid.

m.p.: 141 °C

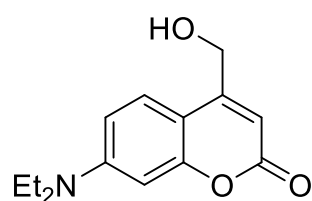
R_f = 0.44 (dichloromethane + 10% methanol)

¹H NMR (400 MHz, CDCl₃, ppm) δ = 10.03 (s, 1H, CHO), 8.30 (d, J = 9.1 Hz, 1H, 5-*H*), 6.62 (dd, J = 9.2, 2.7 Hz, 1H, 6-*H*), 6.52 (d, J = 2.6 Hz, 1H, 8-*H*), 6.45 (s, 1H, 3-*H*), 3.43 (q, J = 7.1 Hz, 4H, 2 × CH₂CH₃), 1.22 (t, J = 7.1 Hz, 6H, 2 × CH₂CH₃).

¹³C NMR (126 MHz, CDCl₃, ppm) δ = 192.5, 161.9, 157.4, 151.0, 143.9, 127.0, 117.3, 109.5, 103.7, 97.6, 44.8, 12.4.

IR (ATR, cm⁻¹) $\tilde{\nu}$ = 2973 (m), 2936 (m), 2900 (w), 2871 (w), 1724 (s), 1697 (vs), 1609 (vs), 1585 (vs), 1519 (vs), 1426 (vs), 1407 (vs), 1375 (vs), 1350 (vs), 1293 (s), 1266 (vs), 1225 (s), 1196 (vs), 1142 (vs), 1078 (vs), 1051 (vs), 1010 (s), 982 (s), 897 (s), 854 (vs), 833 (vs), 796 (vs), 775 (vs), 730 (s), 701 (s), 639 (vs), 543 (m), 509 (m), 470 (vs), 435 (vs), 392 (s).

HRMS (ESI, [M+H]⁺, C₁₄H₁₆NO₃) calcd.: 246.1125, found: 246.1121.

7-(Diethylamino)-4-(hydroxymethyl)-2H-chromen-2-one (47)¹²⁸

7-(Diethylamino)-2-oxo-2H-chromene-4-carbaldehyde **(45)**

(1.05 g, 4.28 mmol, 1.00 equiv) was dissolved in dry tetrahydrofuran (15.0 mL), and sodium borohydride (324 mg, 8.56 mmol, 2.00 equiv) was added at 0 °C, before and the mixture

was allowed to reach room temperature under vigorous stirring. After stirring for 3.5 h at 21 °C, sat. aq. sodium hydrogen carbonate solution was added, and the mixture was extracted with dichloromethane. The combined organic phase was dried over sodium sulfate and filtered, and the solvent was removed under reduced pressure. The crude product was purified *via* flash-chromatography on silica gel using a mixture of cyclohexane/ethyl acetate (1:1) to yield the title compound (793 mg, 3.21 mmol, 75% yield) as a yellow solid.

m.p.: 91 °C

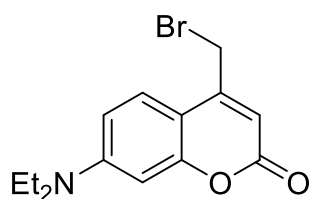
R_f = 0.35 (dichloromethane + 10% methanol)

¹H NMR (400 MHz, CDCl₃, ppm) δ = 7.32 (d, J = 9.0 Hz, 1H, 5-*H*), 6.56 (dd, J = 9.0, 2.6 Hz, 1H, 6-*H*), 6.51 (d, J = 2.6 Hz, 1H, 8-*H*), 6.25 (t, J = 1.4 Hz, 1H, 3-*H*), 4.83 (dd, J = 5.7, 1.1 Hz, 2H, CH₂OH), 3.41 (q, J = 7.1 Hz, 4H, 2 × CH₂CH₃), 1.20 (t, J = 7.1 Hz, 6H, 2 × CH₂CH₃). The spectrum contains traces of silicon grease.

¹³C NMR (101 MHz, CDCl₃, ppm) δ = 162.6, 156.4, 154.5, 150.7, 124.5, 108.7, 106.4, 105.7, 98.0, 61.2, 44.9, 12.6.

IR (ATR, cm⁻¹) $\tilde{\nu}$ = 3434 (m), 2970 (w), 2934 (w), 2897 (w), 1697 (s), 1677 (vs), 1616 (vs), 1601 (vs), 1588 (vs), 1524 (vs), 1441 (s), 1402 (vs), 1375 (m), 1351 (s), 1324 (vs), 1298 (s), 1278 (s), 1232 (s), 1198 (s), 1142 (s), 1086 (vs), 1024 (m), 1006 (m), 989 (m), 948 (w), 907 (w), 861 (w), 843 (s), 830 (vs), 795 (s), 748 (m), 708 (w), 666 (m), 642 (w), 567 (s), 531 (s), 506 (s), 470 (s), 435 (vs), 399 (s).

HRMS (ESI, [M+H]⁺, C₁₄H₁₈NO₃) calcd.: 248.1281, found: 248.1278.

4-(Bromomethyl)-7-(diethylamino)-2H-chromen-2-one (42)¹³⁴

7-(Diethylamino)-4-(hydroxymethyl)-2H-chromen-2-one (47)

(700 mg, 2.83 mmol, 1.00 equiv) was combined with a mixture of dichloromethane (35.0 mL) and triethylamine (573 mg, 789 μ L, 5.66 mmol, 2.00 equiv). It was cooled to 0 °C before adding methanesulfonyl chloride (486 mg, 329 μ L, 4.25 mmol, 1.50 equiv).

After stirring for 2 h at 0 °C, it was quenched with cold sat. aq. sodium hydrogen carbonate solution. It was washed with cold sat. aq. sodium hydrogen carbonate solution, the organic phase was dried over sodium sulfate and filtered, and the solvent was removed under reduced pressure. It was suspended in tetrahydrofuran (30.0 mL) before adding lithium bromide (983 mg, 11.3 mmol, 4.00 equiv). After stirring for 2 h at 21 °C, the solvent was removed under reduced pressure. It was redissolved in dichloromethane and washed with water and brine. The organic phase was dried over sodium sulfate and filtered, and the solvent was removed under reduced pressure. The crude product was purified *via* flash-chromatography on silica gel using a mixture of *n*-pentane/dichloromethane (1:1) to yield the title compound (679 mg, 2.19 mmol, 77% yield) as a yellow solid.

m.p.: 126 °C

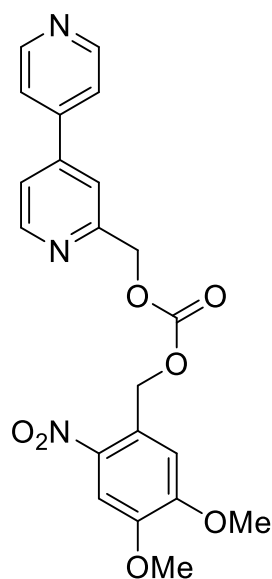
R_f = 0.19 (dichloromethane)

¹H NMR (500 MHz, CDCl₃, ppm) δ = 7.49 (d, J = 9.0 Hz, 1H, 5-*H*), 6.62 (dd, J = 9.0, 2.6 Hz, 1H, 6-*H*), 6.51 (d, J = 2.5 Hz, 1H, 8-*H*), 6.13 (s, 1H, 3-*H*), 4.40 (s, 2H, CH₂Br), 3.42 (q, J = 7.1 Hz, 4H, 2 \times CH₂CH₃), 1.21 (t, J = 7.1 Hz, 6H, 2 \times CH₂CH₃).

¹³C NMR (126 MHz, CDCl₃, ppm) δ = 161.9, 156.8, 151.0, 150.4, 125.5, 109.4, 108.8, 106.3, 98.0, 44.9, 27.3, 12.6.

IR (ATR, cm⁻¹) $\tilde{\nu}$ = 2979 (w), 2931 (w), 2915 (w), 2897 (w), 2864 (w), 2684 (w), 1698 (vs), 1613 (vs), 1596 (vs), 1526 (vs), 1487 (m), 1473 (w), 1448 (s), 1414 (vs), 1375 (s), 1350 (vs), 1336 (s), 1295 (m), 1269 (s), 1227 (vs), 1197 (s), 1170 (m), 1153 (s), 1125 (vs), 1094 (m), 1081 (s), 1051 (vs), 1014 (m), 984 (m), 942 (w), 931 (w), 904 (s), 884 (w), 849 (vs), 820 (vs), 803 (vs), 765 (m), 745 (m), 720 (s), 697 (m), 673 (w), 656 (m), 635 (s), 588 (vs), 552 (s), 538 (m), 524 (m), 503 (m), 449 (vs), 435 (vs), 407 (m), 381 (w).

HRMS (ESI, [M+H]⁺, C₁₄H₁₇⁷⁹BrNO₂) calcd.: 310.0437, found: 310.0434.

[4,4'-Bipyridin]-2-ylmethyl (4,5-dimethoxy-2-nitrobenzyl) carbonate (48)

[4,4'-Bipyridin]-2-ylmethanol (**19**) (60.5 mg, 325 μ mol, 1.00 equiv) was dissolved in dry dichloromethane (8.00 mL) containing 4 Å molar sieves. The mixture was cooled to 0 °C before silver(I) oxide (151 mg, 650 μ mol, 2.00 equiv) and NVOC-Cl (89.6 mg, 325 μ mol, 1.00 equiv) were added, and the mixture was allowed to reach room temperature under vigorous stirring. After stirring for 20 h at 20 °C, the reaction mixture was filtered through a plug of Celite® with dichloromethane and methanol. The solvent was removed under reduced pressure, and the crude product was purified *via* flash-chromatography on silica gel using dichloromethane with 3% to 5% methanol to yield the title compound (55.8 mg, 131 μ mol, 40% yield) as a yellow solid.

R_f = 0.44 (dichloromethane + 10% methanol)

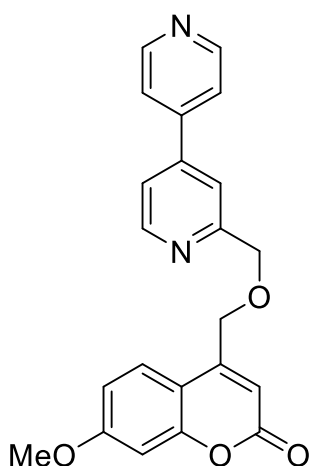
^1H NMR (400 MHz, CDCl_3 , ppm) δ = 8.75 (d, J = 5.2 Hz, 2H, 2'- and 6'-CH), 8.72 (dd, J = 5.1, 0.8 Hz, 1H, 6-CH), 7.73 (s, 1H, ph-CH), 7.63 (d, J = 1.7 Hz, 1H, 3-CH), 7.57 – 7.52 (m, 2H, 3'- and 5'-CH), 7.49 (dd, J = 5.1, 1.8 Hz, 1H, 5-CH), 7.08 (s, 1H, ph-CH), 5.64 (s, 2H, 2-CCH₂), 5.41 (s, 2H, CH₂), 3.96 (d, J = 1.6 Hz, 6H, 2 \times CH₃).

^{13}C NMR (101 MHz, CDCl_3 , ppm) δ = 156.2, 154.6, 153.9, 153.7, 150.8, 150.5, 148.5, 145.3, 139.8, 132.4, 126.3, 121.5, 121.0, 119.4, 111.0, 110.3, 108.3, 108.2, 70.0, 66.9, 56.5 (2C).

IR (ATR, cm^{-1}) $\tilde{\nu}$ = 3094 (w), 3044 (w), 2975 (w), 2934 (w), 2857 (w), 1738 (m), 1707 (vs), 1698 (vs), 1619 (m), 1592 (vs), 1524 (vs), 1463 (m), 1429 (m), 1398 (s), 1337 (vs), 1268 (vs), 1232 (m), 1215 (s), 1197 (vs), 1147 (m), 1125 (vs), 1105 (s), 1065 (s), 1054 (vs), 1027 (w), 1010 (m), 989 (m), 960 (w), 945 (w), 878 (s), 861 (m), 839 (m), 815 (vs), 800 (s), 786 (m), 748 (m), 725 (w), 612 (s), 535 (w), 513 (m), 483 (w), 443 (w), 426 (w), 394 (w).

HRMS (ESI, $[\text{M}+\text{H}]^+$, $\text{C}_{21}\text{H}_{20}\text{N}_3\text{O}_7$) calcd.: 426,1296, found: 426,1292.

4-([4,4'-Bipyridin]-2-ylmethoxy)methyl)-7-methoxy-2H-chromen-2-one (49)



[4,4'-Bipyridin]-2-ylmethanol (**19**) (60.0 mg, 322 μ mol, 1.00 equiv) was dissolved in dry dichloromethane (8.00 mL) containing 4 Å molar sieves. The mixture was cooled to 0 °C before silver(I) oxide (224 mg, 967 μ mol, 3.00 equiv), 2,6-di-*tert*-butylpyridine (185 mg, 209 μ L, 967 μ mol, 3.00 equiv) and 4-(bromomethyl)-7-methoxy-2H-chromen-2-one (86.7 mg, 322 μ mol, 1.00 equiv) were added, and the mixture was allowed to reach room temperature under vigorous stirring. After stirring for 48 h at 20 °C, the reaction mixture was filtered through a plug of

Celite® with dichloromethane and methanol. The solvent was removed under reduced pressure, and the crude product was purified *via* flash-chromatography on silica gel using dichloromethane with 5% methanol to yield the title compound (94.2 mg, 252 μ mol, 78% yield) as a yellow solid.

R_f = 0.37 (dichloromethane + 10% methanol)

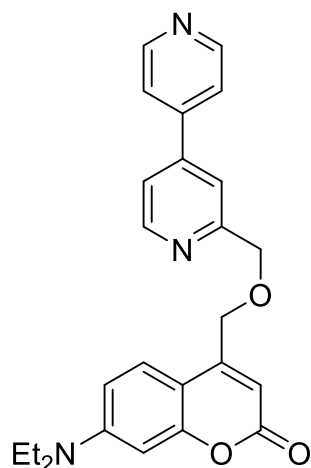
$^1\text{H NMR}$ (400 MHz, CDCl_3 , ppm) δ = 8.78–8.72 (m, 2H, 2'- and 6'-CH), 8.70 (dd, J = 5.1, 0.9 Hz, 1H, 6-CH), 7.70 (d, J = 1.8 Hz, 1H, 3-CH), 7.56–7.51 (m, 2H, 3'- and 5'-CH), 7.51–7.44 (m, 2H), 6.86–6.82 (m, 2H), 6.49 (d, J = 1.4 Hz, 1H), 4.88 (s, 2H, 2-CCH₂), 4.84 (d, J = 1.4 Hz, 2H, OCH₂), 3.87 (s, 3H, OCH₃).

$^{13}\text{C NMR}$ (101 MHz, CDCl_3 , ppm) δ = 162.9, 161.3, 158.8, 155.8, 151.2, 150.9 (2C), 150.3, 145.6, 124.9, 121.6 (2C), 120.7, 119.3, 112.7, 111.2, 110.5, 101.2, 74.1, 68.9, 55.9.

IR (ATR, cm^{-1}) $\tilde{\nu}$ = 3064 (w), 2921 (w), 2847 (w), 1713 (vs), 1612 (vs), 1592 (vs), 1537 (s), 1519 (m), 1465 (m), 1422 (s), 1401 (s), 1349 (s), 1334 (s), 1289 (vs), 1268 (s), 1213 (s), 1152 (vs), 1132 (vs), 1058 (s), 1033 (s), 1021 (s), 983 (vs), 841 (vs), 805 (vs), 730 (s), 701 (s), 613 (vs), 595 (s), 513 (s), 487 (vs), 448 (s), 436 (s).

HRMS (ESI, $[\text{M}+\text{H}]^+$, $\text{C}_{22}\text{H}_{19}\text{N}_2\text{O}_4$) calcd.: 375.1340, found: 375.1335.

4-((([4,4'-Bipyridin]-2-ylmethoxy)methyl)-7-(diethylamino)-2H-chromen-2-one (50)



[4,4'-Bipyridin]-2-ylmethanol (**19**) (60.0 mg, 322 μmol , 1.00 equiv) was dissolved in dry dichloromethane (8.00 mL) containing 4 Å molar sieves. The mixture was cooled to 0 °C before silver(I) oxide (224 mg, 967 μmol , 3.00 equiv), 2,6-di-*tert*-butylpyridine (185 mg, 209 μL , 967 μmol , 3.00 equiv) and 4-(bromomethyl)-7-(diethylamino)-2H-chromen-2-one (**42**) (99.9 mg, 322 μmol , 1.00 equiv) were added, and the mixture was allowed to reach room temperature under vigorous stirring. After stirring for 48 h at 20 °C, the reaction mixture was filtered through

a plug of Celite® with dichloromethane and methanol. The solvent was removed under reduced pressure, and the crude product was purified *via* flash-chromatography on silica gel using dichloromethane with 5% methanol to yield the title compound (83.0 mg, 200 μmol , 62% yield) as a yellow solid.

R_f = 0.38 (dichloromethane + 10% methanol)

^1H NMR (400 MHz, CDCl_3 , ppm) δ = 8.78–8.71 (m, 2H, 2'- and 6'-CH), 8.69 (dd, J = 5.2, 0.8 Hz, 1H, 6-CH), 7.71 (d, J = 1.2 Hz, 1H, 3-CH), 7.56–7.50 (m, 2H, 3'- and 5'-CH), 7.46 (dd, J = 5.2, 1.8 Hz, 1H, 5-CH), 7.39 (d, J = 9.0 Hz, 1H), 6.55 (dd, J = 8.9, 2.6 Hz, 1H), 6.51 (d, J = 2.6 Hz, 1H), 6.27 (d, J = 1.3 Hz, 1H), 4.86 (s, 2H, 2- CCH_2), 4.79 (d, J = 1.3 Hz, 2H, OCH_2), 3.41 (q, J = 7.1 Hz, 4H, 2 \times CH_2), 1.20 (t, J = 7.1 Hz, 6H, 2 \times CH_3).

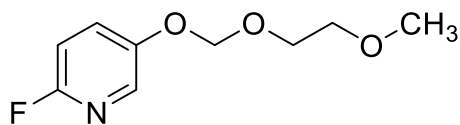
^{13}C NMR (101 MHz, CDCl_3 , ppm) δ = 162.2, 159.1, 156.5, 151.4, 150.9 (2C), 150.7, 150.2, 146.6, 145.6, 124.9, 121.6 (2C), 120.6, 119.2, 108.7, 107.1, 106.6, 98.0, 73.9, 69.1, 44.9 (2C), 12.6 (2C).

IR (ATR, cm^{-1}) $\tilde{\nu}$ = 3094 (w), 3051 (w), 2975 (w), 2921 (w), 2851 (w), 1698 (vs), 1618 (s), 1601 (vs), 1591 (vs), 1526 (s), 1465 (m), 1426 (m), 1398 (m), 1353 (w), 1336 (vs), 1295 (w), 1269 (s), 1215 (w), 1196 (m), 1146 (w), 1125 (vs), 1103 (s), 1074 (m), 1052 (s), 1026 (w), 1010 (m), 989 (w), 878 (m), 861 (m), 837 (m), 815 (vs), 800 (s), 748 (w), 737 (w), 612 (s), 571 (w), 537 (w), 513 (m), 483 (m), 443 (w), 425 (w), 397 (w).

HRMS (ESI, $[\text{M}+\text{H}]^+$, $\text{C}_{25}\text{H}_{26}\text{N}_3\text{O}_3$) calcd.: 416.1969, found: 416.1967.

5.2.2 HINA derivatives

2-Fluoro-5-((2-methoxyethoxy)methoxy)pyridine (54)



To a stirred solution of 6-fluoropyridin-3-ol (3.00 g, 26.5 mmol, 1.00 equiv) in dry tetrahydrofuran (50.0 mL) at 0 °C was added potassium *tert*-butoxide (4.76 g, 42.4 mmol, 1.60 equiv) portion-wise. After stirring the reaction mixture for 30 min, 1-(chloromethoxy)-2-methoxyethane (5.87 g, 5.38 mL, 42.4 mmol, 1.60 equiv) was added at 0 °C. The reaction slowly turned red-orange and a precipitate formed while the reaction mixture was stirred overnight at 21 °C. The crude was extracted with ethyl acetate and washed with water and brine. The combined organic phase was dried over sodium sulfate and filtered, and the solvent was removed under reduced pressure. The crude product was purified *via* flash-chromatography on silica gel using a mixture of cyclohexane/ethyl acetate (2:1 --> 0:1) to yield 2-fluoro-5-((2-methoxyethoxy)methoxy)pyridine (3.44 g, 17.1 mmol, 64% yield) as a light-yellow liquid.

$R_f = 0.41$ (dichloromethane + 2% methanol)

$^1\text{H NMR}$ (500 MHz, CDCl_3 , ppm) $\delta = 7.98$ (dd, $J = 3.1, 1.7$ Hz, 1H, 6-CH), 7.50 (ddd, $J = 8.9, 6.5, 3.1$ Hz, 1H, 4-CH), 6.85 (ddd, $J = 8.9, 3.5, 0.6$ Hz, 1H, 3-CH), 5.24 (s, 2H, OCH_2O), 3.85–3.81 (m, 2H, $\text{CH}_2\text{-CH}_2\text{OCH}_3$), 3.57–3.54 (m, 2H, $\text{CH}_2\text{-OCH}_3$), 3.37 (s, 3H, OCH_3).

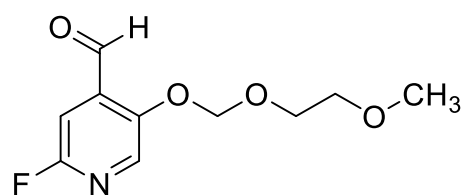
$^{13}\text{C NMR}$ (126 MHz, CDCl_3 , ppm) $\delta = 158.6$ (d, $J = 233.7$ Hz, 2-CF), 151.7 (d, $J = 4.5$ Hz, 5-CO), 135.7 (d, $J = 15.4$ Hz, 6-CH), 129.4 (d, $J = 7.9$ Hz, 4-CH), 109.6 (d, $J = 40.2$ Hz, 3-CH), 94.4 (OCH_2O), 71.5 ($\text{CH}_2\text{-OCH}_3$), 68.0 ($\text{CH}_2\text{-CH}_2\text{OCH}_3$), 59.1 (OCH_3).

$^{19}\text{F NMR}$ (471 MHz, CDCl_3 , ppm) $\delta = -76.4$ (2-CF).

IR (ATR, cm^{-1}) $\tilde{\nu} = 2928$ (w), 2919 (w), 2881 (w), 2820 (w), 1595 (w), 1480 (vs), 1417 (w), 1387 (m), 1368 (w), 1283 (w), 1224 (vs), 1201 (m), 1160 (m), 1101 (vs), 1018 (s), 979 (vs), 878 (w), 850 (s), 829 (s), 786 (w), 731 (s), 659 (w), 438 (w).

MS (EI, 70 eV) m/z (%) = 201 (2) $[\text{M}]^+$, 181 (16), 162 (2), 131 (17), 126 (11), 119 (3), 113 (3), 100 (4), 96 (10), 93 (2), 90 (4), 89 (92), 84 (4), 76 (3), 69 (35), 60 (3), 59 (100), 57 (4).

HRMS (EI, $[\text{M}]^+$, $\text{C}_9\text{H}_{12}\text{FNO}_3$) calcd.: 202.0797, found: 202.0796.

2-Fluoro-5-((2-methoxyethoxy)methoxy)isonicotinaldehyde (57)

To a stirred solution of 2-fluoro-5-((2-methoxyethoxy)methoxy)pyridine (**54**) (246 mg, 1.22 mmol, 1.00 equiv) in dry tetrahydrofuran (4.00 mL) was added *n*-butyllithium (86.0 mg, 537 μ L, 1.34 mmol, 2.50M, 1.10 equiv) dropwise at -78 °C. After stirring for 60 minutes at -78 °C, *N,N*-dimethylformamide (134 mg, 142 μ L, 1.83 mmol, 1.50 equiv) was added to the reaction mixture, and it was stirred for 15 mins at -78 °C. Saturated ammonium chloride solution was added dropwise to the reaction at -78 °C, and the reaction was warmed-up to 21 °C. The crude was extracted with ethyl acetate and washed with water and brine. The combined organic phase was dried over sodium sulfate and filtered, and the solvent was removed under reduced pressure. The crude product was purified *via* automated flash-chromatography on diol-modified silica gel using a mixture of cyclohexane/ethyl acetate (1:0 \rightarrow 0:1) to yield 2-fluoro-5-((2-methoxyethoxy)methoxy)isonicotinaldehyde (278 mg, 1.21 mmol, 99% yield) as a colorless liquid.

R_f = 0.19 (dichloromethane + 2% methanol)

^1H NMR (500 MHz, CD_3CN , ppm) δ = 10.38 (d, J = 2.7 Hz, 1H, 4-CHO), 8.27 (d, J = 1.8 Hz, 1H, 6-CH), 7.25 (d, J = 3.4 Hz, 1H, 3-CH), 5.43 (d, J = 15.6 Hz, 2H, OCH₂O), 3.86–3.83 (m, 2H, CH₂-CH₂OCH₃), 3.51–3.49 (m, 2H, CH₂-OCH₃), 3.25 (s, 3H, OCH₃).

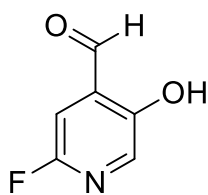
^{13}C NMR (126 MHz, CD_3CN , ppm) δ = 189.3 (d, J = 2.3 Hz, 4-CHO), 159.5 (d, J = 231.9 Hz, 2-CF), 153.2 (d, J = 4.6 Hz, 5-CO), 138.1 (d, J = 15.1 Hz, 4-CCHO), 136.6 (d, J = 6.7 Hz, 6-CH), 106.8 (d, J = 41.8 Hz, 3-CH), 95.9 (OCH₂O), 72.1 (CH₂-OCH₃), 69.4 (CH₂-CH₂OCH₃), 58.8 (OCH₃).

^{19}F NMR (471 MHz, CD_3CN , ppm) δ = -77.1 (2-CF).

IR (ATR, cm^{-1}) $\tilde{\nu}$ = 2975 (vw), 2928 (w), 2883 (w), 2822 (vw), 1698 (vs), 1578 (vw), 1476 (vs), 1388 (vs), 1293 (w), 1264 (w), 1237 (m), 1197 (s), 1162 (m), 1136 (m), 1106 (vs), 1027 (w), 960 (vs), 880 (w), 849 (w), 806 (w), 758 (vw), 730 (w), 626 (w), 492 (vw), 450 (w).

MS (EI, 70 eV) m/z (%) = 229 (1) [M]⁺, 155 (1), 154 (6), 141 (1), 126 (1), 112 (1), 111 (2), 96 (2), 90 (3), 89 (100), 84 (1), 76 (1), 69 (1), 60 (2), 59 (92), 58 (1), 57 (2), 56 (1), 51 (1).

HRMS (EI, [M]⁺, C₁₀H₁₂FNO₄) calcd.: 229.0745, found: 229.0743.

2-Fluoro-5-hydroxyisonicotinaldehyde (66)

To a stirred solution of 2-fluoro-5-((2-methoxyethoxy)-methoxy)isonicotinaldehyde (**57**) (193 mg, 840 μ mol, 1.00 equiv) in dichloromethane (15.0 mL) was added 2,2,2-trifluoroacetic acid (7.45 g, 5.00 mL, 65.3 mmol, 77.8 equiv). After stirring for 15 minutes at 21 °C, it was extracted with ethyl acetate. Then 1 M aqueous NaOH solution was added until pH = 10-11, extracted with ethyl acetate. Then 1 M aqueous HCl solution was added until pH 4-5. It was extracted with a solution of dichloromethane/iPrOH (4:1), dried over sodium sulfate, and filtered, and the solvent was carefully removed under reduced pressure while keeping the temperature of the crude constantly at 20 °C with a water bath. The crude title compound (37.2 mg, 264 μ mol, 31% yield) was obtained as a volatile light-yellow liquid, which proved pure without further purification.

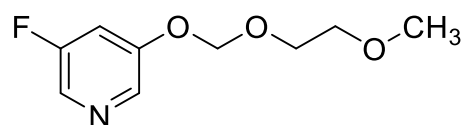
^1H NMR (500 MHz, CD_3CN , ppm) δ = 10.10 (s, 1H, 4-CHO), 9.61 (s, 1H, 5-OH), 8.04 (d, J = 1.7 Hz, 1H, 6-CH), 7.31 (d, J = 3.4 Hz, 1H, 3-CH). The spectrum contains traces of dichloromethane, 2-propanol, and protected starting material.

^{19}F NMR (471 MHz, CD_3CN , ppm) δ = -80.7 (2-CF). The spectrum contains traces of protected starting material.

IR (ATR, cm^{-1}) $\tilde{\nu}$ = 3186 (w), 3111 (w), 3064 (w), 2922 (s), 2873 (m), 2853 (m), 2745 (w), 2681 (w), 1680 (vs), 1622 (m), 1473 (vs), 1414 (vs), 1395 (vs), 1332 (s), 1273 (vs), 1256 (s), 1196 (vs), 1122 (vs), 1109 (vs), 1086 (s), 1040 (s), 989 (m), 966 (s), 871 (m), 832 (w), 822 (w), 799 (vs), 773 (m), 747 (m), 721 (m), 691 (s), 669 (m), 632 (m), 601 (w), 562 (w), 513 (w), 449 (w).

MS (EI, 70 eV) m/z (%) = 142 (5)[$\text{M}+\text{H}$] $^+$, 141 (100)[M] $^+$, 140 (8), 123 (4), 113 (6), 112 (9), 95 (4), 85 (5), 58 (5), 57 (8).

HRMS (EI, [M] $^+$, $\text{C}_6\text{H}_4\text{FNO}_2$) calcd.: 141.0221, found: 141.0221.

3-Fluoro-5-((2-methoxyethoxy)methoxy)pyridine (56)

To a stirred solution of 5-fluoropyridin-3-ol (2.01 g, 17.8 mmol, 1.00 equiv) in dry tetrahydrofuran (40.0 mL) at 0 °C was added potassium *tert*-butoxide (3.18 g, 28.3 mmol, 1.59 equiv) portion-wise. After stirring the reaction mixture for 30 min, 1-(chloromethoxy)-2-methoxyethane (3.92 g, 3.59 mL, 28.3 mmol, 1.59 equiv) was added at 0 °C. The reaction slowly turned red-orange and a precipitate formed while the reaction mixture was stirred overnight at 21 °C. The crude was extracted with ethyl acetate and washed with water and brine. The combined organic phase was dried over sodium sulfate and filtered, and the solvent was removed under reduced pressure. The crude product was purified *via* flash-chromatography on silica gel using a mixture of cyclohexane/ethyl acetate (2:1 --> 0:1) to yield 3-fluoro-5-((2-methoxyethoxy)methoxy)pyridine (1.13 g, 5.63 mmol, 32% yield) as a light-yellow liquid.

$R_f = 0.34$ (dichloromethane + 5% methanol)

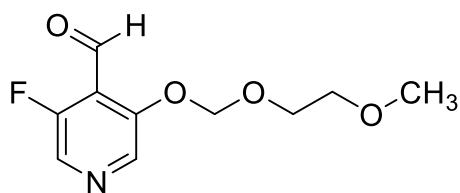
$^1\text{H NMR}$ (500 MHz, CDCl_3 , ppm) $\delta = 8.25$ (dd, $J = 2.5, 1.1$ Hz, 1H, 6-CH), 8.16 (d, $J = 2.4$ Hz, 1H, 2-CH), 7.19 (dt, $J = 10.2, 2.4$ Hz, 1H, 4-CH), 5.30 (s, 2H, OCH₂O), 3.86–3.81 (m, 2H, CH₂-CH₂OCH₃), 3.59–3.53 (m, 2H, CH₂-OCH₃), 3.37 (s, 3H, OCH₃).

$^{13}\text{C NMR}$ (126 MHz, CDCl_3 , ppm) $\delta = 159.8$ (d, $J = 257.9$ Hz, 3-CF), 154.4 (d, $J = 5.4$ Hz, 5-CO), 135.7 (d, $J = 3.6$ Hz, 6-CH), 131.4 (d, $J = 23.1$ Hz, 2-CH), 111.0 (d, $J = 21.0$ Hz, 4-CH), 94.0 (OCH₂O), 71.6 (CH₂-OCH₃), 68.3 (CH₂-CH₂OCH₃), 59.2 (OCH₃).

$^{19}\text{F NMR}$ (376 MHz, CDCl_3 , ppm) $\delta = -125.8$ (3-CF).

IR (ATR, cm^{-1}) $\tilde{\nu} = 2925$ (w), 2878 (w), 2817 (w), 1596 (s), 1578 (s), 1462 (w), 1434 (vs), 1310 (w), 1275 (s), 1230 (w), 1170 (s), 1152 (vs), 1142 (vs), 1101 (vs), 1023 (vs), 994 (vs), 948 (s), 864 (s), 850 (m), 697 (s).

HRMS (ESI, $[\text{M}+\text{Na}]^+$, $\text{C}_9\text{H}_{12}\text{FNO}_3\text{Na}$) calcd.: 224.0693, found: 224.0691.

3-Fluoro-5-((2-methoxyethoxy)methoxy)isonicotinaldehyde (58)

To a stirred solution of 3-fluoro-5-((2-methoxyethoxy)methoxy)pyridine (**56**) (400 mg, 1.99 mmol, 1.00 equiv) in dry tetrahydrofuran (7.00 mL) was added *n*-butyllithium (140 mg, 875 μ L, 2.19 mmol, 2.50M, 1.10 equiv) dropwise at -78 $^{\circ}$ C. After stirring for 60 minutes at -78 $^{\circ}$ C, *N,N*-dimethylformamide (218 mg, 231 μ L, 2.98 mmol, 1.50 equiv) was added to the reaction mixture, and it was stirred for 15 mins at -78 $^{\circ}$ C. Saturated ammonium chloride solution was added dropwise to the reaction at -78 $^{\circ}$ C, and the reaction was warmed-up to 21 $^{\circ}$ C. The crude was extracted with ethyl acetate and washed with water and brine. The combined organic phase was dried over sodium sulfate and filtered, and the solvent was removed under reduced pressure. The crude product was purified *via* automated flash-chromatography on silica gel using a mixture of cyclohexane/ethyl acetate (20:1 to 3:2) to yield 3-fluoro-5-((2-methoxyethoxy)methoxy)isonicotinaldehyde (85.2 mg, 372 μ mol, 19% yield) as a colorless liquid.

^1H NMR (500 MHz, CDCl_3 , ppm) δ = 10.46 (s, 1H, 4-CHO), 8.58 (s, 1H, 6-CH), 8.32 (s, 1H, 2-CH), 5.45 (s, 2H, OCH_2O), 3.91–3.87 (m, 2H, $\text{CH}_2\text{-CH}_2\text{OCH}_3$), 3.58–3.54 (m, 2H, $\text{CH}_2\text{-OCH}_3$), 3.36 (s, 3H, OCH_3).

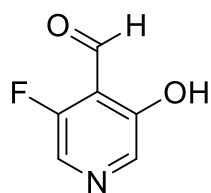
^{13}C NMR (126 MHz, CDCl_3 , ppm) δ = 186.5 (s, 4-CHO), 156.9 (d, J = 272.9 Hz, 3-CF), 153.4 (5-CO), 135.0 (d, J = 5.0 Hz, 6-CH), 133.1 (d, J = 23.6 Hz, 2-CH), 119.2 (d, J = 7.5 Hz, 4-CCHO), 94.8 (OCH_2O), 71.5 ($\text{CH}_2\text{-OCH}_3$), 69.0 ($\text{CH}_2\text{-CH}_2\text{OCH}_3$), 59.2 (OCH_3).

^{19}F NMR (471 MHz, CDCl_3 , ppm) δ = -132.0 (3-CF).

IR (ATR, cm^{-1}) $\tilde{\nu}$ = 3074 (w), 2925 (w), 2894 (w), 2857 (w), 2822 (w), 1734 (w), 1701 (s), 1686 (s), 1611 (m), 1594 (s), 1548 (s), 1466 (vs), 1458 (vs), 1426 (vs), 1363 (s), 1282 (s), 1241 (vs), 1183 (vs), 1102 (vs), 1052 (vs), 1024 (vs), 982 (vs), 931 (vs), 849 (vs), 802 (vs), 717 (vs), 703 (vs), 554 (vs), 535 (vs), 528 (vs), 472 (vs), 446 (vs), 438 (vs), 425 (vs), 395 (vs), 375 (vs).

MS (EI, 70 eV) m/z (%) = 229 (1), 174 (2), 155 (2), 154 (22), 142 (1), 141 (16), 140 (1), 126 (1), 124 (4), 123 (1), 113 (1), 112 (4), 111 (3), 109 (1), 97 (1), 96 (6), 95 (1), 90 (4), 89 (100), 86 (1), 85 (1), 83 (1), 76 (2), 69 (2), 68 (1), 60 (2), 59 (69), 58 (6), 57 (5), 56 (1).

HRMS (EI, $[\text{M}]^+$, $\text{C}_{10}\text{H}_{12}\text{FNO}_4$) calcd.: 229.0745, found: 229.0743.

3-Fluoro-5-hydroxyisonicotinaldehyde (61)

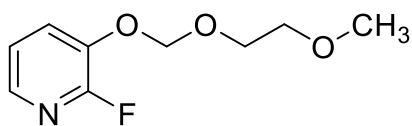
To a stirred solution of 3-fluoro-5-((2-methoxyethoxy)methoxy)isonicotinaldehyde (**58**) (200 mg, 809 μ mol, 1.00 equiv) in dichloromethane (15.0 mL) was added 2,2,2-trifluoroacetic acid (11.2 g, 7.50 mL, 97.9 mmol, 121 equiv). After stirring for 15 minutes at 21 $^{\circ}$ C, it was extracted with ethyl acetate. Then 1 M aqueous NaOH solution was added until pH = 10-11, extracted with ethyl acetate. Then 1 M aqueous HCl solution was added until pH 4-5. It was extracted with a solution of dichloromethane/*i*PrOH (4:1), dried over sodium sulfate, and filtered, and the solvent was carefully removed under reduced pressure while keeping the temperature of the crude constantly at 20 $^{\circ}$ C with a water bath. The crude title compound (5.30 mg, 37.6 μ mol, 5% yield) was obtained as a volatile colorless liquid, which proved pure without further purification. It decomposed after a few days when kept at -18 $^{\circ}$ C under an argon atmosphere.

^1H NMR (500 MHz, CD_2Cl_2 , ppm) δ = 10.72 (br s, 1H, OH), 10.37 (s, 1H, CHO), 8.33 (s, 1H, 2-CH), 8.18 (s, 1H, 6-CH).

^{13}C NMR (126 MHz, CD_2Cl_2 , ppm) δ = 193.0 (d, J = 8.1 Hz, 4-CHO), 158.9 (d, J = 269.2 Hz, 3-CF), 155.6 (5-CO), 138.7 (d, J = 5.0 Hz, 6-CH), 129.1 (d, J = 22.0 Hz, 2-CH), 113.8 (d, J = 10.1 Hz, 4-CCHO).

^{19}F NMR (471 MHz, CD_2Cl_2 , ppm) δ = -139.2 (3-CF).

IR (ATR, cm^{-1}) $\tilde{\nu}$ = 3225 (s), 3189 (s), 2921 (s), 2854 (m), 1677 (m), 1623 (m), 1479 (vs), 1418 (vs), 1388 (vs), 1283 (s), 1272 (s), 1048 (s), 956 (vs), 798 (s).

2-Fluoro-3-((2-methoxyethoxy)methoxy)pyridine (55)

To a stirred solution of 2-fluoropyridin-3-ol (1.00 g, 8.84 mmol, 1.00 equiv) in dry tetrahydrofuran (20.0 mL) at 0 °C was added potassium *tert*-butoxide (1.57 g, 14.0 mmol,

1.58 equiv) portion-wise. After stirring the reaction mixture for 30 min, 1-(chloromethoxy)-2-methoxyethane (1.93 g, 1.77 mL, 14.0 mmol, 1.58 equiv) was added at 0 °C. The reaction slowly turned red-orange and a precipitate formed while the reaction mixture was stirred overnight at 23 °C. The crude was extracted with ethyl acetate and washed with water and brine. The combined organic phase was dried over sodium sulfate and filtered, and the solvent was removed under reduced pressure. The crude product was purified *via* flash-chromatography on silica gel using a mixture of cyclohexane/ethyl acetate (2:1) to yield the title compound (1.23 g, 6.11 mmol, 69% yield) as a light-yellow liquid.

R_f = 0.47 (cyclohexane/ethyl acetate, 1:1)

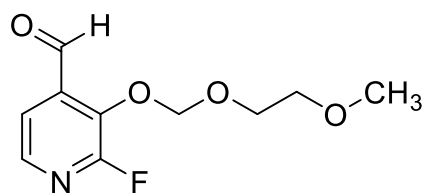
^1H NMR (500 MHz, CDCl_3 , ppm) δ = 7.80 (dt, J = 4.9, 1.7 Hz, 1H), 7.58 (ddd, J = 9.9, 7.9, 1.6 Hz, 1H), 7.10 (ddd, J = 8.0, 4.9, 0.8 Hz, 1H), 5.32 (s, 2H), 3.89–3.83 (m, 2H), 3.56–3.53 (m, 3H), 3.35 (s, 3H). The spectrum contains traces of (2-methoxyethoxy)methanol and silicon grease.

^{13}C NMR (126 MHz, CDCl_3 , ppm) δ = 154.4 (d, J = 238.3 Hz, 2-CF), 140.4 (d, J = 25.5 Hz, 3-CO), 139.1 (d, J = 13.3 Hz, 6-CH), 126.5 (d, J = 4.0 Hz, 4-CH or 5-CH), 121.9 (d, J = 4.4 Hz, 4-CH or 5-CH), 94.5 (OCH₂O), 71.5 (CH₂-OCH₃), 68.4 (CH₂-CH₂OCH₃), 59.1 (OCH₃). The spectrum contains traces of (2-methoxyethoxy)methanol and silicon grease.

^{19}F NMR (471 MHz, CDCl_3 , ppm) δ = -84.0 (2-CF).

IR (ATR, cm^{-1}) $\tilde{\nu}$ = 2928 (w), 2881 (w), 2820 (vw), 1605 (w), 1578 (w), 1453 (vs), 1414 (w), 1269 (m), 1244 (s), 1184 (s), 1099 (vs), 1027 (m), 967 (vs), 853 (m), 798 (s), 758 (m), 745 (s), 579 (w).

HRMS (ESI, $[\text{M}+\text{H}]^+$, $\text{C}_9\text{H}_{13}\text{FNO}_3$) calcd.: 202.0874, found: 202.0872.

2-Fluoro-3-((2-methoxyethoxy)methoxy)isonicotinaldehyde (59)

To a stirred solution of 2-fluoro-3-((2-methoxyethoxy)methoxy)pyridine (**55**) (800 mg, 3.98 mmol, 1.00 equiv) in dry tetrahydrofuran (20.0 mL) was added *n*-butyllithium (280 mg, 1.75 mL, 4.37 mmol, 2.50M, 1.10 equiv) dropwise at -78 °C. After stirring for 60 minutes at -78 °C, *N,N*-dimethylformamide (436 mg, 462 μ L, 5.96 mmol, 1.50 equiv) was added to the reaction mixture, and it was stirred for 15 mins at -78 °C. Saturated ammonium chloride solution was added dropwise to the reaction at -78 °C, and the reaction was warmed-up to 21°C. The crude was extracted with ethyl acetate and washed with water and brine. The combined organic phase was dried over sodium sulfate and filtered, and the solvent was removed under reduced pressure. The crude product was purified *via* automated flash-chromatography on silica gel using a mixture of dichloromethane/methanol (dichloromethane + 1% methanol \rightarrow dichloromethane + 4% methanol) to yield 2-fluoro-3-((2-methoxyethoxy)methoxy)isonicotinaldehyde (903 mg, 3.94 mmol, 99% yield) as a colorless liquid.

^1H NMR (500 MHz, CD_3CN , ppm) δ = 10.42 (d, J = 0.8 Hz, 1H, 4-CHO), 8.04 (ddd, J = 4.9, 1.7, 0.7 Hz, 1H, 6-CH), 7.54 (dd, J = 4.9, 0.9 Hz, 1H, 5-CH), 5.38 (d, J = 1.1 Hz, 2H, OCH_2O), 3.88–3.85 (m, 2H, $\text{CH}_2\text{-CH}_2\text{OCH}_3$), 3.48–3.45 (m, 2H, $\text{CH}_2\text{-OCH}_3$), 3.23 (s, 3H, OCH_3). The spectrum contains traces of dichloromethane.

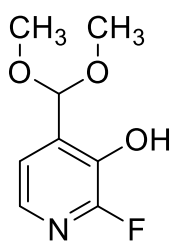
^{13}C NMR (126 MHz, CD_3CN , ppm) δ = 189.4 (d, J = 3.8 Hz, 4-CHO), 158.0 (d, J = 239.4 Hz, 2-CF), 142.3 (d, J = 14.5 Hz, 6-CH), 141.9 (d, J = 27.6 Hz, 3-COH), 139.2 (d, J = 4.5 Hz, 4-CCHO), 119.8 (d, J = 4.9 Hz, 5-CH), 99.5 (d, J = 6.4 Hz, OCH_2O), 72.1 ($\text{CH}_2\text{-OCH}_3$), 70.5 ($\text{CH}_2\text{-CH}_2\text{OCH}_3$), 58.8 (OCH_3).

^{19}F NMR (471 MHz, CD_3CN , ppm) δ = -80.8 (2-CF).

IR (ATR, cm^{-1}) $\tilde{\nu}$ = 2927 (w), 2883 (w), 2820 (vw), 1698 (vs), 1567 (w), 1432 (vs), 1407 (s), 1384 (s), 1368 (w), 1293 (w), 1242 (vs), 1201 (s), 1164 (m), 1140 (s), 1109 (vs), 1075 (vs), 1027 (w), 1001 (w), 966 (m), 922 (vs), 840 (s), 819 (m), 761 (w), 547 (w).

MS (EI, 70 eV) m/z (%) = 229 (15) $[\text{M}]^+$, 201 (100), 89 (100), 59 (96).

HRMS (EI, $[\text{M}]^+$, $\text{C}_{10}\text{H}_{12}\text{FNO}_4$) calcd.: 229.0745, found: 229.0744.

4-(Dimethoxymethyl)-2-fluoropyridin-3-ol (65)

To a stirred solution of 2-fluoro-3-((2-methoxyethoxy)methoxy)isonicotinaldehyde (**59**) (600 mg, 2.62 mmol, 1.00 equiv) in 1,2-dimethoxyethane (10.0 mL) *para*-toluenesulfonic acid (90.2 mg, 524 μ mol, 0.200 equiv) and trimethyl orthoformate (2.78 g, 2.86 mL, 26.2 mmol, 10.0 equiv) was added, and it was stirred for 2 hours at 21 °C. The crude was extracted with ethyl acetate and

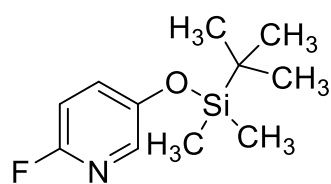
washed with water and brine. The combined organic phase was dried over sodium sulfate and filtered, and the solvent was removed under reduced pressure. The crude was dissolved in dry dichloromethane (20.0 mL), and 2,2,2-trifluoroacetic acid (14.9 g, 10.0 mL, 131 mmol, 49.9 equiv) was added. It was stirred for 15 minutes at 21 °C. It was extracted with ethyl acetate. Then 1 M aqueous NaOH solution was added until pH = 10-11, extracted with ethyl acetate. Then 1 M aqueous HCl solution was added until pH 4-5. It was extracted with a solution of dichloromethane/*i*PrOH (4:1), dried over sodium sulfate, and filtered, and the solvent was carefully removed under reduced pressure while keeping the temperature of the crude constantly at 20 °C with a water bath. The title compound (131 mg, 698 μ mol, 27% yield) was obtained as a volatile colorless liquid.

^1H NMR (500 MHz, D_2O , ppm) δ = 7.07 (dd, J = 5.1, 1.4 Hz, 1H, 5-CH), 6.97 (d, J = 5.1 Hz, 1H, 6-CH), 5.58 (s, 1H, 4-CH(OCH_3)₂), 3.32 (s, 6H, 2 \times CH_3).

^{13}C NMR (126 MHz, D_2O , ppm) δ = 151.5 (d, J = 238.2 Hz, 2-CF), 143.3 (d, J = 26.5 Hz, 3-COH or 4-CCH(OCH_3)₂), 130.3 (d, J = 9.6 Hz, 3-COH or 4-CCH(OCH_3)₂), 121.2 (d, J = 11.8 Hz, 6-CH), 113.4 (4-CCH(OCH_3)₂), 94.2 (d, J = 5.0 Hz, 5-CH), 49.0 (2C, 2 \times OCH_3).

^{19}F NMR (471 MHz, D_2O , ppm) δ = -91.0 (2-CF).

IR (ATR, cm^{-1}) $\tilde{\nu}$ = 2953 (w), 2919 (m), 2850 (w), 1737 (w), 1672 (m), 1655 (m), 1626 (m), 1578 (w), 1561 (w), 1513 (w), 1439 (vs), 1417 (vs), 1364 (s), 1300 (s), 1239 (vs), 1208 (vs), 1096 (s), 1051 (s), 1023 (s), 950 (m), 833 (s), 738 (vs), 718 (vs), 646 (s), 609 (s), 588 (s), 550 (s), 537 (s), 523 (s), 507 (s), 438 (s), 429 (m).

5-((*Tert*-butyldimethylsilyl)oxy)-2-fluoropyridine (67)

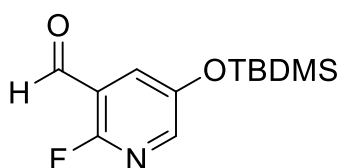
To a stirred solution of 6-fluoro-3-pyridinol (1.00 g, 8.84 mmol, 1.00 equiv) and 1H-imidazole (1.20 g, 17.7 mmol, 2.00 equiv) in *N,N*-dimethylformamide (20.0 mL), TBDMS-Cl (1.47 g, 9.73 mmol, 1.10 equiv) was added. After stirring the reaction mixture for 2 hours at 21 °C, it was extracted with ethyl acetate and washed with water and brine. The title compound (1.30 g, 5.72 mmol, 65% yield) was obtained as a colorless liquid. The crude proved to be pure without further purification.

^1H NMR (500 MHz, CDCl_3 , ppm) δ = 7.75 (dd, J = 3.1, 1.7 Hz, 1H, 6-CH), 7.23 (ddd, J = 8.8, 6.6, 3.0 Hz, 1H, 3-CH), 6.80 (dd, J = 8.7, 3.6 Hz, 1H, 4-CH), 0.98 (s, 9H, $\text{SiC}(\text{CH}_3)_3$), 0.20 (s, 6H, $2 \times \text{SiCH}_3$).

^{13}C NMR (126 MHz, CDCl_3 , ppm) δ = 158.2 (d, J = 233.0 Hz), 150.2 (d, J = 4.4 Hz), 138.4 (d, J = 15.0 Hz), 132.4 (d, J = 8.2 Hz), 109.6 (d, J = 40.5 Hz), 25.7, 18.3, -4.4.

^{19}F NMR (376 MHz, CDCl_3 , ppm) δ = -77.2 (2-CF).

IR (ATR, cm^{-1}) $\tilde{\nu}$ = 2956 (w), 2931 (w), 2895 (vw), 2887 (vw), 2860 (w), 1588 (w), 1479 (vs), 1409 (vw), 1378 (m), 1364 (w), 1286 (m), 1255 (m), 1237 (vs), 1112 (w), 1089 (w), 1035 (w), 1017 (w), 1007 (w), 912 (s), 874 (w), 834 (vs), 781 (vs), 738 (w), 694 (m), 654 (vw), 636 (vw), 572 (vw), 487 (w), 460 (w), 439 (w), 395 (w).

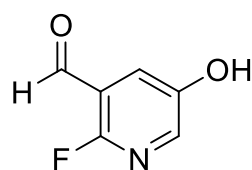
5-((*Tert*-butyldimethylsilyl)oxy)-2-fluoroisonicotinaldehyde (68)

To a stirred solution of 5-((*tert*-butyldimethylsilyl)oxy)-2-fluoropyridine (1.10 g, 4.84 mmol, 1.00 equiv) in dry tetrahydrofuran (15.0 mL) was added *n*-butyllithium (341 mg, 2.13 mL, 5.32 mmol, 2.50M, 1.10 equiv) dropwise at -78 °C. After stirring for 60 minutes at -78 °C, *N,N*-dimethylformamide (530 mg, 562 μ L, 7.26 mmol, 1.49 equiv) was added to the reaction mixture, and it was stirred for 15 mins at -78 °C. Saturated ammonium chloride solution was added dropwise to the reaction at -78 C, and the reaction was warmed-up to 21°C. The crude was extracted with ethyl acetate and washed with water and brine. The combined organic phase was dried over sodium sulfate and filtered, and the solvent was removed under reduced pressure. The crude product was purified *via* automated flash-chromatography on silica gel using a mixture of cyclohexane/dichloromethane (1% \rightarrow 100% dichloromethane) to yield 5-((*tert*-butyldimethylsilyl)oxy)-2-fluoroisonicotinaldehyde (35.5 mg, 139 μ mol, 3% yield) as a colorless liquid.

^1H NMR (400 MHz, CDCl_3 , ppm) δ = 10.23 (s, 1H, 3-CHO), 7.99 (dd, J = 3.3, 1.7 Hz, 1H, 6-CH), 7.66 (dd, J = 7.5, 3.1 Hz, 1H, 4-CH), 0.98 (s, 9H, $\text{SiC}(\text{CH}_3)_3$), 0.22 (s, 6H, $2 \times \text{SiCH}_3$).

^{13}C NMR (101 MHz, CDCl_3 , ppm) δ = 186.6 (3-CHO), 158.6 (d, J = 242.8 Hz, 2-CF), 151.1 (d, J = 4.3 Hz, 5-CO), 144.9 (d, J = 15.9 Hz, 6-CH), 128.7 (d, J = 3.2 Hz, 4-CH), 118.2 (d, J = 25.1 Hz, 3-CCHO), 25.6 (3C, $\text{SiC}(\text{CH}_3)_3$), 18.3 ($\text{SiC}(\text{CH}_3)_3$), -4.4 (2C, $2 \times \text{SiCH}_3$).

^{19}F NMR (376 MHz, CDCl_3 , ppm) δ = -83.7 (2-CF).

2-fluoro-5-hydroxynicotinaldehyde (69)

To a stirred solution of 5-((*tert*-butyldimethylsilyl)oxy)-2-fluoroisonicotinaldehyde (20.0 mg, 78.3 μmol , 1.00 equiv) acetic acid (6.23 mg, 5.94 μL , 104 μmol , 1.00 equiv) in tetrahydrofuran (1.00 mL) was added tetra-*n*-butylammonium fluoride (136 mg, 519 μL , 519 μmol , 1.00M, 5.00 equiv). After stirring for 60 minutes at 23 °C, it was quenched with sat. aq. ammonium chloride solution, extracted with ethyl acetate and washed with water and brine. The combined organic phase was dried over sodium sulfate and filtered, and the solvent was removed under reduced pressure. The crude product was purified *via* automated flash-chromatography on silica gel using a mixture of cyclohexane/ethyl acetate (5% \rightarrow 100% ethyl acetate) to yield 2-fluoro-5-hydroxynicotinaldehyde (6.80 mg, 48.2 μmol , 46% yield) as a colorless solid.

^1H NMR (500 MHz, CD_2Cl_2 , ppm) δ = 10.22 (s, 1H, 3-CHO), 8.06 (d, J = 1.9 Hz, 1H), 7.72 (dd, J = 7.6, 3.2 Hz, 1H).

Due to decomposition, recording a ^{13}C NMR with clearly assignable signals was impossible.

^{19}F NMR (376 MHz, CD_2Cl_2 , ppm) δ = -85.3 (2-CF).

IR (ATR, cm^{-1}) $\tilde{\nu}$ = 3044 (w), 2867 (w), 2764 (w), 2673 (w), 2636 (w), 2572 (w), 1704 (vs), 1594 (m), 1458 (vs), 1442 (vs), 1390 (vs), 1310 (m), 1296 (vs), 1234 (vs), 1205 (vs), 1133 (m), 1123 (m), 993 (m), 911 (vs), 820 (vs), 758 (vs), 745 (vs), 734 (vs), 633 (vs), 575 (m), 568 (s), 486 (m), 477 (m), 398 (m).

MS (EI, 70 eV) m/z (%) = 141 (100) $[\text{M}]^+$, 140 (41) $[\text{M}-\text{H}]^+$, 112 (32), 58 (10), 57 (15).

HRMS (EI, $[\text{M}]^+$, $\text{C}_6\text{H}_4\text{FNO}_2$) calcd.: 141.0226, found: 141.0227.

6 List of Abbreviations

μ	Micro	ELSD	Evaporative light scattering detector
Å	Angstrom		
Ac	Acetyl	EtOH	ethanol
aq.	Aqueous	EWG	Electron withdrawing group
atc	1,3,5,7-Adamantane tetracarboxylate	h	Hours
ATR	Attenuated total reflection	HINA	Isonicotinic acid
BD	Butanediol	HPLC	High-performance liquid chromatography
BINOL	1,1'-Bi-2-naphthol	HRMS	High-resolution mass spectrometry
BIPY,BPY	4,4'-Bipyridine	HSQC	Heteronuclear single-quantum coherence
BPDC	Biphenyl-4,4'-dicarboxylic acid	Hz	Hertz
BTC	1,3,5-Benzenetricarboxylate	Ipr	Isopropyl
Bu	Butyl	IR	Infrared
calcd.	Calculated	LBL	Layer-by-layer
CHCl ₃	Chloroform	LED	Light-emitting diode
CMMT	9-Carboxy-10-(mercaptomethyl) triptycene	LPE	Liquid-phase epitaxy
Cy	Cyclohexyl	M	Molar
D	Debye	m.p.	Melting Point
DABCO	1,4-Diazabicyclo[2.2.2]octane	<i>m/z</i>	Mass-to-charge ratio
dba	Dibenzylideneacetone	MHDA	16-Mercaptohexadecanoic acid
DE-bdc	1,4-Benzenedicarboxylate	min	Minutes
DMSO	Dimethyl sulfoxide	mL	Milliliter
DoM	Directed <i>ortho</i> metalation	mmol	Milimole
<i>e.g.</i>	lat. <i>exempli gratia</i>	MOF	Metal-organic framework
EDG	Electron donating group	MS	Mass spectrometry
EI	Electron impact	MS	Molecular sieve
equiv	Equivalents	MUD	11-Mercaptoundecanol
ESI	Electrospray ionization	NH ₃	Ammonia
Et	Ethyl	NHC	<i>N</i> -Heterocyclic carbene
<i>et al.</i>	lat. <i>et alia</i>	nm	Nanometer

NMR	Nuclear magnetic resonance
NVOC	6-Nitroveratryloxycarbonyl
PEPPSI	Pyridine- enhanced precatalyst preparation stabilization and initiation
PG	Protecting group
Ph	Phenyl
PPG	Photocleavable protecting group
PSS	Photo steady state
ppm	Parts per million
QCM	Quartz crystal microbalance
ref.	reference
<i>R_f</i>	Retardation factor
SAM	Self-assembled monolayer
sat.	Saturated
SBU	Secondary building unit
SHG	Second-harmonic generation
SURMOF	Surface
T	Temperature
t	Time
<i>t</i>	<i>tert</i>
TBAB	Tetrabutylammonium bromide
TBDMS	<i>tert</i> -Butyldimethylsilyl
Tf	Trifluoromethylsulfonyl
TFA	Trifluoroacetic acid
TLC	Thin layer chromatography
TMS	Trimethylsilyl
TPMTA	4'-Carboxyterphenyl-4- methanethiol
UV	Ultraviolet
vis	Visible
W	Watt
XRD	X-Ray diffraction
ZIF	Zeolitic imidazolate framework

7 Bibliography

1. R. Kang, L. Talamini, E. D'Este, B. M. Estevão, L. De Cola, W. Klopper and F. Biedermann, Discovery of a size-record breaking green-emissive fluorophore: small, smaller, HINA, *Chemical Science*, 2021, **12**, 1392-1397.
2. I. M. Ross, The foundation of the silicon age, *Bell Labs Technical Journal*, 2002, **2**, 3-14.
3. N. R. Council, *Opportunities in Chemistry*, The National Academies Press, Washington, DC, 1985.
4. Y. Nakao, Transition-Metal-Catalyzed C-H Functionalization for the Synthesis of Substituted Pyridines, *Synthesis*, 2011, 3209-3219.
5. F. Saitoh, M. Noma and N. Kawashima, The alkaloid contents of sixty Nicotiana species, *Phytochemistry*, 1985, **24**, 477-480.
6. J. W. Daly, H. Martin Garraffo and T. F. Spande, in *Alkaloids: Chemical and Biological Perspectives*, ed. S. W. Pelletier, Pergamon, 1999, vol. 13, pp. 1-161.
7. T. Anderson, Ueber die Producte der trocknen Destillation thierischer Materien, *Annalen der Chemie und Pharmacie*, 1851, **80**, 44-65.
8. J. Clayden, N. Greeves and S. Warren, *Organic chemistry*, Oxford University Press, New York, New York, 2nd edn., 2012.
9. T. Eicher, S. Hauptmann and A. Speicher, *The Chemistry of Heterocycles: Structures, Reactions, Synthesis, and Applications*, Wiley, 2013.
10. C. González-Bello and L. Castedo, in *Modern Heterocyclic Chemistry*, 2011, pp. 1431-1525.
11. K. Eller, E. Henkes, R. Roszbacher and H. Höke, Amines, Aliphatic, *Ullmann's Encyclopedia of Industrial Chemistry*, 2000.
12. C. N. Satterfield, M. Modell and J. F. Mayer, Interactions between catalytic hydrodesulfurization of thiophene and hydrodenitrogenation of pyridine, *AIChE J.*, 1975, **21**, 1100-1107.
13. J. I. Jones, 287. Studies of coal tar bases. Part III. By-products of the hydrogenation of pyridine with raney nickel, *J. Chem. Soc.*, 1950, 1392-1397.
14. S. Sowmiah, J. M. S. S. Esperança, L. P. N. Rebelo and C. A. M. Afonso, Pyridinium salts: from synthesis to reactivity and applications, *Org. Chem. Front.*, 2018, **5**, 453-493.
15. H. Kühner, Synthesis of 4,4'-bipyridines as non-centrosymmetric linkers for surface-mounted metal-organic frameworks holding non-linear optical properties, Karlsruhe Institute of Technology (KIT), 2019.
16. R. Laville, G. Genta-Jouve, C. Urda, R. Fernández, O. Thomas, F. Reyes and P. Amade, Njaoaminiums A, B, and C: Cyclic 3-Alkylpyridinium Salts from the Marine Sponge *Reniera* sp., *Molecules*, 2009, **14**, 4716-4724.

17. C. M. Gordon, M. J. Muldoon, M. Wagner, C. Hilgers, J. H. Davis Jr and P. Wasserscheid, in *Ionic Liquids in Synthesis*, 2007, p. 8.
18. J. A. Joule and K. Mills, *Heterocyclic Chemistry*, Wiley, 2013.
19. A. Klapars and E. Vedejs, Activation of Pyridinium Salts for Electrophilic Acylation: a Method for Conversion of Pyridines into 3-Acylpyridines, *Chemistry of Heterocyclic Compounds*, 2004, **40**, 759-766.
20. E. F. V. Scriven, in *Comprehensive Heterocyclic Chemistry*, eds. A. R. Katritzky and C. W. Rees, Pergamon, Oxford, 1984, pp. 165-314.
21. in *Nomenclature of Organic Chemistry: IUPAC Recommendations and Preferred Names 2013*, The Royal Society of Chemistry, 2014, pp. 1-129.
22. L.-M. Duan, F.-T. Xie, X.-Y. Chen, Y. Chen, Y.-K. Lu, P. Cheng and J.-Q. Xu, Syntheses, Structures, and Magnetic Properties of Three Novel Metal–Malate–Bipyridine Coordination Polymers with Layered and Pillared Topology, *Crystal Growth & Design*, 2006, **6**, 1101-1106.
23. Z.-E. Lin, J. Zhang, S.-T. Zheng and G.-Y. Yang, A New Inorganic-Organic Hybrid with Zinc Phosphate Layers Pillared by the 4, 4'-Bipyridine Units, *Z. Anorg. Allg. Chem.*, 2005, **631**, 155-159.
24. C. Ruiz-Pérez, P. A. Lorenzo-Luis, M. Hernández-Molina, M. M. Laz, P. Gili and M. Julve, Supramolecular Loop-Chain Network of Pillared Layers via 4,4'-Bipyridine, *Crystal Growth & Design*, 2004, **4**, 57-61.
25. J. Qiao, X. Liu, X. Liu, X. Liu, L. Zhang and Y. Liu, Two urea-functionalized pcu metal–organic frameworks based on a pillared-layer strategy for gas adsorption and separation, *Inorganic Chemistry Frontiers*, 2020, **7**, 3500-3508.
26. P. Metrangolo and G. Resnati, Halogen Bonding: A Paradigm in Supramolecular Chemistry, *Chemistry – A European Journal*, 2001, **7**, 2511-2519.
27. J. A. Davidson, M. Sacchi, F. Gorrec, S. M. Clarke and S. J. Jenkins, Halogen Bonding in Bicomponent Monolayers: Self-Assembly of a Homologous Series of Iodinated Perfluoroalkanes with Bipyridine, *Langmuir*, 2021, **37**, 627-635.
28. T. Anderson, Ueber die Producte der trockenen Destillation thierischer Materien, *Annalen der Chemie und Pharmacie*, 1870, **154**, 270-286.
29. H. Weidel and M. Russo, Studien über das Pyridin, *Monatsh. Chem.*, 1882, **3**, 850-885.
30. G. M. Badger and W. H. F. Sasse, in *Adv. Heterocycl. Chem.*, ed. A. R. Katritzky, Academic Press, 1963, vol. 2, pp. 179-202.
31. Estimated Annual Agricultural use of Paraquat, <https://water.usgs.gov/nawqa/pnsp/usage/maps/county-level/>, (accessed 03.08.2022).
32. F. Kubel and J. Strähle, Polymere Dimethyl- und Diphenylglyoximatokomplexe des Cobalts und Eisens mit 4,4'-Bipyridin als Brückenligand. Die Kristallstruktur des Bis(dimethylglyoximato)4,4'-bipyridincobalt(II), *Z. Naturforsch.*, 1982, **37b**, 272.

33. T. J. Meyer, Photochemistry of metal coordination complexes: metal to ligand charge transfer excited states, *Pure Appl. Chem.*, 1986, **58**, 1193-1206.
34. A. Juris, V. Balzani, F. Barigelletti, S. Campagna, P. Belser and A. von Zelewsky, Ru(II) polypyridine complexes: photophysics, photochemistry, electrochemistry, and chemiluminescence, *Coord. Chem. Rev.*, 1988, **84**, 85-277.
35. J.-M. Lehn, Supramolecular Chemistry—Scope and Perspectives Molecules, Supermolecules, and Molecular Devices(Nobel Lecture), *Angew. Chem. Int. Ed.*, 1988, **27**, 89-112.
36. C. S. John, in *Encyclopedia of Supramolecular Chemistry*, CRC Press, 2004, ch. Spherands.
37. J. W. Steed and J. L. Atwood, *Supramolecular Chemistry*, Wiley, 2022.
38. F. M. Menger, Supramolecular chemistry and self-assembly, *Proceedings of the National Academy of Sciences*, 2002, **99**, 4818-4822.
39. Y. Yang and M. W. Urban, Self-Healing of Polymers via Supramolecular Chemistry, *Advanced Materials Interfaces*, 2018, **5**, 1800384.
40. S. R. Batten, N. R. Champness, X.-M. Chen, J. Garcia-Martinez, S. Kitagawa, L. Öhrström, M. O’Keeffe, M. P. Suh and J. Reedijk, Terminology of metal–organic frameworks and coordination polymers (IUPAC Recommendations 2013), *Pure Appl. Chem.*, 2013, **85**, 1715-1724.
41. O. M. Yaghi, M. O’Keeffe, N. W. Ockwig, H. K. Chae, M. Eddaoudi and J. Kim, Reticular synthesis and the design of new materials, *Nature*, 2003, **423**, 705-714.
42. H. Furukawa, K. E. Cordova, M. O’Keeffe and O. M. Yaghi, The Chemistry and Applications of Metal-Organic Frameworks, *Science*, 2013, **341**, 1230444.
43. M. J. Kalmutzki, N. Hanikel and O. M. Yaghi, Secondary building units as the turning point in the development of the reticular chemistry of MOFs, *Sci Adv*, 2018, **4**, eaat9180.
44. K. Yukio, M. Ikuo, H. Taiichi and S. Yoshihiko, The Crystal Structure of Bis(adiponitrilo)copper(I) Nitrate, *Bull. Chem. Soc. Jpn.*, 1959, **32**, 1221-1226.
45. H. Li, M. Eddaoudi, T. L. Groy and O. M. Yaghi, Establishing Microporosity in Open Metal–Organic Frameworks: Gas Sorption Isotherms for Zn(BDC) (BDC = 1,4-Benzenedicarboxylate), *J. Am. Chem. Soc.*, 1998, **120**, 8571-8572.
46. H. Li, M. Eddaoudi, M. O’Keeffe and O. M. Yaghi, Design and synthesis of an exceptionally stable and highly porous metal-organic framework, *Nature*, 1999, **402**, 276-279.
47. O. M. Yaghi and H. Li, Hydrothermal Synthesis of a Metal-Organic Framework Containing Large Rectangular Channels, *J. Am. Chem. Soc.*, 1995, **117**, 10401-10402.
48. O. M. Yaghi, M. J. Kalmutzki, C. S. Diercks and L. Wiley Online, *Introduction to reticular chemistry : metal-organic frameworks and covalent organic frameworks*, Wiley-VCH Verlag GmbH & Co, Weinheim, Germany, 1st edn., 2019.
49. H. Furukawa and O. M. Yaghi, Storage of Hydrogen, Methane, and Carbon Dioxide in Highly Porous Covalent Organic Frameworks for Clean Energy Applications, *J. Am. Chem. Soc.*, 2009, **131**, 8875-8883.

50. H. Furukawa, K. E. Cordova, M. O'Keeffe and O. M. Yaghi, The Chemistry and Applications of Metal-Organic Frameworks, *Science*, 2013, **341**.
51. W. Lu, Z. Wei, Z.-Y. Gu, T.-F. Liu, J. Park, J. Park, J. Tian, M. Zhang, Q. Zhang, T. Gentle Iii, M. Bosch and H.-C. Zhou, Tuning the structure and function of metal-organic frameworks via linker design, *Chem. Soc. Rev.*, 2014, **43**, 5561-5593.
52. J. H. Fendler, Self-Assembled Nanostructured Materials, *Chem. Mater.*, 1996, **8**, 1616-1624.
53. J.-M. Lehn, Perspectives in Supramolecular Chemistry—From Molecular Recognition towards Molecular Information Processing and Self-Organization, *Angew. Chem. Int. Ed.*, 1990, **29**, 1304-1319.
54. M. Shimomura and T. Sawadaishi, Bottom-up strategy of materials fabrication: a new trend in nanotechnology of soft materials, *Current Opinion in Colloid & Interface Science*, 2001, **6**, 11-16.
55. A. J. Blake, N. R. Champness, P. Hubberstey, W.-S. Li, M. A. Withersby and M. Schröder, Inorganic crystal engineering using self-assembly of tailored building-blocks, *Coord. Chem. Rev.*, 1999, **183**, 117-138.
56. D. Philp and J. F. Stoddart, Self-Assembly in Natural and Unnatural Systems, *Angew. Chem. Int. Ed.*, 1996, **35**, 1154-1196.
57. D. Zacher, O. Shekhah, C. Wöll and R. A. Fischer, Thin films of metal-organic frameworks, *Chem. Soc. Rev.*, 2009, **38**, 1418.
58. M. A. Herman, W. Richter and H. Sitter, in *Epitaxy: Physical Principles and Technical Implementation*, Springer Berlin Heidelberg, Berlin, Heidelberg, 2004, pp. 63-80.
59. O. Shekhah, H. Wang, S. Kowarik, F. Schreiber, M. Paulus, M. Tolan, C. Sternemann, F. Evers, D. Zacher, R. A. Fischer and C. Wöll, Step-by-Step Route for the Synthesis of Metal-Organic Frameworks, *J. Am. Chem. Soc.*, 2007, **129**, 15118-15119.
60. O. Shekhah, H. Wang, T. Strunskus, P. Cyganik, D. Zacher, R. Fischer and C. Wöll, Layer-by-Layer Growth of Oriented Metal Organic Polymers on a Functionalized Organic Surface, *Langmuir*, 2007, **23**, 7440-7442.
61. A. Bétard and R. A. Fischer, Metal-Organic Framework Thin Films: From Fundamentals to Applications, *Chem. Rev.*, 2012, **112**, 1055-1083.
62. O. Shekhah, J. Liu, R. A. Fischer and C. Wöll, MOF thin films: existing and future applications, *Chem. Soc. Rev.*, 2011, **40**, 1081.
63. J. C. Love, L. A. Estroff, J. K. Kriebel, R. G. Nuzzo and G. M. Whitesides, Self-Assembled Monolayers of Thiolates on Metals as a Form of Nanotechnology, *Chem. Rev.*, 2005, **105**, 1103-1170.
64. S. Wannapaiboon, A. Schneemann, I. Hante, M. Tu, K. Epp, A. L. Semrau, C. Sternemann, M. Paulus, S. J. Baxter, G. Kieslich and R. A. Fischer, Control of structural flexibility of layered-pillared metal-organic frameworks anchored at surfaces, *Nature Communications*, 2019, **10**.
65. D. R. Smith, W. J. Padilla, D. C. Vier, S. C. Nemat-Nasser and S. Schultz, Composite Medium with Simultaneously Negative Permeability and Permittivity, *Phys. Rev. Lett.*, 2000, **84**, 4184-4187.

66. J. B. Pendry, Negative Refraction Makes a Perfect Lens, *Phys. Rev. Lett.*, 2000, **85**, 3966-3969.
67. P. Ronan, EM spectrum, https://upload.wikimedia.org/wikipedia/commons/3/30/EM_spectrumrevised.png, (accessed 31st October, 2020).
68. B. Pilkington, Metamaterials: An Overview., <https://www.azom.com/article.aspx?ArticleID=21097>, (accessed 11.10.2022, 2022).
69. S. Guenneau, A. Movchan, G. Pétursson and S. Anantha Ramakrishna, Acoustic metamaterials for sound focusing and confinement, *New Journal of Physics*, 2007, **9**, 399-399.
70. G. Oliveri, D. H. Werner and A. Massa, Reconfigurable Electromagnetics Through Metamaterials—A Review, *Proceedings of the IEEE*, 2015, **103**, 1034-1056.
71. M. Brun, S. Guenneau and A. B. Movchan, Achieving control of in-plane elastic waves, *Appl. Phys. Lett.*, 2009, **94**, 061903.
72. D. J. Williams, Organic Polymeric and Non-Polymeric Materials with Large Optical Nonlinearities, *Angew. Chem. Int. Ed.*, 1984, **23**, 690-703.
73. G. He and S. H. Liu, *Physics of nonlinear optics*, World Scientific, 1999.
74. M. O. Senge, M. Fazekas, E. G. A. Notaras, W. J. Blau, M. Zawadzka, O. B. Locos and E. M. Ni Mhuircheartaigh, Nonlinear Optical Properties of Porphyrins, *Adv. Mater.*, 2007, **19**, 2737-2774.
75. S. R. Marder, J. E. Sohn and G. D. Stucky, *Materials for nonlinear optics chemical perspectives*, American Chemical Society Washington DC, 1991.
76. J. M. Cole, Single-crystal X-ray diffraction studies of photo-induced molecular species, *Chem. Soc. Rev.*, 2004, **33**, 501-513.
77. R. W. Boyd, in *Nonlinear Optics (Third Edition)*, ed. R. W. Boyd, Academic Press, Burlington, 2008, pp. 1-67.
78. R. Menzel, *Photonics : linear and nonlinear interactions of laser light and matter*, Springer, Berlin ; New York, 2nd edn., 2007.
79. D. Gonzalez-Andrade, A. Dias, J. M. Luque-Gonzalez, J. Gonzalo Wanguemert-Perez, A. Ortega-Monux, R. Halir, I. Molina-Fernandez, P. Cheben and A. V. Velasco, 2020.
80. L. Raju, K.-T. Lee, Z. Liu, D. Zhu, M. Zhu, E. Poutrina, A. Urbas and W. Cai, Maximized Frequency Doubling through the Inverse Design of Nonlinear Metamaterials, *ACS Nano*, 2022, **16**, 3926-3933.
81. Z. L. Sámson, K. F. Macdonald, F. De Angelis, B. Gholipour, K. Knight, C. C. Huang, E. Di Fabrizio, D. W. Hewak and N. I. Zheludev, Metamaterial electro-optic switch of nanoscale thickness, *Appl. Phys. Lett.*, 2010, **96**, 143105.
82. W. Zhu, I. D. Rukhlenko and M. Premaratne, Graphene metamaterial for optical reflection modulation, *Appl. Phys. Lett.*, 2013, **102**, 241914.

83. S. Xiao, T. Wang, T. Liu, C. Zhou, X. Jiang and J. Zhang, Active metamaterials and metadevices: a review, *J. Phys. D: Appl. Phys.*, 2020, **53**, 503002.
84. Y. Yao, Z. Liao, Z. Liu, X. Liu, J. Zhou, G. Liu, Z. Yi and J. Wang, Recent progresses on metamaterials for optical absorption and sensing: a review, *J. Phys. D: Appl. Phys.*, 2021, **54**, 113002.
85. J. M. Cole, Organic materials for second-harmonic generation: advances in relating structure to function, *Philosophical Transactions of the Royal Society of London. Series A: Mathematical, Physical and Engineering Sciences*, 2003, **361**, 2751-2770.
86. H. S. Nalwa, T. Watanabe and S. Miyata, in *Nonlinear Optics of Organic Molecules and Polymers*, CRC press, 2020, pp. 89-350.
87. J. F. W. Herschel, IV. 'Αμόρφωτα, no. I.— on a case of superficial colour presented by a homogeneous liquid internally colourless, *Philosophical Transactions of the Royal Society of London*, 1845, **135**, 143-145.
88. G. G. Stokes, XXX. On the change of refrangibility of light, *Philosophical Transactions of the Royal Society of London*, 1852, **142**, 463-562.
89. A. Jabłoński, Über den Mechanismus der Photolumineszenz von Farbstoffphosphoren, *Zeitschrift für Physik*, 1935, **94**, 38-46.
90. M. Zimmer, GFP: from jellyfish to the Nobel prize and beyond, *Chem. Soc. Rev.*, 2009, **38**, 2823.
91. L. Möckl, D. C. Lamb and C. Bräuchle, Super-resolved Fluorescence Microscopy: Nobel Prize in Chemistry 2014 for Eric Betzig, Stefan Hell, and William E. Moerner, *Angew. Chem. Int. Ed.*, 2014, **53**, 13972-13977.
92. A. Jain, C. Blum and V. Subramaniam, in *Advances in Biomedical Engineering*, ed. P. Verdonck, Elsevier, Amsterdam, 2009, pp. 147-176.
93. B. Valeur and M. N. Berberan-Santos, *Molecular Fluorescence: Principles and Applications*, Wiley, 2012.
94. P. Pantazis, J. Maloney, D. Wu and S. E. Fraser, Second harmonic generating (SHG) nanoprobe for in vivo imaging, *Proceedings of the National Academy of Sciences*, 2010, **107**, 14535-14540.
95. I. Berlman, *Handbook of fluorescence spectra of aromatic molecules*, Elsevier, 2012.
96. J. R. Albani, *Structure and Dynamics of Macromolecules: Absorption and Fluorescence Studies*, Elsevier Science, 2011.
97. Y. Sato, S. Ichinosawa and H. Kanai, Operation characteristics and degradation of organic electroluminescent devices, *IEEE Journal of Selected Topics in Quantum Electronics*, 1998, **4**, 40-48.
98. J. Liu, Y.-Q. Sun, H. Zhang, H. Shi, Y. Shi and W. Guo, Sulfone-Rhodamines: A New Class of Near-Infrared Fluorescent Dyes for Bioimaging, *ACS Applied Materials & Interfaces*, 2016, **8**, 22953-22962.

99. L. D. Lavis and R. T. Raines, Bright Building Blocks for Chemical Biology, *ACS Chemical Biology*, 2014, **9**, 855-866.
100. Y. Fu and N. S. Finney, Small-molecule fluorescent probes and their design, *RSC Advances*, 2018, **8**, 29051-29061.
101. M. Cooper, A. Ebner, M. Briggs, M. Burrows, N. Gardner, R. Richardson and R. West, Cy3B™: Improving the Performance of Cyanine Dyes, *Journal of Fluorescence*, 2004, **14**, 145-150.
102. A. Loudet and K. Burgess, BODIPY Dyes and Their Derivatives: Syntheses and Spectroscopic Properties, *Chem. Rev.*, 2007, **107**, 4891-4932.
103. K. Źamojć, W. Wiczak, B. Zaborowski, D. Jacewicz and L. Chmurzyński, Fluorescence quenching of 7-amino-4-methylcoumarin by different TEMPO derivatives, *Spectrochimica Acta Part A: Molecular and Biomolecular Spectroscopy*, 2015, **136**, 1875-1880.
104. R. N. Dsouza, U. Pischel and W. M. Nau, Fluorescent Dyes and Their Supramolecular Host/Guest Complexes with Macrocycles in Aqueous Solution, *Chem. Rev.*, 2011, **111**, 7941-7980.
105. G. Hong, A. L. Antaris and H. Dai, Near-infrared fluorophores for biomedical imaging, *Nature Biomedical Engineering*, 2017, **1**, 0010.
106. H. Kühner, L. Leyen, Z. Hassan, C. Wöll and S. Bräse, Synthesis of Non-centrosymmetric Dipolar 4,4'-Bipyridines: Molecular Tectons for Programmed Assembly of Supramolecular Systems, *ChemPlusChem*, 2022.
107. , Nobel Prizes 2010: Richard F. Heck / Ei-ichi Negishi / Akira Suzuki, *Angew. Chem. Int. Ed.*, 2010, **49**, 8300-8300.
108. N. Miyaura, T. Ishiyama, M. Ishikawa and A. Suzuki, Palladium-catalyzed cross-coupling reactions of B-alkyl-9-BBN or trialkylboranes with aryl and 1-alkenyl halides, *Tetrahedron Lett.*, 1986, **27**, 6369-6372.
109. C. Len, S. Bruniaux, F. Delbecq and V. Parmar, Palladium-Catalyzed Suzuki–Miyaura Cross-Coupling in Continuous Flow, *Catalysts*, 2017, **7**, 146.
110. N. Miyaura, T. Yanagi and A. Suzuki, The Palladium-Catalyzed Cross-Coupling Reaction of Phenylboronic Acid with Haloarenes in the Presence of Bases, *Synth. Commun.*, 1981, **11**, 513-519.
111. A. Suzuki, Recent advances in the cross-coupling reactions of organoboron derivatives with organic electrophiles, 1995–1998, *J. Organomet. Chem.*, 1999, **576**, 147-168.
112. C. Amatore, A. Jutand and G. Le Duc, Mechanistic Origin of Antagonist Effects of Usual Anionic Bases (OH⁻, CO₃²⁻) as Modulated by their Counteranions (Na⁺, Cs⁺, K⁺) in Palladium-Catalyzed Suzuki–Miyaura Reactions, *Chemistry – A European Journal*, 2012, **18**, 6616-6625.
113. S. Grosjean, Z. Hassan, C. Wöll and S. Bräse, Diverse Multi-Functionalized Oligoarenes and Heteroarenes for Porous Crystalline Materials, *Eur. J. Org. Chem.*, 2019, **2019**, 1446-1460.
114. T. Ohmura, Y. Morimasa and M. Suginome, Organocatalytic Diboration Involving “Reductive Addition” of a Boron–Boron σ -Bond to 4,4'-Bipyridine, *J. Am. Chem. Soc.*, 2015, **137**, 2852-2855.

115. D. Bulfield and S. M. Huber, Synthesis of Polyfluorinated Biphenyls; Pushing the Boundaries of Suzuki–Miyaura Cross Coupling with Electron-Poor Substrates, *J. Org. Chem.*, 2017, **82**, 13188-13203.
116. J. Clayden, N. Greeves, S. Warren, F. Glauner, K. Mühle and K. von der Saal, *Organische Chemie*, Springer Berlin Heidelberg, 2017.
117. F. Schroeter and T. Strassner, Understanding Anionic “Ligandless” Palladium Species in the Mizoroki–Heck Reaction, *Inorg. Chem.*, 2018, **57**, 5159-5173.
118. D. Guest, V. H. Menezes da Silva, A. P. de Lima Batista, S. M. Roe, A. A. C. Braga and O. Navarro, (N-Heterocyclic Carbene)-Palladate Complexes in Anionic Mizoroki–Heck Coupling Cycles: A Combined Experimental and Computational Study, *Organometallics*, 2015, **34**, 2463-2470.
119. D. Borah, B. Saha, B. Sarma and P. Das, A new PEPPSI type N-heterocyclic carbene palladium(II) complex and its efficiency as a catalyst for Mizoroki–Heck cross-coupling reactions in water, *Journal of Chemical Sciences*, 2020, **132**.
120. L. Heinke, M. Cakici, M. Dommaschk, S. Grosjean, R. Herges, S. Bräse and C. Wöll, Photoswitching in Two-Component Surface-Mounted Metal–Organic Frameworks: Optically Triggered Release from a Molecular Container, *ACS Nano*, 2014, **8**, 1463-1467.
121. X. Yu, Z. Wang, M. Buchholz, N. Füllgrabe, S. Grosjean, F. Bebensee, S. Bräse, C. Wöll and L. Heinke, cis-to-trans isomerization of azobenzene investigated by using thin films of metal–organic frameworks, *Physical Chemistry Chemical Physics*, 2015, **17**, 22721-22725.
122. A. Baeyer, Nitrosobenzol und Nitrosonaphtalin, *Berichte der deutschen chemischen Gesellschaft*, 1874, **7**, 1638-1640.
123. C. Mills, XCIII.—Some new azo-compounds, *Journal of the Chemical Society, Transactions*, 1895, **67**, 925-933.
124. J. Kohl-Landgraf, F. Buhr, D. Lefrancois, J.-M. Mewes, H. Schwalbe, A. Dreuw and J. Wachtveitl, Mechanism of the Photoinduced Uncaging Reaction of Puromycin Protected by a 6-Nitroveratryloxycarbonyl Group, *J. Am. Chem. Soc.*, 2014, **136**, 3430-3438.
125. A. S. C. Fonseca, M. S. T. Gonçalves and S. P. G. Costa, Photocleavage studies of fluorescent amino acid conjugates bearing different types of linkages, *Tetrahedron*, 2007, **63**, 1353-1359.
126. A. V. Pinheiro, P. Baptista and J. C. Lima, Light activation of transcription: photocaging of nucleotides for control over RNA polymerization, *Nucleic Acids Res.*, 2008, **36**, e90-e90.
127. R. O. Schönleber, J. Bendig, V. Hagen and B. Giese, Rapid photolytic release of cytidine 5'-diphosphate from a coumarin derivative: a new tool for the investigation of ribonucleotide reductases, *Biorg. Med. Chem.*, 2002, **10**, 97-101.
128. T. Weinrich, M. Gränz, C. Grünewald, T. F. Prisner and M. W. Göbel, Synthesis of a Cytidine Phosphoramidite with Protected Nitroxide Spin Label for EPR Experiments with RNA, *Eur. J. Org. Chem.*, 2017, **2017**, 491-496.
129. G. Sauerbrey, Verwendung von Schwingquarzen zur Wägung dünner Schichten und zur Mikrowägung, *Zeitschrift für Physik*, 1959, **155**, 206-222.

130. J. Liu, B. Lukose, O. Shekhah, H. K. Arslan, P. Weidler, H. Gliemann, S. Bräse, S. Grosjean, A. Godt, X. Feng, K. Müllen, I.-B. Magdau, T. Heine and C. Wöll, A novel series of isorecticular metal organic frameworks: realizing metastable structures by liquid phase epitaxy, *Scientific Reports*, 2012, **2**.
131. A. Nefedov, R. Haldar, Z. Xu, H. Kühner, D. Hofmann, D. Goll, B. Sapotta, S. Hecht, M. Krstić, C. Rockstuhl, W. Wenzel, S. Bräse, P. Tegeder, E. Zojer and C. Wöll, Avoiding the Center-Symmetry Trap: Programmed Assembly of Dipolar Precursors into Porous, Crystalline Molecular Thin Films, *Adv. Mater.*, 2021, **33**, 2103287.
132. J. Lu, X. Liu, M. Zhao, X.-B. Deng, K.-X. Shi, Q.-R. Wu, L. Chen and L.-M. Wu, Discovery of NLO Semiorganic C₅H₆ON⁺(H₂PO₄)⁻: Dipole Moment Modulation and Superior Synergy in Solar-Blind UV Region, *J. Am. Chem. Soc.*, 2021, **143**, 3647-3654.
133. W. R. Dolbier, *Guide to Fluorine NMR for Organic Chemists*, Wiley, 2009.
134. I. Seven, T. Weinrich, M. Gränz, C. Grünewald, S. Brüß, I. Krstić, T. F. Prisner, A. Heckel and M. W. Göbel, Photolabile Protecting Groups for Nitroxide Spin Labels, *Eur. J. Org. Chem.*, 2014, 4037-4043.

8 Appendix

8.1 Curriculum Vitae

Personal Details

Name:	Hannes Fabian Kühner
Date of Birth:	November 11, 1992
Place of Birth	Bad Friedrichshall
Address:	Westmarkstr. 30, 76227 Karlsruhe, Germany

Education

01/2020 – present	Collège des Ingénieurs (CDI), Munich MBA Fellow, Science and Management Program
09/2019 – 02/2023	Karlsruhe Institute of Technology (KIT), Karlsruhe Ph.D. in Organic Chemistry (Prof. Dr. Stefan Bräse) - “Synthesis and applications of functional pyridines for metamaterials and fluorophores”
04/2017 – 08/2019	Karlsruhe Institute of Technology (KIT), Karlsruhe M.Sc. in Chemical Biology (1.1) Master Thesis (Prof. Dr. Stefan Bräse) – “Synthesis of 4,4'-bipyridines as non-centrosymmetric linkers for surface-mounted metal-organic frameworks holding non-linear optical properties”
10/2013 – 04/2017	Karlsruhe Institute of Technology (KIT), Karlsruhe B.Sc. in Chemical Biology (1.8) Bachelor Thesis (Prof. Dr. Stefan Bräse) – “Beiträge zur Semisynthese von Calotropin: Synthese und Gegenüberstellung vicinaler 2,3-Steroiddiele
09/2009 – 07/2012	Christiane-Herzog-Schule, Heilbronn Abitur, Allgemeine Hochschulreife (1.6)

8.2 List of Publications

- (1) Sarah Al Muthafer, Christoph Schissler, Vanessa Koch, Hannes Kühner, Martin Nieger and Stefan Bräse, *accepted*. Stereoselective Semisynthesis of Uzarigenin and allo-Uzarigenin, *Organic Chemistry Frontiers*, 2022.
- (2) H. Kühner, L. Leyen, Z. Hassan, C. Wöll and S. Bräse, Synthesis of Non-centrosymmetric Dipolar 4,4'-Bipyridines: Molecular Tectons for Programmed Assembly of Supramolecular Systems, *ChemPlusChem*, 2022, e202200425.
- (3) Nefedov, R. Haldar, Z. Xu, H. Kühner, D. Hofmann, D. Goll, B. Sapotta, S. Hecht, M. Krstić, C. Rockstuhl, W. Wenzel, S. Bräse, P. Tegeder, E. Zojer and C. Wöll, Avoiding the Center-Symmetry Trap: Programmed Assembly of Dipolar Precursors into Porous, Crystalline Molecular Thin Films, *Adv. Mater.*, 2021, **33**, 2103287.
- (4) J. M. O'Brien, E. Sitte, K. J. Flanagan, H. Kühner, L. J. Hallen, D. Gibbons and M. O. Senge, Functionalization of Deutero- and Protoporphyrin IX Dimethyl Esters via Palladium-Catalyzed Coupling Reactions, *J. Org. Chem.*, 2019, **84**, 6158-6173.

8.3 Acknowledgements

At this point of the thesis, I would like to highlight all of those people and organizations that have contributed in a special way to the realization of this thesis by supporting me directly or indirectly in my endeavor. I chose to prepare parts of the Acknowledgements in German or English for better understanding of the persons that are mentioned.

An dieser Stelle der Arbeit möchte ich noch all diejenigen Menschen und Organisationen hervorheben, die im besonderen Maße zur Umsetzung dieser Doktorarbeit beigetragen haben, indem sie mich bei meinem Unterfangen direkt oder indirekt unterstützt haben. Ich habe mich dafür entschieden, Teile der Danksagungen auf Deutsch oder Englisch zu verfassen, um ein besseres Verständnis für die erwähnten Personen zu ermöglichen.

Bereits für meine Bachelorarbeit hat Prof. Stefan Bräse mich in seinem Arbeitskreis herzlich aufgenommen und mir früh im Studium eine Perspektive gegeben sowie die die Chance diese zu verfolgen. Über die Jahre habe ich ihn als Mensch und Doktorvater schätzen gelernt. Seine gutmütige und professionelle Unterstützung während der Anfertigung dieser Arbeit haben maßgeblich zum Gelingen beigetragen. Ich bedanke mich für das Vertrauen und die Freiheit, die ich während meiner Zeit im Arbeitskreis genießen durfte. Außerdem möchte ich mir für die Bereitstellung des Arbeitsplatzes bedanken und dafür, dass er jederzeit ein offenes Ohr für Anliegen jeglicher Art hatte.

Durch die Unterstützung von Prof. Wöll wurde es erst ermöglicht dieses interdisziplinäre Forschungsprojekt durchzuführen und neuartige SURMOFs herzustellen. Des Weiteren möchte ich mich freundlich für die Annahme des Korreferats bedanken. Auch bei Benedikt Sapotta, der mir durch seine unkomplizierte und kollegiale Hilfe stets zur Seite stand, sowie bei Dr. Ritesh Haldar möchte ich mich bedanken.

Außerdem bin ich 3DMM20 und 3MET nicht nur für die finanzielle Unterstützung dankbar, sondern auch für die Möglichkeiten, die sich mir durch Netzwerk- und Schulungsveranstaltungen boten.

Next, I want to thank Dr. Zahid Hassan for being the best advisor during my thesis that I could have wished for. His ideas and purposefulness were of inestimable value for the professional work and with his encouraging words he cheered me up whenever I needed it most.

I am grateful that Dr. Ksenia Kutonova has included me in her select circle of "Ksenia's Jünger", her support in finding topics and her straightforward help during my work.

Während meiner Zeit im AK Bräse bin ich dem 1. Stock stets treu geblieben. Hierbei bin ich mit vielen Menschen in Kontakt gekommen, die mich während meiner alltäglichen Arbeit unterstützten und an vielen Tagen einen durchschnittlichen zu einem großartigen Arbeitstag machten. Ganz besonders möchte ich mich jedoch bei Dr. Christin Bednarek bedanken, die mich durch ihr offenes Ohr und mit ihren Ratschlägen stets unterstützte.

Mein Dank geht ebenso an die Verwaltung des Fachbereichs und das Institut, insbesondere an Christiane Lampert, Janine Bolz, Karolin Kohnle, Dr. Andreas Rapp, Dr. Norbert Foitzik und Angelika Mösle. Darüber hinaus bin ich für die Zusammenarbeit mit den AK Bräse Mitarbeitenden am Campus Nord dankbar, hier möchte ich besonders Dr. Nicole Jung und Simone Gräßle erwähnen.

Ich kann mich glücklich schätzen mit dem AK Bräse eine Arbeitsgruppe gefunden zu haben, in der ich viele fröhliche Momente erleben durfte. Die beiläufigen Gespräche auf dem Gang oder in der Küche, die Diskussionen bei den AK Barbecues und nach der Arbeit bedeuteten für mich viel mehr, als es die alltäglichen Situationen erahnen ließen. Mein besonderer Dank gilt Dr. Susanne Kirchner, Dr. Stefan Marschner, Dr. Nicolai Rosenbaum, Dr. Christina Retich sowie Dr. Jasmin Busch, von denen ich stets praktische Ratschläge bekam und die mich sehr herzlich in den Arbeitskreis aufgenommen haben.

Durch die Betreuung von Studierenden und Auszubildenden konnte ich Gelerntes weitergeben, während ich selbst Neues lernen durfte. Für die Unterstützung während meiner Arbeit danke ich den drei Auszubildenden Sina Jaschik, Michelle Karsten und Lisa Wanner und den Studierenden Lisa Rieger, Severin Stelter und Louis Leyen für das gemeinsame Arbeiten und Diskutieren und wünsche ihnen allen das Beste für die Zukunft.

Wie viel Unterstützung man erfährt, zeigt sich besonders in Zeiten, in denen man auf die Hilfe anderer angewiesen ist. Ich danke den Rettern in der Not: Jens Hohmann und Angelika Seliwjorstow.

Für die gemeinsame Zeit auf 3DMM20 Seminaren in Bad Herrenalb, Diskussionen und Scherze in und zwischen den Laboren, sowie die Unterstützung während meiner gesamten Promotion bin ich Simon Oßwald ganz besonders dankbar.

Den beiden Collège des Ingénieurs-Fellows Gloria Hong und Steffen Otterbach möchte ich für die schöne gemeinsame Zeit während der Seminare in Paris, die akribische Vorbereitung auf das Vorstellungsgespräch und für die ausgedehnten Diskussionen über Alltägliches danken.

There are more people that made the first floor unique, and I want to thank Lisa-Lou Gracia and Céline Leonhardt for amazing coffee breaks and after-hour activities. I will never forget discussions about hair styles, amazing food and many more. I am grateful for the time I spent with Cecilia Bruschi during my PhD, and I will never forget the laughs we had.

Schon vor dem Studium sind Dr. Christoph Schissler und ich uns begegnet und ich kann mich glücklich schätzen, mit ihm meine Studienzeit verbracht haben zu dürfen. Ich bin dankbar für die gemeinsame Zeit, tiefgreifende Diskussionen und größere und kleinere Späße im Alltag.

Weiterhin möchte ich mich bei allen bedanken, die mir diese Arbeit ermöglicht haben:

Mein besonderer Dank gebührt meinen Eltern, die mir mein Studium erst ermöglichten und mir stets liebevoll und voller Verständnis zur Seite standen. Ganz besonderen Dank dafür, dass Sie immer das Beste für meine Geschwister und mich tun und alles Erdenkliche bereit sind, dafür zu geben.

Meinen Geschwistern Lisa und Anna möchte ich für die unschätzbar wertvolle gemeinsame Zeit, die schwesterliche Unterstützung und den Rat danken, den ihr mir jederzeit habt zuteilwerden lassen. Bei euch und „euren Männern“ Daniel, Rico und Louis kann ich die Arbeit hinter mir lassen.

Ein großer Dank geht auch an meine Tanten und Onkel Christine und Peter sowie Uta und Claus, die mich stets in meinem Weg bestärkt haben und auf deren Unterstützung ich jederzeit bauen konnte.

Für die Unterstützung von Familie Osterberg, die mich von Beginn an wie ein Mitglied der Familie aufgenommen haben, möchte ich mich herzlich bedanken.

Natalia Kiseleva, it is a pleasure to get inspired by your ideas and thoughts and you show me again and again that life is more than a career. Thank you.

Ich möchte mich bei Ina Wendland für die langjährige Freundschaft, die vielen Telefonate danken. Die WG-Partys und Spieleabende werde ich nicht vergessen und haben mir gezeigt, wofür Freundschaft da ist.

Für eine ausgezeichnete Beobachtungsgabe, Diskussionen über Brotteige und gemeinsame Party und Spieleabende bin ich Sarah Al Muthafer dankbar. Darüber hinaus bedanke ich mich für die Telefonate in der Schreibphase und die Laborkonsultationen, die zermürende Momente in Schöne verwandelt haben.

Dass während Corona nicht alles schlecht war, hat mir Daniel Feser gezeigt. Für die zahlreichen Schachabende und exquisiten Cocktail- und Kochevents bin ich dir wahnsinnig dankbar.

Für endlose Bank-Sessions mit Pamina Frisch und eine stabile Stütze während den letzten Jahren bin ich sehr dankbar. Mit deiner einzigartigen und herzlichen Art faszinierst du mich immer wieder aufs Neue und ich möchte dich nicht missen.

Zuletzt möchte ich jedoch Janine Osterberg danken, da es wohl keinen Menschen gibt, der die guten und die schlechten Zeiten so intensiv mit mir erlebt und verbracht hat. Für die bedingungslose Unterstützung, das Vertrauen und die Liebe bin ich unendlich dankbar.